In vitro Effects of Selenium on DNA Damage in *BRCA1* Cell Lines

A thesis

submitted in fulfilment

of the requirements for the degree

of

Masters of Science Research in Biology

at

The University of Waikato

by

Kirsty Mayall

THE UNIVERSITY OF
WAIKATO
Te Whare Wānanga o Waikato

2015

Abstract

Cancer of the breast is the most common cancer affecting women, with a 1 in 9 lifetime risk of developing breast cancer. Carriers of mutations in the breast cancer susceptibility gene, *BRCA1,* present with an increased lifetime risk of 80-95% of developing breast cancer. *BRCA1* is a tumour-suppressor gene that is involved in DNA repair of double-strand breaks and transcriptional regulation.

Studies have shown that oral supplementation with Selenium (Se) could potentially be an effective preventive agent against *BRCA1*-mutation carriers. Se is an essential trace mineral that plays critical roles in maintaining health in humans. Se functions by protecting lipid membranes, proteins and DNA from free radical damage and is involved in redox regulation in the cell. These functions are mediated through specific Se-dependent proteins termed selenoproteins, in which Se is incorporated.

Se supplementation may exert its benefits by enhancing the DNA damage repair response. The effects also appear to be dependent on selenoprotein genotypes and concentration of Se in the body/diet. It is possible that Se supplementation may be effective in reducing the risk of breast cancer in *BRCA1* carriers, but the use of organic Se compounds is likely to be preferable, but the dose-response needs to be determined.

The objectives of this research thesis are to evaluate the dose-response of sodium selenite and methylseleninic acid (MSA) in two *BRCA1*-mutated cancer cell lines *in vitro.* The MTT assay was used to monitor cell activity, along with the comet assay to evaluate the DNA damage level using a dose-response curve of the two Se compounds on control and bleomycin-induced DNA damaged cells. In addition, DNA from each cell line was sequenced to confirm the presence of the published *BRCA1* mutation.

The data presented within this thesis demonstrates that a commonly-used inorganic form of Se, sodium selenite, is more genotoxic than the organic Se compound, MSA, in malignant *BRCA1*-mutated cells. Sodium selenite also has more direct cytotoxicity in *BRCA1*-mutated cells than MSA, as

demonstrated by the MTT assay. However the enhanced repair capacity from Se on DNA damage in cells demonstrated by others has not been reproduced. Preliminary data showed potential at much lower doses (2 µM) of Se. Interestingly, the volatile metabolites produced from MSA appear to reduce DNA damage, supportive of this hypothesis. In order to understand if the effects observed are linked specifically to the *BRCA1* mutation or breast cancer in general, future research should include the investigation of the effects of Se on breast cancer using alternative breast cancer cell lines, as well as non-malignant cells.

Acknowledgments

First and foremost I would like to thank my two supervisors, Dr Linda Peters, and Dr Michael Jameson, for taking me on as their student and giving me this opportunity to undertake research in such an interesting and important area. Linda, all your help with the lab work and the writing up of this thesis has been extremely valuable to me. Without your guidance, this research would not have been possible. And Michael, your enthusiasm and knowledge in this area of research is contagious, and it kept me excited to keep going, even when I was at my wits ends with experiments not working. So, to both of you, a huge thank you, without you, this wouldn't have been possible.

A big thank you to Olivia Patty and Sari Karppinen for all your training and technical help in the lab. You taught me many skills which I am very grateful for.

Another big thank you to Dr Ray Cursons, Dr Steve Bird, Steve Evans, and Dr Greg Jacobson for your expertise and help throughout this thesis. Your input has been very valuable to me, and I greatly appreciated your help. To everyone else in the Molecular Genetics lab, thanks for your help and company, especially those in the Master's office (you know who you are) who put up with me and my craziness for the year, you guys are awesome!

Also, thank you to Dr Ryan Martinus and Kerry Allen from the Biochemistry Cell Culture lab for your help and expertise, and to Alice Wang who went through it all with me - we made it!

Thank you to the University of Waikato for the Research Scholarship that has helped support me during this thesis, and to the School of Science for supporting travel to attend the Queenstown Molecular Biology conference. Also, thank you to the Waikato Clinical School for the Summer Studentship.

To mum and dad, a huge thank you for your absolute support you have given me right throughout my entire life; for letting me live at home and save while studying, for reading assignments (and my thesis!), even though you didn't fully understand what you were reading, and your constant love. It means the world to me. So thank you and love you! Also, to the rest of my family, thank you for your support in my 'boob science' research, you were great distractions, but kept me motivated to get the work done. Also, a special thanks to my brother, Jay, for proofreading my thesis.

Last, but certainly not least, thank you to my partner, Sam, for your constant support and patience throughout the last two years of my Masters. Your faith and positivity in me got me through the most stressful of times, and I couldn't have done it without you. I can finally say I'm finished, and now we can start a new adventure together!

Table of Contents

List of Figures

List of Tables

List of Equations

Abbreviations

+ve	Positive
°C	Degrees Celsius
2288delT	Deletion of a thymine at position 2288
3'	Three prime DNA end
5'	Five primer DNA end
5396 + 1G>A	Base substitution from a guanine to an adenine one nucleotide after position 5396
8-oxoGUa	8-hydroxydeoxyguanine
A	Adenine nucleotide
A. laidlawii	*Acholeplasma laidlawii*
aa	Amino acid(s)
ATP	Adenosine triphosphate
B1	Buffer 1
B2	Buffer 2
BASC	*BRCA1*-associated genome surveillance complex
BER	Base excision repair
Bl	Blank
BLAST	Basic local alignment search tool
bp	Base pair(s)
BRCA1	Breast cancer susceptibility gene 1

BRCA2	Breast cancer susceptibility gene 2
CI	Confidence interval
CO_2	Carbon dioxide
d.f	Dilution factor
DMSO	Dimethyl sulfoxide
DNA	Deoxyribonucleic acid
dNTP	Deoxyribonucleotide
DSMZ	Deutsche Sammlung von Mikroorganismen und Zellkulturen GmbH
EDTA	Ethylenediaminetetraacetic acid
eEFSec	Sec-specific translation elongation factor
ER	Oestrogen receptor
ER^+	Oestrogen receptor positive
et al	And others
FASTA	File format for nucleotide and protein sequences
FBS	Fetal bovine serum
g	G-force
g	Gram(s)
G	Guanine nucleotide
Gadd45	Growth arrest and DNA-damage-inducible 45
GC	Growth control
gDNA	Genomic DNA
GPx-1	Glutathione peroxidase 1

H_2O_2	Hydrogen peroxide
HC	Hydrocortisone
HCC	Hannah Crossan
HCl	Hydrochloric acid
HER2	Human epithelial growth factor receptor 2
$HER2^+$	Human epithelial growth factor receptor 2 positive
hr	Hour(s)
IC_{50}	Concentration required to inhibit 50% of the population
IDT	Integrated DNA Technologies
kb	Kilobase
KM	Kirsty Mayall
L	Litre(s)
LMP	Linda Marie Peters
LMPA	Low melting point agarose
LOD	Logarithm of odds
M	Molar
mA	Milliampere(s)
mcm^5U	5-methylcarboxymethyluridine
mcm^5Um	5-methylcarboxymethyluridine-2'-O-methylribose
mg	Milligram(s)
$MgCl_2$	Magnesium chloride
min	Minute(s)

mL	Millilitre(s)
mM	Millimolar
mm	Millimeter
MPI	Ministry for Primary Industries
mQ H_2O	milliQ water
mRNA	Messenger RNA
MSA	Methylseleninic acid
MTT	3-(4,5-dimethylthiazol-2-yl)-2,5-diphenyl tetrazolium bromide
Na	Sodium
NaOAc	Sodium acetate
NaOH	Sodium hydroxide
NCBI	National Center for Biotechnology Information
ng	Nanogram(s)
nm	Nanometer
NMPA	Normal melting point agarose
OD	Optical density
OGG1	8-oxoguanine DNA glycosylase enzyme
ORF	Open reading frame
PBMC	Peripheral blood mononuclear cells
PBS	Phosphate buffered saline
PC2	Physical containment facility level 2
PCR	Polymerase chain reaction

Pen/strep	Penicillin and streptomycin
ppm	Parts per million
PR	Progesterone receptor
PR^+	Progesterone receptor positive
PSA	Prostate-specific antigen
PSTK	Phosphoseryl-$tRNA^{[Ser]Sec}$ kinase
rDNA	Ribosomal DNA
RING	Really Interesting New Gene
RNA	Ribonucleic acid
ROS	Reactive oxygen species
rpm	Revolutions per minute
RT	Room temperature
SBS2	SECIS binding protein 2
SC	Solvent control
SCGE	Single cell gel electrophoresis
sd	Standard deviation
SDS	Sodium dodecyl sulfate
Se	Selenium
sec	Second(s)
Sec	Selenocysteine
SECIS	Sec insertion sequence
SecS	Selenocysteine synthase
SELECT	Selenium and Vitamin E Cancer Prevention Trial

SEM	Standard error of the mean
Ser	Serine
SerS	seryl-tRNA synthetase
SPS2	Selenophosphate synthetase 2
T	Thymine nucleotide
TAE	Tris-Acetate-EDTA
TE	Tris-EDTA
tRNA	transfer RNA
$tRNA^{[Ser]Sec}$	Sec tRNA
U	Enzyme units
Um34	2'-O-methylribose at position 34
UTR	3'-untranslated region
UV	Ultra violet
UVA	Ultra violet radiation A (long-wave)
V	Volt(s)
-ve	Negative
µg	Microgram
µl	Microlitre
µM	Micromolar

Chapter One

Introduction and Literature Review

1.1 Introduction to Cancer

Cancer is defined as a group of diseases which are characterised by uncontrolled cell growth and the invasion and spread of cells from the origin site to other sites throughout the body as a result of changes to the mammalian genome. Over 100 different types of cancer have been classified. The tissue of origin allows cancers to be classified due to cancer tissues having distinguishing characteristics. For example, the most common cancers occur in epithelial cells and are classified as carcinomas; cancers derived from the mesoderm cells (e.g. bone, muscle) are called sarcomas; and cancers of glandular tissue (e.g. breast) are called adenocarcinomas (Pecorino, 2005). Even with the diverse range of cancer types, there are alterations of eight essential functions in cell physiology that lead to carcinogenesis (the development of cancer); these are known as the eight hallmarks of cancer (Hanahan & Weinberg, 2011). The following hallmarks are common to most, if not all cancers: self-sufficiency in growth signals; evasion of growth inhibitory signals; evasion of apoptosis (programmed cell death); unlimited replicative potential; sustained angiogenesis (formation of new blood vessels); tissue invasion and metastasis (spreading of cancer cells from one organ to another); reprogramming of energy metabolism; and evading immune destruction. These eight hallmarks are the capabilities required by cells to combat the anticancer defence mechanism that leads to the growth of tumours (Figure 1).

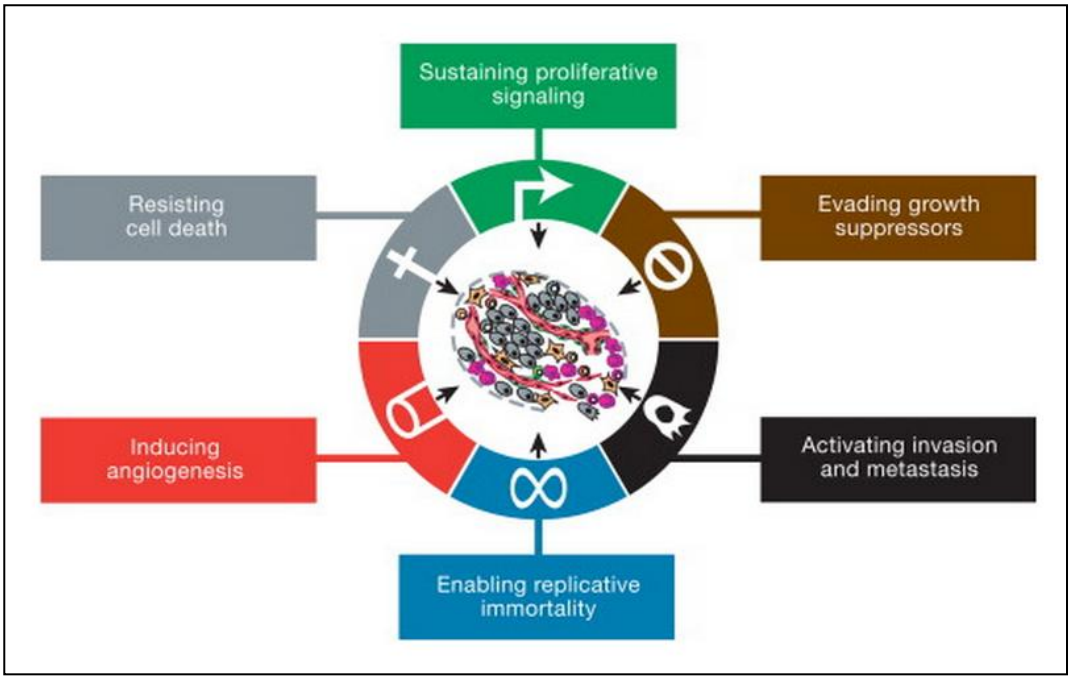

Figure 1. The six, original, hallmarks of cancer. The six hallmarks impact the growth and viability of tumour cells (present in the centre of the figure). The two new hallmarks that have recently been identified (not present in the figure) are reprogramming of energy metabolism, and evading immune destruction. Source: Hanahan & Weinberg, 2011.

1.2 Breast Cancer

Breast cancer is a heterogeneous disease caused by the formation of malignant cancerous cells in breast tissue (Li, Uribe, & Daling, 2005; Weigelt, Geyer, & Reis-Filho, 2010; Yerushalmi, Hayes, & Gelmon, 2009). These cells have the ability to metastasise. The tissue that most breast tumours are derived from is the mammary ductal epithelium, predominantly the terminal duct-lobular unit, regardless of the histological type (Arpino, Bardou, Clark, & Elledge, 2004; Arps, Healy, Zhao, Kleer, & Pang, 2013; Li et al., 2005; Weigelt, Geyer, et al., 2010; Weigelt & Reis-filho, 2009; Yerushalmi et al., 2009). Breast cancer can be categorised and divided into subtypes due to the fact that tumours have different biological factors (expression of tumour markers, histological type, behaviour and molecular profiles), as well as clinical behaviours (response to therapy) (Arps et al., 2013; Li et al., 2005; Weigelt, Geyer, et al., 2010; Yerushalmi et al., 2009). Breast cancer phenotypes can be classified based on histopathological characteristics such as histological tumour type

and tumour grade, or their molecular gene expression profile focusing on the oestrogen-receptor (ER), progesterone-receptor (PR), and the human epithelial growth factor receptor 2 (HER2) status (Arpino et al., 2004; Arps et al., 2013; Sørlie et al., 2001; Weigelt, Baehner, & Reis-Filho, 2010; Weigelt & Reis-filho, 2009). However, in regards to deciding which treatment method should be utilised for each breast cancer case, three main types are determined: endocrine receptor (ER/PR) positive, HER2 positive, or triple negative (no hormone receptors - ER/PR and HER2 negative).

1.2.1 Epidemiology of Breast Cancer

Breast cancer is the most common cancer affecting women, with a 1 in 9 (11%) lifetime risk of developing breast cancer (Barber, Thomas, & Dixon, 2008; Davies, 2012; Judson & Van Le, 1998; Key, Verkasalo, & Banks, 2001; Ministry of Health, 2012; Murray, 2010; Murray & Davies, 2013; Sasco, 2001; Wang & Chung, 2012; Washbrook, 2006). In New Zealand, it accounted for 28.7% of all new registered female patients with cancer in 2011 (Ministry of Health, 2014). Breast cancer can also be developed in males, but at a much lower rate. The rate of registration of breast cancer from 2001 to 2011 has remained relatively stable. However, the death rate due to breast cancer fell during this time period by 19.6% (Ministry of Health, 2014).

Numerous factors have been identified that affect the risk of breast cancer in individuals. The factors that have the highest impact on breast cancer risk are age; reproductive factors; and genetics; with other factors such as hormonal status, lifestyle and radiation exposure also playing a part in the aetiology of breast cancer (Figure 2) (Barber et al., 2008; Davies, 2012; Key et al., 2001; MacMahon, 2006; Murray & Davies, 2013; Sasco, 2001; Vanderhaeghe, 2004; Wang & Chung, 2012; Washbrook, 2006).

Established and probable risk factors for breast cancer

Risk factor	Relative risk	High-risk group
Age	› 10	Elderly
Reproductive factors		
Age at menarche	3	Menarche before age 11
Age at menopause	2	Menopause after age 54
Age at first pregnancy	3	Nulliparous or first child in early 40s
Lifestyle factors		
Diet	1.5	High intake of saturated fat
Body weight (postmenopausal)	2	Body mass index › 35
Alcohol	1.3	Excessive intake
Hormonal status		
Oral contraceptives	1.24	Current use
Hormone replacement therapy	1.35	Use for ≥ 10 years
Radiation	3	Abnormal exposure after age 10
Family history	≥ 2	Breast cancer in first-degree relative when young

Figure 2. Risk factors associated with breast cancer. The relative risk of each factor on the incidence of breast cancer is rated from 1 (lowest relative risk of breast cancer) through to 10 (highest relative risk of breast cancer). Therefore, age can be clearly determined as the biggest influencing factor on the relative risk of breast cancer incidence with a rating of greater than 10, through to oral contraceptives having the lowest relative risk of breast cancer with a rating of 1.24. Source: Washbrook, 2006.

1.3 Breast Cancer Genetics

Genetic variance is a determining factor in breast cancer epidemiology (Figure 3). The genetic variation associated with breast cancer is due to the familial (hereditary) inheritance of germline mutations, resulting in autosomal dominant inheritance patterns, and these account for 20% of all breast cancer cases (Figure 3). Therefore, to inherit the disease requires the transmission of the abnormal gene from one parent only, and the child then becomes a carrier. Individuals who have inherited one copy are termed carriers. (Boeri, Canzonieri, Cagioni, Ornati, & Danesino, 2011; Judson & Van Le, 1998; Key et al., 2001; Nathanson, Wooster, & Weber, 2001; Thompson & Easton, 2004). The heritable genetic variants are, however, only found to be responsible for 5-25% of breast cancer cases (Barber et al., 2008; Judson & Van Le, 1998; Key et al., 2001; Murray & Davies, 2013; Thompson & Easton, 2004). Studies on familial breast

cancer have shown that those with an affected first-degree relative have a two-fold increased risk of breast cancer, with a lower risk for affected second-degree relatives (e.g. grandmothers, aunts) (Judson & Van Le, 1998; Key et al., 2001; Thompson & Easton, 2004).

The biggest contributing genetic variants to the disease are the breast cancer susceptibility genes; breast cancer susceptibility gene 1 (*BRCA1*) and breast cancer susceptibility gene 2 (*BRCA2*). Mutations in these genes result in an increased risk of breast and ovarian cancer, along with other specific cancers such as prostate, pancreatic, and fallopian tube cancer (Barber et al., 2008; Boeri et al., 2011; Judson & Van Le, 1998; Murray, 2010; Murray & Davies, 2013; Nathanson et al., 2001; Sasco, 2001; Thompson & Easton, 2004).

Research into the disease-causing genes of breast cancer was carried out in the early 1990s using epidemiological research and collections of family data. From this data, linkage was identified with polymorphic markers on chromosome 17 (logarithm of the odds (LOD) score of +5.98) (Hall et al., 1990). Following this initial investigation, *BRCA1* was identified in 1993 as the first gene responsible for hereditary breast cancer (Hall et al., 1990). After the identification of *BRCA1,* a larger data set of families segregating breast cancer were ascertained, and using linkage analysis (total LOD score of -16.63) (excluding *BRCA1*), *BRCA2* was identified (Boeri et al., 2011; Hall et al., 1990; Thompson & Easton, 2004).

It is considered that the *BRCA* genes are responsible for 20% of all familial cases of breast cancer, and carriers of these mutations present with an increased lifetime risk of 80-95% (Judson & Van Le, 1998). The *BRCA* genes are considered high-risk mutations as they are highly penetrant (e.g. those who have a specific genetic variant express it to produce a correlated phenotype) (Judson & Van Le, 1998; Key et al., 2001; Lymberis, Parhar, Katsoulakis, & Formenti, 2004; Nathanson et al., 2001; Thompson & Easton, 2004). Families that have these high-risk mutations often show clustering of early-onset (<50 years old) breast cancer.

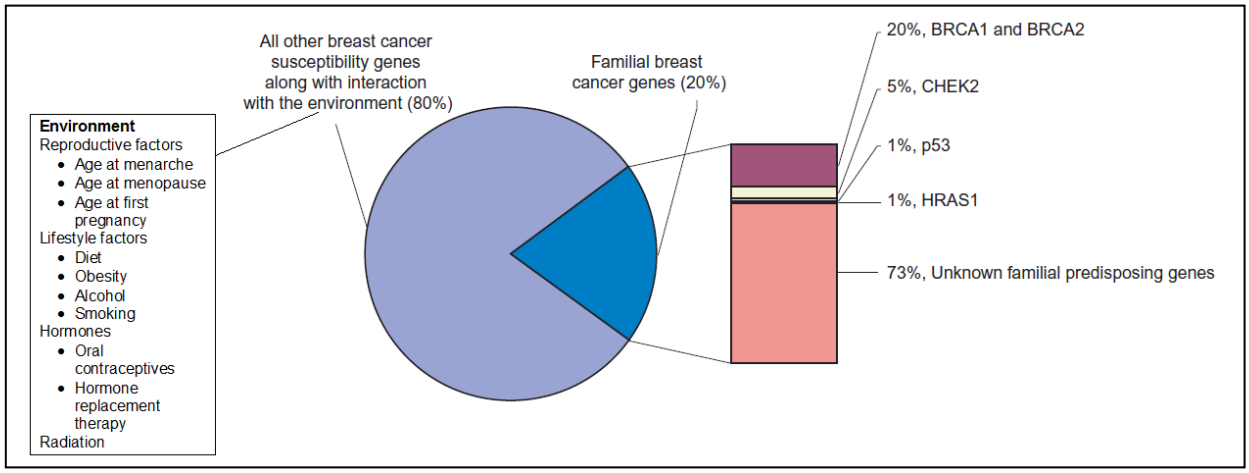

Figure 3. Epidemiology of breast cancer. Environment versus familial genetic factors and their influence on the incidence of breast cancer. Modified from: Lymberis, Parhar, Katasoulakis, & Formenti, 2004.

1.3.1 *BRCA1* and *BRCA2* genes

Familial *BRCA1* and *BRCA2* inherited high-risk germline mutations are only responsible for less than 5% of all breast cancer cases (20% of familial breast cancers) (Boeri et al., 2011; Judson & Van Le, 1998; Murray & Davies, 2013; Nathanson et al., 2001; Thompson & Easton, 2004). *BRCA1* (Accession number: NG_005905 (NCBI GenBank, 2013a)) is a large gene comprised of 24 coding exons located on human chromosome 17q21, spanning 100 kilobases (kb) of genomic DNA, and encodes a protein product of 1863 amino acids (aa) (Boeri et al., 2011; Judson & Van Le, 1998; Lymberis et al., 2004; Murray, 2010; Murray & Davies, 2013; Nathanson et al., 2001; Thompson & Easton, 2004). Six variant transcripts have been identified and accepted for the *BRCA1* gene as a result of alternative splicing (UCSC Genome Bioinformatics, 2013a). These alternative transcripts play a role in the localisation to specific tissues and the various functions of the *BRCA1* gene (NCBI GenBank, 2013a; Orban & Olah, 2003). *BRCA2* (Accession number: NG_012772 (NCBI GenBank, 2013b)) is even larger than *BRCA1*, comprising of 27 exons located on chromosome 13q12, spanning around 70 kb, and encoding a protein product of 3418 aa (Boeri et al., 2011; Judson & Van Le, 1998; Lymberis et al., 2004; Murray, 2010; Murray & Davies, 2013; Nathanson et al., 2001; Thompson & Easton, 2004). In comparison to

BRCA1, *BRCA2* does not appear to have any alternative splicing transcript variants (UCSC Genome Bioinformatics, 2013b).

BRCA1 is a tumour-suppressor gene that forms a large multi-subunit protein complex called the *BRCA1*-associated genome surveillance complex (BASC) through the association with other tumour suppressors, DNA damage sensors, and signal transducers. BASC is suggested to act as a sensor for DNA damage, and can then aid in the repair mechanisms to maintain the integrity of the genome during DNA replication. Through this association of *BRCA1* in BASC, it points to *BRCA1* having a key role in the DNA repair process (Wang et al., 2000). *BRCA2* is also a tumour-suppressor gene which, along with *BRCA1*, is involved in cell processes such as DNA repair of double-strand breaks and transcriptional regulation (NCBI GenBank, 2013a, 2013b; Thompson & Easton, 2004; Welcsh & King, 2001).

Breast carcinogenesis can be attributed to the 'two-hit hypothesis'; the loss of the gene product through mutation of both alleles which leads to tumourigenesis susceptibility (Boeri et al., 2011; Judson & Van Le, 1998; Murray, 2010; Murray & Davies, 2013; Thompson & Easton, 2004). Somatic mutations are genetic changes that occur in the cells of an organism which are not passed on to the offspring through the germline and they occur over time. Therefore, it will take many years for an individual to gain two mutations in the *BRCA* genes (which results in the development of breast cancer). Whereas, if an individual has inherited a germline mutation in one of their *BRCA* alleles from their parent, they only have to gain one somatic mutation to result in breast cancer, therefore, giving carriers a greater risk of breast carcinogenesis.

Mutations such as small frameshift insertions or deletions (<20 bp), and nucleotide substitutions can occur anywhere along the entire length of the *BRCA* gene, with most resulting in truncation of the protein. For example, 70% of *BRCA1* mutations and 90% of *BRCA2* mutations result in protein truncation, and as a result, loss of protein function (Thompson & Easton, 2004). More than 1600 genetic variants in *BRCA1* and 1880 genetic

variants in *BRCA2* have been identified as pathogenic mutations (Boeri et al., 2011). One online database, ClinVar (NCBI ClinVar, 2013b), outlines identified genetic variations that have an associated risk, or are considered as pathogenic variants. For example, one such identified pathogenic genetic variation of hereditary breast and ovarian cancer is the deletion of two nucleotides, adenine and guanine, at position 68 and 69 of the *BRCA1* gene, resulting in a frameshift of the open reading frame (NM_007294.3:c.68_69delAG) (NCBI ClinVar, 2013a).

The mutations identified in familial cases of breast cancer are generally found to be 'individual' mutations (only present in the family), with the exception of a few common mutations which can be found in certain populations such as the Icelandic and Ashkenazi Jews (Boeri et al., 2011; Judson & Van Le, 1998; Lymberis et al., 2004; Murray, 2010; Murray & Davies, 2013; Nathanson et al., 2001; Thompson & Easton, 2004). In these situations, the recurrent mutation has been passed on from a single founder present in a small founder population. For example, three founder mutations have been identified in the Ashkenazi Jewish population: 185delAG and 5382insC in *BRCA1*, and 617delT in *BRCA2*. Nearly all of the reported cases of *BRCA1* and *BRCA2* mutations found in this population can be attributed to these three mutations (Thompson & Easton, 2004).

Even though the function of *BRCA1* and *BRCA2* are similar, they are not closely related at the nucleotide and protein level. When their protein nucleotide sequences are aligned and compared against each other (blastn), the results show that they only share 31% identity between them. There are five regions that show higher conservation, but they only show identity values ranging between 24% - 50% (Figure 4) (NCBI BLAST (Basic Local Alignment Search Tool), 2013). From these results, it can be clearly demonstrated that these two genes do not share a common recent ancestor. They are both ubiquitously expressed, showing the most elevated concentrations in the ovaries, testis, and thymus (Thompson & Easton, 2004). Finally, both genes show relatively high conservation of their amino acid sequences between species. Four conserved protein

domains have been identified: serine-rich domain, ethylene-insensitive 3, breast cancer suppressor protein, carboxy-terminal domain, and the RING-finger (Really Interesting New Gene) domain (NCBI HomoloGene, 2013). Also, using the UCSC Genome Bioinformatics database, the *BRCA1* transcript (Figure 5) and the *BRCA2* transcript (Figure 6) show great conservation of their amino acid sequence with closely related species such as rhesus macaque (*Macaca mulatta*), and their sequence conservation decreases in less closely related species such as zebrafish (*Danio rerio*) (UCSC Genome Bioinformatics, 2013a, 2013b).

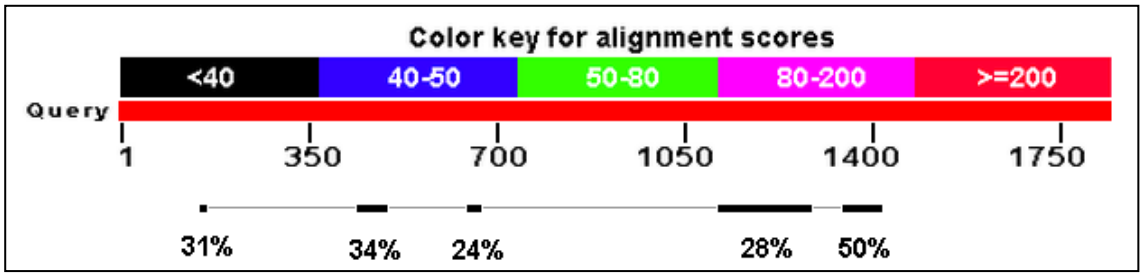

Figure 4. Blastn of *BRCA1* nucleotide sequence against *BRCA2* nucleotide sequence. The score of each alignment is indicated by one of five different colours. Below this, is a solid red bar which represents the query sequence (*BRCA1* gene from nucleotide 1–2000). Underneath is a black line that shows the five regions of higher conservation in bold, showing relative identities of each region. Source: NCBI BLAST, 2013.

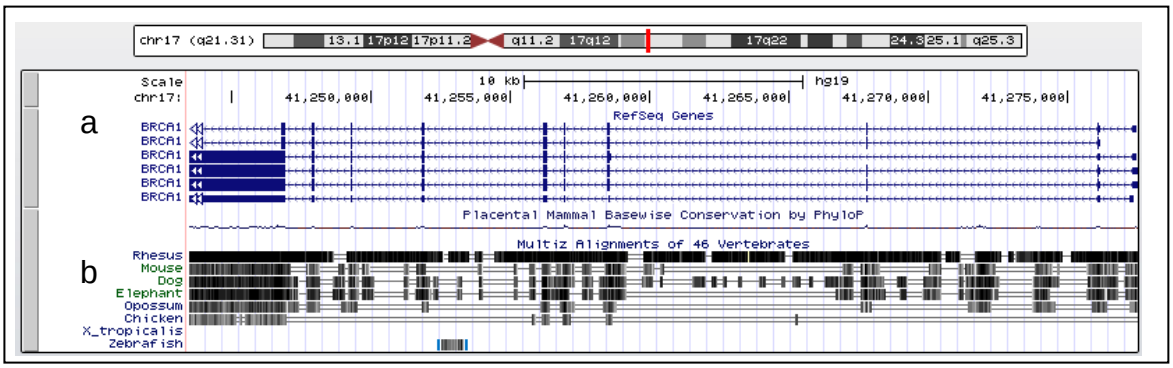

Figure 5. Chromosome 17 ideogram. The ideogram shows the *BRCA1* gene located at chr17q21.31 (red vertical bar) using the UCSC Genome Bioinformatics database, and this region is expanded in the box below. a) Six antisense variant mRNA transcripts as a result of alternative splicing. The vertical bars represent the break between each coding exon. b) Amino acid sequence comparison between humans and various other species. Dark regions show areas of strong sequence correlation. Rhesus shows greater sequence conservation than the other species. Source: UCSC Genome Bioinformatics, 2013a.

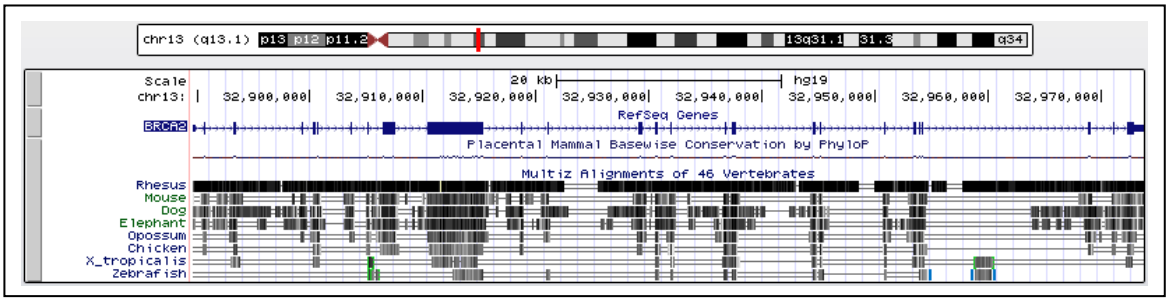

Figure 6. Chromosome 13 ideogram. The ideogram shows the *BRCA2* gene located at chr13q13.1 (red vertical bar) using the UCSC Genome Bioinformatics database, and this region is expanded in the box below. a) Only one sense mRNA transcript identified. The vertical bars represent the break between each coding exon. b) Amino acid sequence comparison between humans and various other species. Dark regions show areas of strong sequence correlation. Rhesus shows greater sequence conservation than other species. Source: UCSC Genome Bioinformatics, 2013b.

1.3.2 Risk Reduction in Carriers of *BRCA1* or *BRCA2*

This greatly increased risk that *BRCA* carriers have, at this time, can only be reduced through drastic prophylactic (risk-reducing) surgery - having both breasts removed (bilateral prophylactic mastectomy) to reduce the risk of breast cancer, and removal of the ovaries and fallopian tubes (bilateral prophylactic salpingo-oophorectomy) to reduce the risk of ovarian cancer. This can, however, be considered to be quite a drastic and mutilating procedure, so another, not quite so intrusive method to reduce the risk of breast cancer in *BRCA* carriers would be very beneficial.

Cases, such as celebrity Angelina Jolie publicly announcing her preventive double mastectomy due to her being a carrier of a rare *BRCA* mutation, have created a greater awareness for *BRCA* testing/screening and preventive options for women at high risk of breast cancer (Kamenova, Reshef, & Caulfield, 2014). However, media publications do not communicate enough information to give the audience a broad understanding of the issues, and the testing and treatment options available (Borzekowski, Guan, Smith, Erby, & Roter, 2014). Although, in Jolie's case, a double mastectomy was a reasonable decision, in many other cases, those drastic measures are not necessary, but due to the influence that celebrities have, many women may be making rash decisions into certain surgeries that could be avoided with a better understanding of the risks (Borzekowski et al., 2014; Kluger & Park, 2013).

There is clearly a pressing need for a less drastic method to reduce the risk of breast, ovarian and other cancers in carriers of pathogenic mutations in these genes. Studies have shown that oral supplementation with the trace mineral selenium (Se) could potentially be an effective preventive agent against breast cancer in this group (Kowalska et al., 2005). In the next section, the biology and chemistry of Se will be reviewed.

1.4 Selenium

Se was discovered in 1817 by Jöns Jacob Berzelius, a Swedish chemist (Weekley & Harris, 2013). It was originally thought to be toxic to humans (*Homo sapiens*) but this view has since changed as it has been revealed through further investigation that Se is an essential trace mineral that plays critical roles in maintaining health (Painter, 1941; Rayman, 2012).

1.4.1 Selenium Bioavailability and Health

Se is present throughout the terrestrial environment in rocks and soils, and enters the food chain when it is taken up by plants; the Se content of animals is directly correlated to their diet. Similarly, the most important source of Se for humans is through the diet (Rayman, 2012; Valdiglesias, Pásaro, Méndez, & Laffon, 2010). The intake of Se varies greatly throughout the human population due to the varying concentrations of Se present in different countries as well as within a single country. For example, New Zealand, Finland, and parts of China have very low soil Se concentrations (<0.05 ppm), and Se deficiency is known to cause diseases in livestock, and adversely affect the health of humans (Aro, Alfthan, & Varo, 1995; Navarro-Alarcon & Cabrera-Vique, 2008; Thomson & Robinson, 1980; Yang, Wang, Zhou, & Sun, 1983). In comparison, countries such as Canada, USA, Venezuela, Ireland and other parts of China have very high soil Se concentrations (>5 ppm) and are considered to be seleniferous (Se-rich) (Navarro-Alarcon & Cabrera-Vique, 2008;

Yang et al., 1983). Se concentration in plants is directly linked to the bioavailability of Se in the soils. The status, distribution and availability of Se in our food systems is therefore dependent on factors, such as: the species of Se; soil pH; the types of rocks and redox potentials in the soil; the presence of other organic or inorganic compounds that could complex with Se; and climatic conditions. All of these factors influence the overall bioavailability of Se to plants and thus to animals and humans (Aro et al., 1995; Combs, 2001; Johnson, Fordyce, & Rayman, 2010; Westermarck, Latvus, & Atroshi, 2014). The availability of this essential micronutrient to humans is therefore dependant on the concentration of Se in the food, and following this, the amount of food consumed (Navarro-Alarcon & Cabrera-Vique, 2008).

Se was first identified as an essential micronutrient in 1957 when it was demonstrated that liver necrosis could be prevented by the supplementation of Se in vitamin E deficient rats and chicks (Schwarz & Foltz, 1957). Se deficiency has now been linked to several human diseases, some of which are found to be quite common place in areas of China where Se soil levels are sub optimal. For example, Keshan disease is an endemic cardiomyopathy found in Chinese children, and Kashin-Beck disease results in chronic arthritis (Yang et al., 1983; Zhou et al., 2003). Low levels of Se can also be linked to other conditions such as increased risk of cancer and cardiovascular disease, decreased immunity and thyroid function, decreased survival in HIV-positive patients, and low fertility in men (Hatfield, Tsuji, Carlson, & Gladyshev, 2014; Rayman, 2012).

1.4.2 Selenium Chemistry

The form of Se influences its bioavailability; organically bound Se compounds are more readily metabolised than inorganic Se compounds. Also, it is generally considered that the inorganic forms of Se are found to be more genotoxic than the organic forms (Abdulah, Miyazaki, Nakazawa, & Koyama, 2005; Valdiglesias et al., 2010). The two Se compounds that this research thesis reviews are organic methylseleninic acid (MSA) (Figure 7a) and inorganic sodium selenite (Figure 7b).

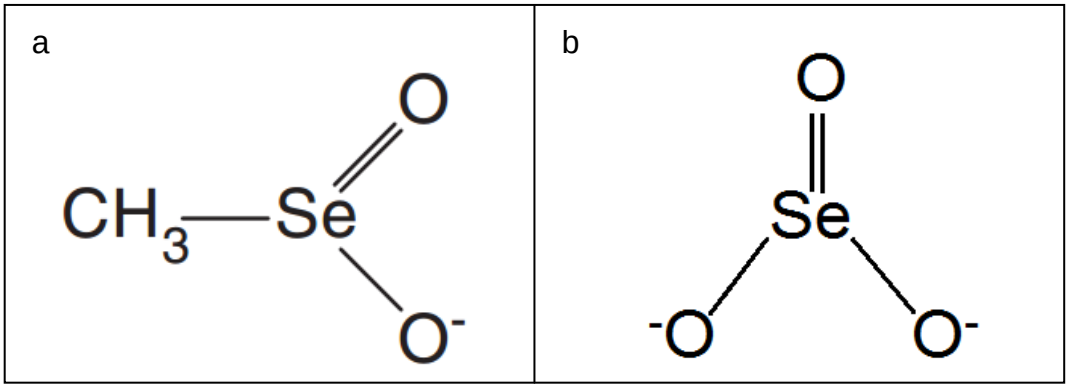

Figure 7. Chemical structure of Se compounds. a) MSA (CH_4O_2Se). b) Selenite (Na_2SeO_3). Source: Abdulah, Miyazaki, Nakazawa, & Koyama, 2005.

1.5 Selenoproteins

Se functions by protecting lipid membranes, proteins and DNA from free radical damage and is involved in redox regulation in the cell (Rayman, 2012). These functions are mediated through specific Se-dependent proteins termed selenoproteins which are all characterised as being oxidoreductases (Lobanov, Hatfield, & Gladyshev, 2009). There are at least 25 different human selenoproteins making up the selenoproteome, and the active centre of these proteins is home to what is known as the 21st amino acid, selenocysteine (Sec). Sec is unique among the standard 20 amino acids as it is biosynthesised by its own tRNA, $tRNA^{[Ser]Sec}$. This tRNA is 90 nucleotides in length, compared to ~75 nucleotides of other tRNA molecules, and as a result of this longer overall length, it has a remarkably long variable arm (Diamond, Dudock, & Hatfield, 1981;

Diamond et al., 1993). Sec tRNA is recognised by the codon UGA, which normally codes for a stop codon (Berry et al., 1991; Kryukov et al., 2003). The UGA codon is recognised as Sec instead of termination by a group of cis- and trans-acting elements (Labunskyy, Hatfield, & Gladyshev, 2014).

1.5.1 Sec tRNA Biosynthesis

The *Trsp* gene encodes the selenocysteine $tRNA^{[Ser]Sec}$. *Trsp* is a single copy gene that produces two different isoforms which differ by a single 2'-*O*-methylribose at position 34 (Um34) (Hatfield, Carlson, Xu, Mix, & Gladyshev, 2006). The first isoform, 5-methylcarboxymethyluridine, (mcm^5U) lacks Um34 and acts as the precursor for the second isoform, 5-methylcarboxymethyluridine-2'-O-methylribose (mcm^5Um), and this final methylation changes the final tertiary structure of the tRNA (Hatfield, Lee, Hampton, & Diamond, 1991; Hatfield et al., 2006). Se status can alter the relative distribution of which isoform is present in cells. During times of Se deficiency, mcm^5U is more abundant than mcm^5Um, as mcm^5U is less dependent on Se status, and during times of rich Se availability (i.e. supplementation), an inverse ratio is observed as mcm^5Um is largely dependent on Se status and is only expressed during times of Se adequacy (Diamond et al., 1993; Hatfield et al., 1991; Hatfield et al., 2006).

Before Sec can be synthesised, $tRNA^{[Ser]Sec}$ is first aminoacylated with serine (Ser) to form an intermediate (Lee, Worland, Davis, Stadtman, & Hatfield, 1989; Westermarck et al., 2014). This process is catalysed by an enzyme that is thought to only recognise Ser and not Sec, seryl-tRNA synthetase (SerS). The elements that differentiate between these two are located in the long arm and wobble base of Sec tRNA, and consequently are necessary for Ser aminoacylation by SerS (Ohama, Yang, & Hatfield, 1994; Wu & Gross, 1993). Phosphoseryl-$tRNA^{[Ser]Sec}$ kinase (PSTK) then converts seryl-$tRNA^{[Ser]Sec}$ to phosphoseryl-$tRNA^{[Ser]Sec}$, another intermediate. The final step in the production of Sec is the conversion of the phosphoserine moeity to a Se-accepting molecule, resulting in

selenocysteyl-tRNA$^{[Ser]Sec}$. Selenocysteine synthase (SecS) catalyses this final step by incorporating the active form of Se, selenophosphate, into the amino acid backbone, forming the final product, Sec-tRNA (Figure 8) (Xu et al., 2006; Yuan et al., 2006). Selenophosphate synthetase 2 (SPS2) is the enzyme responsible for the synthesis of selenophosphate (from selenide and ATP), and as SPS2 is itself a selenoprotein, it suggests that it acts as an autoregulator of its own biosynthesis (Guimarães et al., 1996).

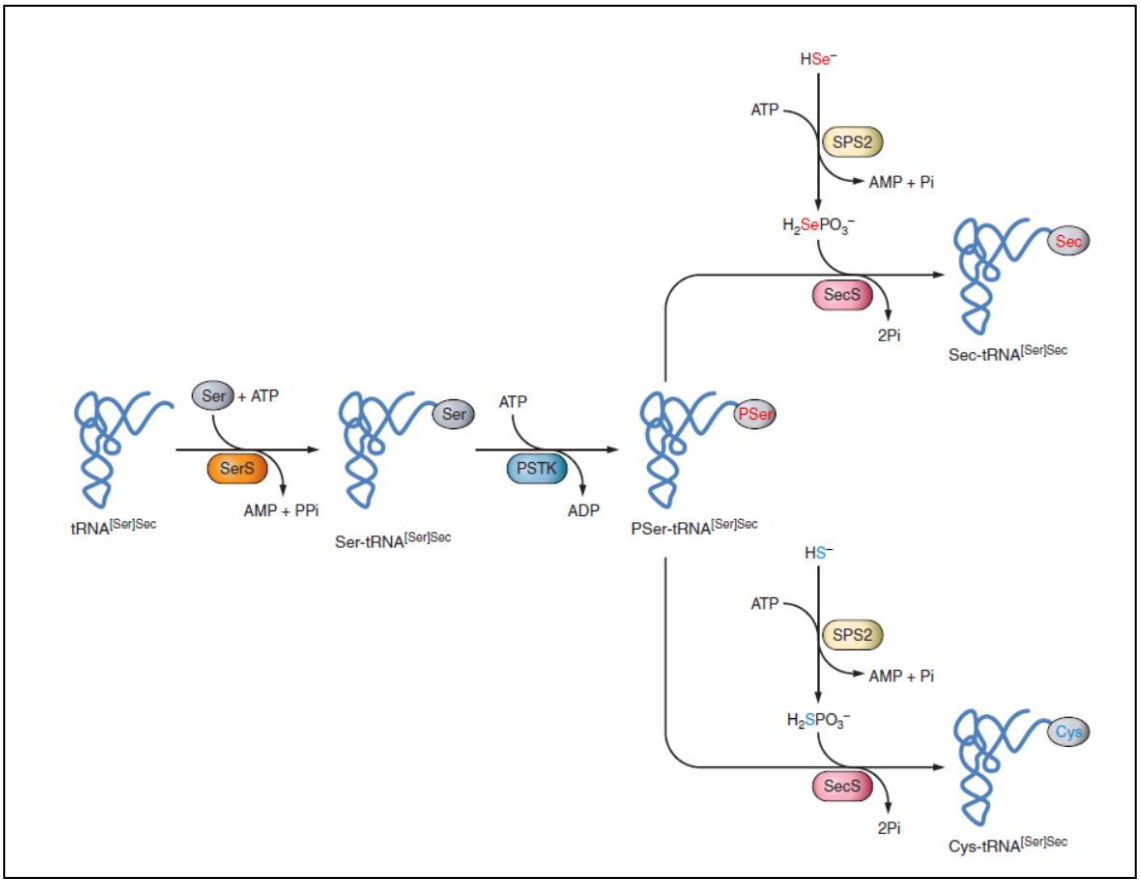

Figure 8. Mechanism of the biosynthesis of Sec tRNA. Source: Labunskyy, Hatfield, & Gladyshev, 2014.

Following the completion of Sec-tRNA biosynthesis, incorporation into the growing polypeptide chain is necessary. During the process of normal protein synthesis, the mRNA transcript moves through the ribosome, with each codon being read by a tRNA (for a specific amino acid) with the complementary anti-codon. Each new tRNA transfers its amino acid to the

growing polypeptide chain until a termination (or stop codon) is read, which results in release of the polypeptide chain, and the separation of the mRNA transcript and the ribosome. However, for Sec-tRNA to be incorporated into the polypeptide chain, the UGA termination codon needs to be recoded as a Sec-tRNA. This process cannot occur by Sec-tRNA interactions alone; other cis- and trans-acting elements play a crucial role in the recoding of UGA as Sec instead of introducing a stop codon (Figure 9). The exclusive cis-acting element, Sec insertion sequence (SECIS), is located in the 3'-untranslated region (UTR) stem-loop structure of eukaryotic selenoprotein mRNAs (Berry et al., 1991; Böck, 2000; Tujebajeva et al., 2000) and is essential for recoding (Krol, 2002). Mutations in non-conserved areas of SECIS reduce the recoding frequency, and can therefore be a factor in the cause of human selenoprotein deficiency related diseases. SECIS binding protein 2 (SBS2) (Copeland, Fletcher, Carlson, Hatfield, & Driscoll, 2000; Low, Grundner-Culemann, Harney, & Berry, 2000) and Sec-specific translation elongation factor (eEFSec) (Tujebajeva et al., 2000) are two of the trans-acting factors that, along with SECIS, are required for Sec recoding. SBS2, which is associated with ribosomes, binds to SECIS with high affinity by the L7Ae RNA-binding domain, as well as interacting with eEFSec. Sec-tRNA$^{[Ser]Sec}$ is then recruited and Sec is incorporated into the growing polypeptide chain by the interactions of eEFSec (Figure 9) (Tujebajeva et al., 2000). Other binding proteins have also been identified as being involved in Sec incorporation: ribosomal protein L30 (Chavatte, Brown, & Driscoll, 2005), nucleolin (Miniard, Middleton, Budiman, Gerber, & Driscoll, 2010), and eukaryotic initiation factor eIF4a3 (Budiman et al., 2009).

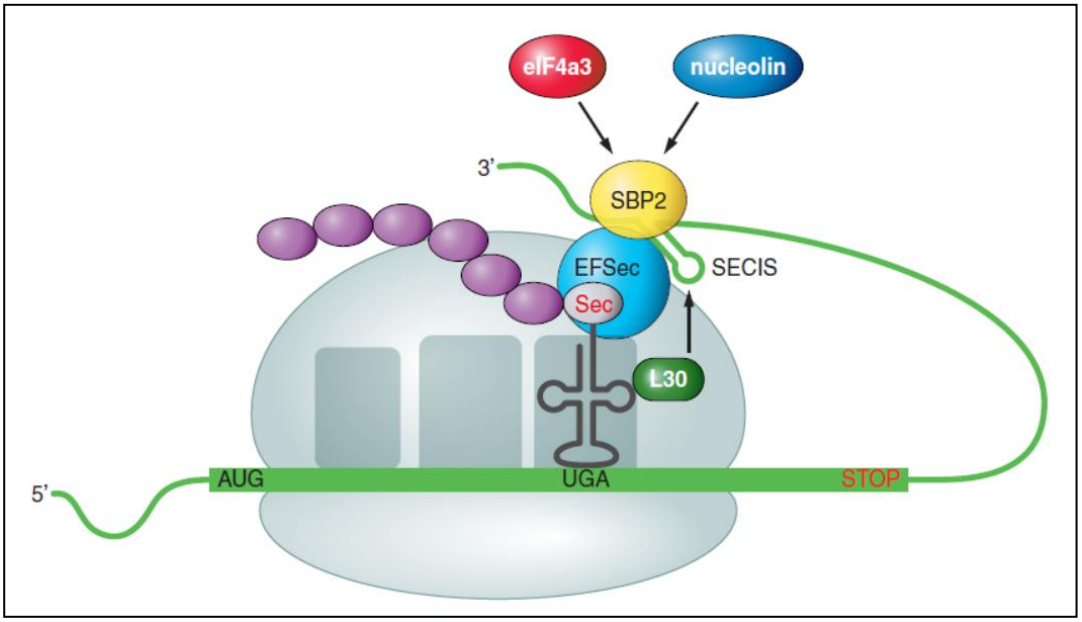

Figure 9. Sec insertion into eukaryotes. The green bar depicts the mRNA transcript travelling through the ribosome (grey) being translated, showing the start codon (AUG) at the 5' end and the Sec tRNA bound to the UGA codon. The mRNA is surrounded by the ribosome and the amino acids (purple ovals) represent the translated polypeptide chain. Source: Labunskyy, Hatfield, & Gladyshev, 2014.

1.6 Selenium for Cancer Prevention

Animal models, *in vitro* mammalian cell studies and human clinical trials have provided evidence that Se could potentially be an effective preventive agent against cancer (Bera, Rosa, Rachidi, & Diamond, 2013; Rayman, 2005; Valdiglesias et al., 2010; Weekley & Harris, 2013). However, the mechanism(s) by which Se might function as a chemopreventive agent against cancer remains to be fully determined. It is known that Se is required for maintenance of health in humans and animals due to its antioxidant properties, but the optimal form and concentration of supplemented Se that will result in protection of genetic material without inducing toxic effects still remains a subject of debate. Published studies indicate that Se supplementation may exert its benefits by enhancing the DNA damage repair response, but the effects also appear to be dependent on selenoprotein genotypes and concentration of Se in the body/diet (Bera et al., 2013; Valdiglesias et al., 2010).

1.6.1 Mechanisms of Action of Se

It has been evident that Se supplementation leads to the increased expression of selenoproteins. Many selenoproteins are antioxidants (e.g. glutathione peroxidase 1 (GPx-1) and thioredoxin reductase (TrxR)), and are therefore responsible for the detoxification of reactive oxygen species (ROS). As a result, the levels of DNA damage present in cells can be reduced due the action of these selenoproteins on ROS before they are able to induce lesions to the DNA caused by oxidative stress. However, how Se enhances the DNA repair process in damaged cells is poorly understood.

One possibility for Se actions is through the elevation of selenoprotein activity. When DNA is under major oxidative stress conditions, a lesion known as 8-hydroxydeoxyguanine (8-oxoGua) is formed (Roszkowski, Jozwicki, Blaszczyk, Mucha-Malecka, & Siomek, 2011), and accumulation of this oxidative DNA lesion can lead to diseases such as cancer. The DNA glycosylase, 8-oxoguanine (OGG1) enzyme is responsible for the repair of these 8-oxoGua lesions via the base excision repair process (BER) (Bravard et al., 2009). The activity of OGG1 requires that the enzyme remains in a reduced state. Due to the presence of highly sensitive redox residues in OGG1, it is necessary for antioxidants to be present to maintain this enzyme in its reduced and active state (Bera et al., 2013). Therefore, Se may enhance this BER process by increasing the levels of selenoproteins, and as a result, enhance the repair of these oxidative DNA lesions. Another example of selenoproteins enhancing other repair processes was demonstrated in mice that were supplemented with Se. The mice showed increased levels of the selenoprotein GPx-1, which in turn then promoted the expression of the DNA damage repair protein, growth arrest and DNA-damage-inducible 45 (Gadd45) (Zeng, Davis, & Finley, 2003).

1.6.2 *In vivo* Animal Studies

Extensive research investigating the chemopreventive effects of Se supplementation doses in animals has been conducted and shown a reduction in cancer incidence (Combs & Lü, 2006; Combs Jr & Gray, 1998). For example, researchers have shown that supplementation with supranutritional levels (e.g. 5 ppm) of Se in the diet or drinking water reduces tumour size and increases inhibition of tumourigenesis in the mammary tissue of laboratory animals (Ip, 1981; Ip & Ip, 1981; Ip & Sinha, 1981; Medina & Shepherd, 1980; Schrauzer, White, & Schneider, 1976). As promising as such animal studies have been, the levels of Se supplementation that were used are much higher than is required to prevent deficiency in humans, and therefore makes it difficult to extrapolate the data for human use. However, one study investigating the effects of Se supplementation in male beagle dogs (*Canis lupus familiaris*) used a dose that is acceptable for humans (Waters et al., 2003). This study reported that supplementation with either selenomethionine or high-Se yeast resulted in lower levels of DNA damage with increased levels of apoptosis in damaged epithelial cells.

1.6.3 *In vitro* Studies using Mammalian Cell Lines

Studies using cell culture methods have also indicated that Se may function by reducing DNA damage in cells. One such study by Seo, Sweeney and Smith, (2002) used pre-treated human, non-tumourigenic fibroblast cell lines with non-toxic levels of selenomethionine. These cells were exposed to UV-light and the levels of damage to the DNA were assessed. The authors concluded that this pre-treatment with Se reduced the levels of DNA damage present. Similarly, another research group was able to show that DNA repair was enhanced with pre-treatment of human leukocytes with selenomethionine that were subjected to DNA strand breaks by the antibiotic bleomycin (Laffon, Valdiglesias, Pásaro, & Méndez, 2010).

The effects of Se on a range of different cancer cell lines has been investigated. Baliga *et al.,* 2007 showed that supplementation of human breast cancer cells (MCF-7) with sodium selenite resulted in the protection of the cells against UV-induced chromosome damage and a reduction in gene mutations (Baliga, Wang, Zhuo, Schwartz, & Diamond, 2007). In addition, the beneficial effect of Se supplementation was reported by de Rosa et al., (2012). This study investigated the effects of two different Se compounds (sodium selenite and selenomethionine) in human prostate adenocarcinoma cells (LNCaP) when treated with UVA or hydrogen peroxide (H_2O_2). The authors concluded that both Se compounds appeared to show protective capabilities against cell toxicity and genotoxicity and increased DNA repair activity in response to oxidative stress. Through examples such as these, it is evident that both inorganic (e.g. sodium selenite) and organic (e.g. selenomethionine) Se compounds appear to show similar repair and protection properties, despite the different effects they have on biological systems (Gammelgaard, Jackson, & Gabel-Jensen, 2011; Zeng, Jackson, Cheng, & Combs, 2011).

1.6.4 Human Clinical Trials

The use of animal models and *in vitro* mammalian cell culture studies are beneficial to improve our understanding of the mode of action of Se. However, these studies can only provide insight to the actual outcome of supplementation with Se in humans. Therefore, it is necessary for human intervention trials to be undertaken to fully understand the effects and outcomes of Se supplementation.

A New Zealand clinical study of a cohort of 43 men at elevated risk of prostate cancer (with high serum PSA but a negative prostate biopsy) showed an inverse association between Se status and accumulated DNA damage, with these men having serum Se concentrations below the average of 97.8 ng/ml (Karunasinghe et al., 2004).

Kowalska et al., (2005) reported that bleomycin-induced DNA damage was significantly greater in peripheral blood mononuclear cells (PBMC)

from 20 *BRCA1* mutation carriers than in 20 non-carriers (0.58 versus 0.39; $p<10^{-4}$), and that supplementation with selenite, 140 µg daily for 1-3 months could reduce bleomycin-induced DNA damage in PBMC from *BRCA1* mutation carriers down to the level of non-carriers (mean, 0.63 breaks per cell versus 0.40; $p<10^{-10}$). Bleomycin is a chemotherapy drug that induces breakage in the DNA strand. These results suggest the potential for Se to prevent breast cancer in *BRCA1* mutation carriers, a strategy subsequently tested in a randomised placebo-controlled trial in Poland of selenite, 250 µg daily in 1135 *BRCA1* mutation carriers. Unfortunately the incidence of breast cancer was higher in the Se treatment group, with 60 incident cases of cancer diagnosed in comparison to 45 cases diagnosed in the placebo group (hazard ratio 1.4; 95% CI: 0.9 to 2.0) (Lubinski et al., 2011). The authors speculated that this counterintuitive result represented use of an excessive dose of Se. While the plasma levels after supplementation with selenite were not reported in the *BRCA1* trial, it is possible that the 250 µg dose resulted in excessive plasma Se concentrations.

There are, however, other possible causes to explain this observation. Other researchers have reported that the inorganic forms of Se are generally more genotoxic (DNA-damaging) than the organic forms, such as selenomethionine and methylselenocysteine, especially at higher doses (Valdiglesias et al., 2010). Clinical evidence to support this comes from a randomised placebo-controlled trial (SELECT) of selenomethionine, 200 µg daily in 35,000 American men in which no increase (or fall) in incidence of prostate or other cancers was observed (Lippman, Klein, Goodman, & et al., 2009). This cohort had much higher baseline Se plasma levels (approximately two-fold) than the *BRCA1* cohort from Poland. The effects of Se on preventing cancer appear to follow a U-shaped curve, with reductions achieved in those with low baseline Se levels (e.g. <1.65 µM), but an increase in those with higher levels (e.g. >1.65 µM). In general, for human health, plasma levels approximating 130 ng/ml (~1.65 µM) appear to be optimal (Rayman, 2012).

Another possible explanation of the excess incidence of breast cancer seen with Se supplementation in *BRCA1* mutation carriers is that the form of Se used, selenite, is likely to be genotoxic at these doses, unlike organic forms. It is possible that Se supplementation may be effective in reducing the risk of breast cancer in *BRCA1* mutation carriers, but the use of organic Se compounds is likely to be preferable, and the dose-response needs to be determined. One way to investigate this is to use *in vitro* human breast cancer cell lines.

1.7 The Biology of Human Breast Cancer Cell Lines

To date, hundreds of human breast cancer cell lines have been described in the literature. For the purposes of this study, four human female breast cancer cell lines were used to investigate the effects of Se on DNA damage (Elstrodt et al., 2006). The cell lines used were SUM149PT, MDA-MB-436, MDA-MB-231 and MCF-7, respectively (Table 1).

Table 1. The breast cancer cell lines used during this research project. ER^+ = oestrogen receptor positive; $HER2^+$ = human epidermal growth factor receptor 2.

Cell Line	*BRCA1* mutation	ER^+	$HER2^+$	Cancer type	Patient age (y)
SUM149PT	2288delT	-	-	Inflammatory breast cancer	35
MDA-MB-436	5396+1G>A	-	-	Adenocarcinoma	43
MDA-MB-231	-	-	-	Adenocarcinoma	51
MCF-7	-	+	-	Adenocarcinoma	69

1.7.1 SUM149PT

SUM149PT is a *BRCA1*-mutated breast cancer cell line that was derived from a 35 year old patient with inflammatory breast carcinoma in 1993 (Chavez, Garimella, & Lipkowitz, 2010; Elstrodt et al., 2006; Ethier, Mahacek, Gullick, Frank, & Weber, 1993; Forozan et al., 1999). These cells are a ductal epithelial cell line that is adherent when cultured (Asterand, 2014). SUM149PT cells express a truncated *BRCA1* protein due to a non-pathogenic mutation, 2288delT: a deletion of a thymine nucleotide in the coding region of the *BRCA1* mRNA, exon 11 at position 2288. This results in a reading frame shift which leads to an insertion after codon 723 of 12 new aa, which is then followed by a termination codon (Elstrodt et al., 2006).

1.7.2 MDA-MB-436

MDA-MB-436 is also a *BRCA1*-mutated breast cancer cell line that was derived from a 43 year old patient with adenocarcinoma of the breast in 1976 (Brinkley et al., 1980; Chavez et al., 2010; Elstrodt et al., 2006). These cells are pleomorphic and adherent when cultured (ATCC, 2014c; Cailleau, Olivé, & Cruciger, 1978). The identified 5396+1G>A *BRCA1* mutation, which refers to a substitution of a guanine nucleotide for an adenine nucleotide one nucleotide after position 5396 (at the splice donor site of exon 20), is pathogenic. This mutation can result in two alternative transcripts: 1) exon 20 is skipped, resulting in an in-frame deletion of 28 amino acids, and 2) an insertion of 7 codons (of intron sequence) followed by a termination codon as a result of splicing at a cryptic splice site in intron 20 (Elstrodt et al., 2006). Therefore, both transcripts result in a truncated protein.

1.7.3 MDA-MB-231

MDA-MB-231 is a breast cancer cell line that, similar to SUM149PT and MDA-MB-436, is classed as triple-negative but, in comparison to them, does not have a mutation in the *BRCA1* gene (Chavez et al., 2010). These are adherent epithelial cells that were obtained from a 51 year old patient with adenocarcinoma of the mammary gland in 1973 (ATCC, 2014b; Brinkley et al., 1980).

1.7.4 MCF-7

MCF-7 is one of the most commonly used breast cancer cell lines and was developed in 1973 at the Michigan Cancer Foundation (Soule, Vazquez, Long, Albert, & Brennan, 1973). The reason these cells are so commonly used is because they are oestrogen receptor positive (ER^+), which makes then a great tool for studying responses to hormone treatments (Levenson & Jordan, 1997). These cells are adherent epithelial cells that were obtained from a 69 year old patient with adenocarcinoma of the breast (ATCC, 2014a).

1.8 Research Aims

We hypothesise that the chemical form and dose of Se supplementation is important in optimising a chemoprotective agent against breast cancer. The aim of this research thesis is to investigate the toxicity of inorganic and organic Se compounds at various concentrations *in vitro* on human *BRCA1*-mutated cancer cells as well as non-*BRCA1*-mutated cancer cells. While this *in vitro* project is evaluating Se effects in cancer cells as opposed to *BRCA1*-mutated non-malignant cells (which are not available as cell lines for *in vitro* use), this will provide preliminary data on DNA damage modification with differing Se concentrations and compounds and may suggest appropriate dosing guidelines when further studies are performed in *BRCA1* carriers.

1.9 Research Objectives

The objectives of this research thesis are to evaluate the dose-response of lethality of sodium selenite and MSA in *BRCA1*-mutated cancer cell lines *in vitro* using the MTT assay, and to evaluate the dose-response of those two Se compounds on native and bleomycin-induced DNA damage as assessed by the comet assay.

Chapter Two

Methodology and Materials

All cell culture work was carried out in the E.3.13 Physical Containment Level 2 (PC2) mammalian cell facility at the University of Waikato, Hamilton, New Zealand. All other work was carried out in the C.2.03 Molecular Biology Laboratory at the University of Waikato. Solutions were prepared using autoclaved 15-18 megohm-cm double distilled deionised water (mQ H_2O) (Barnstead double distilled/deionisation system). All plastic ware used was sterile and all glassware was washed in the dishwasher and autoclaved before use. All experiments were carried out using aseptic techniques on bench top surfaces cleaned with 70% ethanol. Recipes for all solutions can be found in Appendix 1.

2.1 Mammalian Cell Culture

Cell culture is the artificial growth of cells isolated from an animal or plant in a favourable environment. The cells used during this study are human commercial cell lines (see 1.8 for more information) sourced from the Auckland Cancer Society Research Centre, University of Auckland cell line inventory, from Euphemia Leung. They were cultured in T25/T75 culture flasks (Guangzhou Jet Bio-Filtration) that contained a substrate/growth medium which supplied the cells with essential nutrients, growth factors and hormones. The flasks were stored in a humidified incubator set to 37°C with 5% CO_2.

SUM149PT cell lines were cultured with a growth media consisting of Ham's F-12 Medium, 5% fetal bovine serum (FBS), 10 mM HEPES, 5 µg/ml insulin, 1 µg/ml hydrocortisone, and 1X Penicillin-Streptomycin (pen/strep). MDA-MB-436 cell lines were cultured with a growth media

consisting of minimal essential medium (MEM), 10% FBS, 10 µg/ml insulin, and 1X pen/strep.

2.1.1 Thawing/Reviving Frozen Cells

Frozen cells were stored at -80°C in cryotubes in the freezer in the C.2.10 Proteins laboratory. Before thawing/reviving a cryotube of cells, they needed to be removed from the -80°C and transferred to a polystyrene box containing ice, and transported to a designated cell culture laboratory. The frozen cells were then thawed by spraying the cryotube with 70% ethanol and swirling it in a 37°C water bath for no longer than one minute. After this, the cryotube of thawed cells was wiped down, sprayed with 70% ethanol again, and transferred to a cell culture hood where the remainder of the work was carried out. Using a sterile transfer pipette, 500 µl of the appropriate pre-warmed (to 37°C) growth media was added drop wise to the thawed cells and mixed gently by pipetting up and down. All liquid from the cryotube was then added drop wise to 2.5 ml of pre-warmed growth media in a 15 ml Falcon tube and gently mixed. Cells were pelleted by centrifuging the tube at 200 g for 5 minutes at room temperature (RT) in a Heraeus Megafuge 1.0 centrifuge. The supernatant was then discarded, and the cell pellet was resuspended in 3 ml of pre-warmed growth media and transferred to a T25 cell culture flask. The thawed cells were visualised under the inverted microscope (Nikon Eclipse TS100) to determine the level of confluence and then transferred to 37°C incubator with 5% CO_2.

2.1.2 Maintaining and Subculturing Cells

Cell growth media was replaced every 2-3 days by carefully removing old media without disturbing the cell monolayer, and replacing it with pre-warmed media (3 ml for T25 flasks and 10 ml for T75 flasks). Cell growth was monitored by viewing the cells on an inverted microscope (Nikon Eclipse TS100). Cells need to be subcultured (passaged) when they reach

90-95% confluency. To subculture, the cells were harvested by removing the growth media from the flask, cells were washed with 1X phosphate buffered saline (PBS) solution (pH 7.4), trypsin was added (2 ml for T25 and 4 ml for T75 flasks), and the flasks were left to incubate for 3-10 minutes. After all cells became unattached from the bottom of the flask, growth media was added to dilute the trypsin (4 ml for T25 and 5ml for T75 flasks), and all the contents of the flasks was transferred to a 15 ml Falcon tube. Cells were then pelleted by centrifuging the tube at 200 g for 5 minutes at RT, the supernatant removed, and the pellet resuspended in the appropriate volume of growth media to passage the cells at a 1:2 ratio.

2.1.3 Measurement of Cell Concentration

The cell concentration was measured using a haemocytometer. A haemocytometer is a microscope chamber slide that has a 3 mm x 3 mm square etched onto the surface of each chamber (2 chambers/slide) of the slide. Each square is divided into nine 'large' 1 mm x 1 mm squares. When counting cells, a cover slip (22 mm x 22 mm) is placed on the central area of the haemocytometer. The area between the cover slip and slide is 0.1 mm, therefore making the volume above each 'large' square 0.1 mm^3 (1 mm x 1 mm x 0.1 mm). Consequently, to calculate the number of cells/ml in solution, the cell count needs to be multiplied by 10,000. When counting cells, one 'large' square is one count, and the more squares counted, the more accurate the calculation. A general rule when counting cells is to count cells that are touching the top and left limits, and ignoring cells touching the bottom and right limits.

To count the number of cells in solution, a concentration range of 250,000 - 2.5 million cells/ml is ideal for a good estimation of cell concentration. If the original solution was not within this range, it was diluted with 1X PBS to obtain an appropriate concentration. The dilution factor will then need to be incorporated into the final cell concentration calculation. After a suitable dilution of the cells (if necessary) had been made, they were then stained with 0.4% Trypan Blue (Sigma Life Science) in a 1:1 ratio (50 µl cell

suspension to 50 µl Trypan Blue). Trypan Blue was used to determine cell viability as it is able to permeate the cell if membrane integrity has been lost, resulting in a stained dark blue cytoplasm. These dark blue cells are considered to be dead and therefore not viable. The Trypan Blue/cell solution was then added to the haemocytometer with a cover slip placed on top by pipetting 10 µl of the solution gently at the edge of the cover slip and allowing it to enter the chamber by capillary action. This step was repeated for both chambers of the slide. The cells were then visualised by placing the haemocytometer on the microscope. The four 'large' squares in the outer corners of each chamber were counted, giving a total of eight counts which were averaged to calculate the cell concentration. To calculate the concentration of cells, the following equation was used:

$$average\ cell\ count\ \times\ 2\ (Trypan\ Blue\ d.f)\times\ 10{,}000\ \left(\frac{volume}{square}\right)\ =\ cell/ml$$

Equation 1. Number of cells per 1 ml.

The total number of cells in solution was then calculated by:

$$cell/ml\ \times\ volume\ of\ original\ solution\ =\ total\ cells$$

Equation 2. Total number of cells in solution.

2.1.4 Freezing Cells for Storage

When there was a surplus of cells during subculturing, the remainder were frozen down with a protective agent, dimethyl sulfoxide (DMSO), and stored at -80°C. To freeze down cells, the cells were harvested (see 2.1.2), counted (see 2.1.3), and the cell pellet was resuspended in an appropriate volume of freezing media (total media with 5% DMSO) to freeze them at a concentration of 1.6 x 10^6 - 2.2 x 10^6 cells/ml. The cells were then aliquoted in cryotubes with a final volume of 1 ml into each tube, and the cells were stored in the -80°C freezer. When cells are first transferred to the freezer, they are stored in a Mr Froster™ freezing container which controls the freezing rate of the cells to 1°C/min at -80°C.

The cells can be transferred to a -80°C freezer box after being stored in Mr Froster™ for at least 4 hours.

2.2 DNA Extraction

Two of the cell lines used in this research had known *BRCA1* mutations. For validity, it was required that these mutations were identified in the cells received. In order to test for the mutations, DNA was extracted from the cells for further downstream testing of the mutation. The initial step before the DNA could be extracted was to pellet a flask of cells (preferably two passages after reviving). To do this, the cells were harvested (see 2.1.2) and, once pelleted, the supernatant was removed. The pellet was then resuspended in 200 µl digestion buffer containing freshly thawed proteinase K, transferred to a new tube (2 ml), and allowed to digest overnight at 65°C in a 600 rpm shaking thermomixer (Eppendorf). The sample was allowed to cool to RT, followed by vigorous vortexing for 20 seconds, and then an equal volume of chloroform was added to remove protein. Vortexing was repeated and then the sample was mixed using a rotating wheel for 5 minutes at RT. Following this, it was centrifuged for 5 minutes at RT at 10,000 g, and the top layer (~200 µl) was transferred to a new 1.7ml Eppendorf tube. The DNA was then precipitated with two volumes of ice-cold absolute ethanol (100%) and 1/10 volume of 3M Sodium Acetate (NaOAc) (pH 5.2), and incubated in the -20°C freezer for at least an hour. After the incubation period, the sample was centrifuged at maximum speed (>16,000 g) for 20 minutes at 4°C. The supernatant was then carefully removed without disturbing the pellet, washed by adding 1 ml of 70% ethanol and inverting it several times, followed by centrifugation it at maximum speed (>16,000 g) for 15 minutes at 4°C. After centrifugation, the supernatant was removed and the pellet was allowed to air dry at RT for 5 minutes. Finally, the DNA was resuspended in 100 µl 10 mM Tris-Cl (pH 8.0), the concentration was measured using the NanoDrop™ 8000 Spectrophotometer (NanoDrop), and the DNA was stored at -20°C.

2.3 NanoDrop

The NanoDrop™ 8000 Spectrophotometer is able to measure the nucleotide concentration and purity of a sample by comparing a purified product resuspended in a known solution to a blank (the known solution). The concentration of nucleic acids is determined by the absorbance reading at 260 nm, the purity of the sample by the 260/280 nm ratio, and any contaminants present by the 260/230 nm ratio. Initially the NanoDrop is blanked by adding 2 µl of the known solution, and then the samples were measured after that. DNA samples that had a 260/280 nm ratio outside of the range 1.8-2.0, and a 260/230 nm ratio outside of the range 2.0-2.2 were classified as impure/low quality and required purification.

2.4 PCR

Polymerase chain reaction (PCR) is a method used to amplify desired DNA regions. The DNA extracted from the cell lines (protocol 2.2) was used to identify the expected *BRCA1* mutation in the cells, and to test for *Mycoplasma* contamination within the cell cultures. All PCR reactions were carried out in a BIORAD T100™ Thermal Cycler, using single 200 µl PCR tubes (Axygen). While setting up a PCR reaction, all solutions were kept on ice. Preparation and aliquoting of master mixes into individual PCR tubes was carried out in a dedicated PCR UV hood. The primers and template DNA were then added on dedicated PCR benches that were wiped down with 70% ethanol before use. All PCR sample preparation used dedicated PCR pipettes with sterile DNase and RNase-free filtered pipette tips.

The working PCR reaction mix can be seen in Table 2. All PCR reactions were tested with a negative control (no template) to ensure the reaction components were not contaminated, and a positive control using a primer set that is known to work to confirm that the cell DNA extracted was of a high quality.

Table 2. PCR reaction set up showing concentration and volumes required for each PCR tube

Component	Working conc.	Final conc.	Volume
HOT FIREPol® DNA Polymerase (Solis BioDyne)	5U/µl	0.05 U/µl	0.2 µl
Buffer B2 (Solis BioDyne)	10X	1X	2 µl
$MgCl_2$	25 mM	1.9 µM	1.5 µl
dNTP	10 mM	200 µM	0.4 µl
Forward primer	10 µM	0.25 µM	0.5 µl
Reverse primer	10 µM	0.25 µM	0.5 µl
DNA template	50-500 ng/µl	5-100 ng/µl	1-2 µl
PCR grade H_2O			Make up to 20 µl

All PCR reactions were run with the cycling conditions outlined in Table 3 unless otherwise stated. The reactions were stored at 4°C until gel electrophoresis.

Table 3. PCR machine settings showing the temperatures and times required for each cycle.

Cycle step	Temp.	Time	Cycles
Initial denaturation	95°C	15 min	1
Denaturation	95°C	20 sec	34
Annealing	61°C	20 sec	
Elongation	72°C	60 sec	
Final elongation	72°C	12 min	1

2.4.1 Primer Design

Primers for the two *BRCA1*-mutated cell lines (SUM149PT and MDA-MB-436) were designed using Geneious® R7 software (Biomatters) to confirm their deleterious mutation. The complete 5711 bp coding *BRCA1* mRNA sequence (Genbank U14680.1) was used to identify the region where the mutations were found (Elstrodt et al., 2006). The desired region of the *BRCA1* gene containing the mutation was then selected using the Geneious software, and multiple primer pairs were suggested, and the best one was ordered from Integrated DNA Technologies, Inc, USA (IDT). The lyophilised primers were resuspended in TE Buffer (pH8.0) to a final concentration of 100 µM and stored at -20°C. The primers used to target the two mutations in the *BRCA1* gene can be seen in Table 4.

Table 4. Primer sequences used throughout this thesis. The naming of these primers is according to KM (Kirsty Mayall) or HCC (Hannah Crossan), in the order they were ordered, and the strand in which they bind, either forward (F), reverse complement (R), or internal reverse (IR).

Primer name	Sequence (5'-3')	Cell line	Target mutation	IDT melting temperature (°C)	Annealing temperature (°C)	Product length (bp)
KM2F	ACATGACAGCGATACTTTCCC	SUM149PT	2288delT	54.8	61	250
KM2R	ACCAGGTACCAATGAAATACTGC	SUM149PT	2288delT	55.1	61	250
KM4F	TGGTTGGGATGGAAGAGTGA	MDA-MB-436	5396+1G>A	55.8	61	400
KM4R	GATCTGCCTGCCTCAGTCTC	MDA-MB-436	5396+1G>A	57.4	61	400
KM5R	GATCTGCCTGCCTCAGTCTC	MDA-MB-436	5396+1G>A	53.6	-	400
HCC37F	CAAGAAGGTGGTGAAGCAGG	-	-		60	516
HCC38R	GATGGTACATGACAAGGTGC	-	-		60	516

2.4.2 Agarose Gel Electrophoresis

Owl agarose gel electrophoresis systems were used to visualise the resulting PCR products for identification and quantification purposes. A room dedicated to agarose gel electrophoresis was always used for post-PCR analysis, and all gels were prepared using 1X TAE buffer and RedSafe™ dye (Intron Biotechnology, USA). The amount of agarose used to make the gel was dependant on the amplicon size being electrophoresed. As the expected product size of the PCR products being tested was 250-516 base pairs (bp) in length, a 1.5% agarose TAE gel was used. For a single gel cast, 35 ml of 1X TAE buffer was added to 0.525 g dry HyAgarose™ LE Agarose (Hydragene, USA), and heated on medium heat in a 650 watt microwave (stirring intermittently) until all crystals had been dissolved. Once fully dissolved, the liquid gel was cooled to approximately 50°C and 2 µl of RedSafe™ dye was added, mixed, and then poured into a level gel caster. Any bubbles were removed (pushed to the edge) and two combs were placed into the liquid gel before it was allowed to set at RT. Once set, the gel caster was positioned into an electrophoresis tank and filled with enough 1X TAE buffer to cover the gel. Ten microlitres of PCR product was mixed with 2 µl of 6X loading dye and then loaded onto the agarose gel. The loaded samples were run alongside a 100 bp ladder (500 ng, GenScript) with known DNA band lengths and concentrations for comparison purposes. After all samples were loaded, the gel was electrophoresed for 30 minutes at 90 volts (V) at RT, and then visualised using a Safe Imager (Invitrogen), and photographed using a COHU High Performance CCD camera and Scion Image software.

2.4.3 PCR Product Purification

PCR products containing the desired product were required to be purified before being able to be sequenced. This was necessary to remove the dNTPS and primers. The Zymo Research DNA Clean and Concentrate™ kit was used according to the manufacturer to purify the remaining PCR product, and the resulting product was quantified using the NanoDrop.

Briefly, five volumes of DNA binding buffer was added to each volume of DNA sample and this mixture was then added to a Zymo-Spin™ column in a collection tube and centrifuged at full speed (≥10,000 g) for 30 seconds. The flow through was discarded and the DNA was washed twice by adding 200 µl of DNA wash buffer to the column and centrifuging it for 30 seconds. Finally, the Zymo-Spin™ column was transferred to a new 1.5 ml tube, 30 µl of DNA elution buffer was added directly to the column matrix, and the tube was centrifuged for 30 seconds to elute the DNA.

2.4.4 DNA Sequencing

Purified PCR products were sent to the University of Waikato DNA Sequencing Facility (Hamilton, New Zealand) to be sequenced using an Applied Biosystems 3130xl Genetic Sequence Analyser. Table 4 shows the appropriate primers used to sequence the two amplified purified PCR products, KM2F/KM2R and KM4F/KM4R, including the internal reverse primer, KM5R, for the cell lines SUM149PT and MDA-MB-436. The resulting DNA sequences were analysed using the Geneious software.

2.4.5 *Mycoplasma* Contamination PCR

New cell lines, as well as cell lines in continuous culture, should be tested at regular intervals for *Mycoplasma* contamination. *Mycoplasma* is a bacteria that can contaminate cell cultures very easily. This contaminant can often go undetected for many years, but its presence can affect research results and cell culture products, which makes it a major issue when carrying out biological and medical research using cell cultures (Uphoff & Drexler, 1999; Uphoff & Drexler, 2011).

Currently, the mammalian cell facility uses regular inspection of cell morphology under the inverted microscope, evidence of cloudy media, and DAPI staining of cells to monitor for contamination. To improve sensitivity to *Mycoplasma* contamination in cell cultures, a molecular protocol was developed. The protocol was adapted according to procedures published

by Cord C. Uphoff and Hans G. Drexler (Uphoff & Drexler, 2011). This protocol is able to detect many different species of *Mycoplasma* with high sensitivity and specificity by targeting the 16S ribosomal DNA (rDNA) region (Uphoff & Drexler, 1999). When carrying out this diagnostic PCR reaction, an internal control DNA sample is included. An internal control was obtained from Leibniz Institute DSMZ (Deutsche Sammlung von Mikroorganismen und Zellkulturen GmbH) in Germany. The lyophilised internal control DNA sample was resuspended in 100 uL sterile mQ H_2O and diluted 1:10 according the DSMZ guidelines. The internal control DNA is a 3995 bp plasmid that contains a (516 bp) DNA fragment derived from the *Mycoplasma* strain, *Acholeplasma laidlawii*. This fragment is disrupted by the insertion of a 476 bp Taq I fragment from pUC-19 plasmid DNA (Appendix 2). Due to this disruption, the internal control product will appear as a different sized band (1 kb) on the agarose gel to the amplified *Mycoplasma* positive sample (502-520 bp) (C. Uphoff & Drexler, 1999). This will demonstrate that the primers are working efficiently and therefore the internal control DNA sample is incorporated into the PCR reaction mix for every sample reaction. The internal control is added at a limiting dilution to the PCR reaction mixture (resuspension volume and dilution of sample according to DSMZ recommendations), and the sensitivity of the PCR reaction will therefore be shown (Uphoff & Drexler, 2011).

For every PCR reaction, a *Mycoplasma* positive sample is included to show that the reaction conditions were effective, and determine that any samples run alongside the positive control were not contaminated. As a precaution, a negative/water control is also run. This control contains no template DNA (only water) to ensure that the reaction mixture is not contaminated.

The cells used for the purpose of this thesis were transferred from the University of Auckland with a Ministry for Primary Industries (MPI) transfer permit (759). Information received from the University about the cells did not include a status for *Mycoplasma* contamination. Therefore, testing of the cell lines for the reliability of results was necessary.

Table 5 shows the six primers published in the Uphoff and Drexler (1999) protocol for the diagnostic PCR reaction (four forward and two reverse). All six primers were combined into a 5 µM working primer mix stock solution, with the primers containing accessory symbols (e.g. w or r) having molarities reduced by 50%, and needing to be modified accordingly. As a result, 20 µl of LMP13, LMP14, LMP15 and LMP17, and 10 µl of LMP16 and LMP18 was added to 100 µl sterile mQ H_2O to make a 200 µl primer mix stock at a final concentration of 5 µM. All primers were stored at -20°C.

Table 5. Primer sequences used to test for *Mycoplasma* contamination in cell cultures. Source of all primer sequences is from Uphoff & Drexler, 2011. Naming is according to LMP (Linda Marie Peters) in the order that they were ordered. R = A or G; W = A or T.

Primer name	Sequence (5'-3')	Direction	Species and gene target	IDT melting temperature	Product length
LMP13	CGCCTGAGTAGTACGTWCGC	Forward	*A. laidlawii* (internal control) 16S ribosomal RNA	57.6°C	986
LMP14	TGCCTGRGTAGTACATTCGC	Forward	*Mycoplasma* 16S ribosomal RNA	55.8°C	502-520
LMP15	CRCCRGAGTAGTATGCTCGC	Forward	*Mycoplasma* 16S ribosomal RNA	56.4°C	502-520
LMP16	CGCCTGGGTAGTACATTCGC	Forward	*Mycoplasma* 16S ribosomal RNA	58.1°C	502-520
LMP17	GCGGTGTGTACAARACCCGA	Reverse	*Mycoplasma* 16S ribosomal RNA	58.9°C	502-520
LMP18	GCGGTGTGTACAAACCCCGA	Reverse	*A. laidlawii* (internal control) 16S ribosomal RNA	60.3°C	986

Mycoplasma positive control (1 X 10^6 cells/ml of heat inactivated cell lysate of a NIH 3T3 mouse embryo fibroblast cell line contaminated with *Mycoplasma*) was obtained from Crown Research Institute AgResearch, Hamilton, New Zealand. The 50 µl *Mycoplasma* positive cell sample was run through Quick-gDNA™ MiniPrep DNA extraction kit (Zymo Research) as instructed by the manufacturer to obtain *Mycoplasma* DNA in a final elution volume of 25 µl. The extracted gDNA was stored at -20°C.

A commercial 2X PCR Master Mix Solution (i-Taq™) (Intron) was used in order to reduce the preparation time for the diagnostic test. This solution contains 2.5 U i-Taq™ DNA Polymerase (5 U/µl), 2.5 mM of each dNTP, 1X PCR reaction buffer and 1X gel loading buffer. Two different PCR reaction mixes of 25 µl were made: one mix containing the sample DNA (Table 6) and the other mix containing the sample DNA as well as the internal control DNA (Table 7). When testing a DNA sample from a cell line, six individual PCR reactions were required: 1) sample DNA; 2) sample DNA + internal control; 3) *Mycoplasma* positive control 4) *Mycoplasma* positive control + internal control; 5) internal control only; and 6) water control (no template).

Table 6. PCR reaction components for reactions containing sample DNA only (cell culture DNA/positive control sample DNA/negative control).

Reagent	Final concentration	Volume per reaction
2X PCR Master Mix (Intron)	1X	12.5 µl
5 uM Primer mix (LMP13-18)	0.2 µM	1 µl
Test DNA	5-100 ng/µl	1 µl
H_2O		10.5 µl
Total		25 µl

Table 7. PCR reaction components for reactions containing sample + internal control DNA.

Reagent	Final concentration	Volume per reaction
2X PCR Master Mix (Intron)	1X	12.5 µl
5 µM Primer mix (LMP13-18)	0.2 µM	1 µl
Internal DNA	-	1 µl
Test DNA	5-100 ng/µl	1 µl
H_2O		9.5 µl
Total		25 µl

The specific PCR conditions optimised are outlined in Table 8.

Table 8. PCR machine settings showing the temperatures and times required for each cycle.

Cycle step	Temp.	Time	Cycles
Initial denaturation	94°C	2 min	1
Denaturation	94°C	20 sec	35
Annealing	63°C	20 sec	
Elongation	72°C	60 sec	
Final elongation	72°C	5 min	1

Following PCR, a 10 µl volume of PCR products were run on a 1.3% TAE agarose gel with RedSafe™ stain (protocol 2.4.2).

2.5 Selenium Compounds

The Se compounds used during this study were made up to a final concentration of elemental Se within the compound. The proportion of Se within the compound was calculated based on the molecular weight of Se (78.96). The Se compounds stocks were made up in 1X PBS to a concentration of 1M elemental Se. Diluted stocks of 100 mM, 10 mM, 1 mM, and 100 µM were then made up using 1X PBS and stored at -20°C.

2.6 MTT Assay

The tetrazolium salt, MTT (3-(4,5-dimethylthiazol-2-yl)-2,5-diphenyl tetrazolium bromide), is used in a colourimetric assay that was first developed in 1983 and measures cell viability (Mosmann, 1983). The pale yellow MTT is converted by active enzymes found in mitochondria, into blue formazan crystals, which can then be read on a scanning multiwell microplate spectrophotometer. As mitochondria activity is generally considered constant for viable cells, the MTT assay can therefore be used to determine the cytotoxic effects of drugs at various concentrations in a quick and reliable way.

In this study, the MTT assay was used to determine the cytotoxicity of sodium selenite and MSA in *BRCA1*-mutated cell lines. The two Se compounds were tested in the concentration range of 0-1000 µM, with triplicates of each concentration per experiment and three independent experiments conducted for each compound on each cell line. The protocol used in this thesis was based on a publication by Meerloo, Kaspers, and Cloos, (2011) in conjunction with the protocol outlined in the MTT Cell Proliferation Assay Kit (Intron Biotechnology) used. The top and bottom row of the 96-well, clear, flat-bottom culture plate (Guangzhou Jet Bio-Filtration) was filled with 100 µl 1X PBS to minimise evaporation throughout the experiment. Designated wells on either side of the plate were used for controls: 'blanks' containing growth media/PBS solutions,

growth controls containing growth media and cells, and solvent controls containing growth media/PBS solutions and cells.

2.6.1 Initial Set Up of Cells, Growth Media and Selenium

Cells were harvested (protocol 2.1.2), counted (protocol 2.1.3) and resuspended in an appropriate volume of growth media to prepare a cell concentration on 2.5 x 10^5 cells/ml. Using flat-bottomed 96-well microplates, 200 µl of cells was added to each well (excluding the designated 'blank' wells in which 200 µl of growth media alone was added) (Figure 10), and incubated overnight for the MDA-MB-436 cell line, or for 72 hrs for the SUM149PT cell line, at 37°C with 5% CO_2 to allow the cells to adhere and grow. Following this incubation, the Se compound dilutions in growth media (Table 9-12) were made freshly and the growth media was replaced with the Se/growth media solutions according to Figure 10 and incubated for 24 hrs at 37°C with 5% CO_2. The 'blank' and solvent control wells were replaced with 190 µl growth media plus 10 µl 1X PBS, and the growth control wells were replaced with growth media.

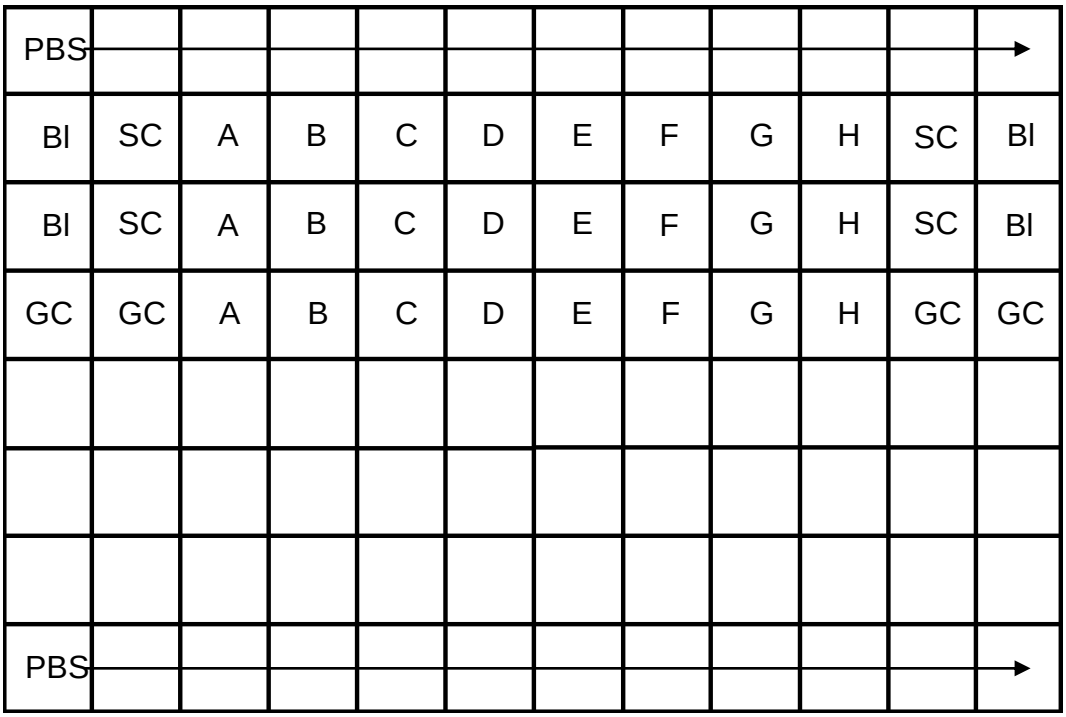

Figure 10. Schematic diagram of a 96-well plate setting for an MTT assay. A separate plate was used for each experiment and each treatment to ensure no fumes produced from one treatment could affect another. PBS was placed in the wells of the top and bottom row to minimise evaporation. Bl= blank; GC = growth control; SC = solvent control; A = 1 µM; B = 5 µM; C = 10 µM; D = 50 µM; E = 100 µM; F = 250 µM; G = 500 µM; H = 1000 µM.

Table 9. Preparation of growth media/Se solutions for a single well of 200 µl for establishing an MTT assay analysis of the SUM149PT cell line.

	Final Selenium Concentration (µM)								
Reagents	**0**	**1**	**5**	**10**	**50**	**100**	**250**	**500**	**1000**
	200 µl Volume per single well (µl)								
FBS	10	10	10	10	10	10	10	10	10
HEPES	2	2	2	2	2	2	2	2	2
Insulin	1	1	1	1	1	1	1	1	1
HC	0.2	0.2	0.2	0.2	0.2	0.2	0.2	0.2	0.2
Pen/Strep	2	2	2	2	2	2	2	2	2
Se - 100 µM	-	2	10	-	-	-	-	-	-
Se - 1 mM	-	-	-	2	10	20	-	-	-
Se - 10 mM	-	-	-	-	-	-	5	10	20
F-12 Ham	184.8	182.8	174.8	182.8	174.8	164.8	179.8	174.8	164.8
Total (µl)	200	200	200	200	200	200	200	200	200

Table 10. Preparation of growth media/Se stock solutions for each treatment run in triplicate to give a total volume of 700 µl (200 µl x 3.5) for the SUM149PT cell line.

	Final Selenium Concentration (µM)								
Reagents	**0**	**1**	**5**	**10**	**50**	**100**	**250**	**500**	**1000**
	Volume in triplicate master mix (µl)								
FBS	35	35	35	35	35	35	35	35	35
HEPES	7	7	7	7	7	7	7	7	7
Insulin	3.5	3.5	3.5	3.5	3.5	3.5	3.5	3.5	3.5
HC	0.7	0.7	0.7	0.7	0.7	0.7	0.7	0.7	0.7
Pen/Strep	7	7	7	7	7	7	7	7	7
Se - 100 µM	-	7	35	-	-	-	-	-	-
Se - 1 mM	-	-	-	7	35	70	-	-	-
Se - 10 mM	-	-	-	-	-	-	17.5	35	70
F-12 Ham	646.8	639.8	611.8	639.8	611.8	576.8	629.3	611.8	576.8
Total (µl)	700	700	700	700	700	700	700	700	700

Table 11. Preparation of growth media/Se solutions for a single well of 200 µl for establishing an MTT assay analysis of the MDA-MB-436 cell line.

	Final Selenium Concentration (µM)								
Reagents	**0**	**1**	**5**	**10**	**50**	**100**	**250**	**500**	**1000**
	200 µl Volume per single well (µl)								
FBS	20	20	20	20	20	20	20	20	20
Insulin	2	2	2	2	2	2	2	2	2
Pen/Strep	2	2	2	2	2	2	2	2	2
Se - 100 µM	-	2	10	-	-	-	-	-	-
Se - 1 mM	-	-	-	2	10	20	-	-	-
Se - 10 mM	-	-	-	-	-	-	5	10	20
F-12 Ham	176	166	174	166	156	171	166	156	174
Total (µl)	200	200	200	200	200	200	200	200	200

Table 12. Preparation of growth media/Se stock solutions for each treatment run in triplicate to give a total volume of 700 µl (200 µl x 3.5) for the MDA-MB-436 cell line.

	Final Selenium Concentration (µM)								
Reagents	**0**	**1**	**5**	**10**	**50**	**100**	**250**	**500**	**1000**
	Volume in triplicate master mix (µl)								
FBS	70	70	70	70	70	70	70	70	70
Insulin	7	7	7	7	7	7	7	7	7
Pen/Strep	7	7	7	7	7	7	7	7	7
Se - 100 µM	-	7	35	-	-	-	-	-	-
Se - 1 mM	-	-	-	7	35	70	-	-	-
Se - 10 mM	-	-	-	-	-	-	17.5	35	70
F-12 Ham	609	581	609	581	546	598.5	581	546	609
Total (µl)	700	700	700	700	700	700	700	700	700

2.6.2 MTT Assay Protocol

To perform the MTT Cell Proliferation Assay, the instructions were followed according to the manufacturer (Intron Biotechnology). Following the 24 hr incubation period with the Se compounds, all solutions were removed from the wells and replaced with 200 µl fresh growth media, and then 10 µl of MTT (5 mg/ml) was added to each well and left to incubate for 4 hrs at 37°C with 5% CO_2. The media/MTT was then removed carefully, ensuring that the cells were not disturbed, and 100 µl of the provided solubilisation solution was added. The 96-well microplate was then placed onto an IKA® MS1 Minishaker plate shaker for 5 minutes, and then incubated for up to 1 hr at 37°C (or until the solubilising solution has dissolved all the formazan crystals). Once all the formazan crystals were dissolved, the absorbance was measured at 570 nm, with a background reference reading at 655 nm, on a Bio-Rad Microplate reader (Model 680).

2.6.3 MTT Assay Data Analysis

For each well, the background reference measurement (655 nm) was subtracted from the 570 nm absorbance reading, and then the mean optical density (OD) values for every test concentration and control was calculated. The sample and solvent control (SC) means were then corrected by subtracting the mean OD of the blanks from the mean OD of the samples/SC. The relative inhibition activity of the Se compounds was then calculated as a percent of SC using the equation:

$$\%\ inhibition\ =\ 100 - \left(corrected\ mean\ OD\ sample\ \times \frac{100}{corrected} mean\ OD\ SC\right)$$

Equation 3. Relative inhibitory rate expressed as percent of solvent control.

The concentration of Se that inhibited growth to 50% of the actively growing cells (IC_{50}) was then determined graphically using Microsoft Excel 2007. Data (mean ± sd) were considered to be statistically significant when the two-tailed *p*-value was <0.05.

2.7 Comet Assay

The single cell gel electrophoresis (SCGE) assay, or comet assay, which was first described in 1984 by (Ostling & Johanson), is a method used to assess DNA damage in cells. It was given the name 'comet assay' as the resulting product of the protocol appears with a 'head' of intact DNA, and a 'tail' of damaged DNA. A few years after the initial description of the SCGE assay by Ostling and Johanson, the protocol was adapted to include an alkaline step (Singh, McCoy, Tice, & Schneider, 1988). The alkaline SCGE became the most commonly used variant of the comet assay, and is the protocol used in this thesis. The recipes for all stock solutions used were taken from Tice and Vasquez's protocol (1998) and can be found in Appendix 1.

2.7.1 Preparation of Drug Exposure Assays

In this study, the alkaline comet assay was used to measure the levels of DNA damage in *BRCA1*-mutated cell lines when treated with each of the two Se compounds. The initial steps for plating and treating the cells with Se can be found in MTT assay initial set up (2.6.1). However, a flat-bottomed 24-well culture plate (Guangzhou Jet Bio-Filtration) was used instead of a 96-well plate. Therefore, 1 ml of cells was added to each well (Figure 11), as opposed to the 200 µl added for the MTT assay, and the recipe calculations were based on Table 9 and Table 11 for SUM149PT and MDA-MB-436, respectively.

All solutions required for the comet assay were incubated in the cold room (4°C) a day prior to being used to ensure all solutions were chilled before use.

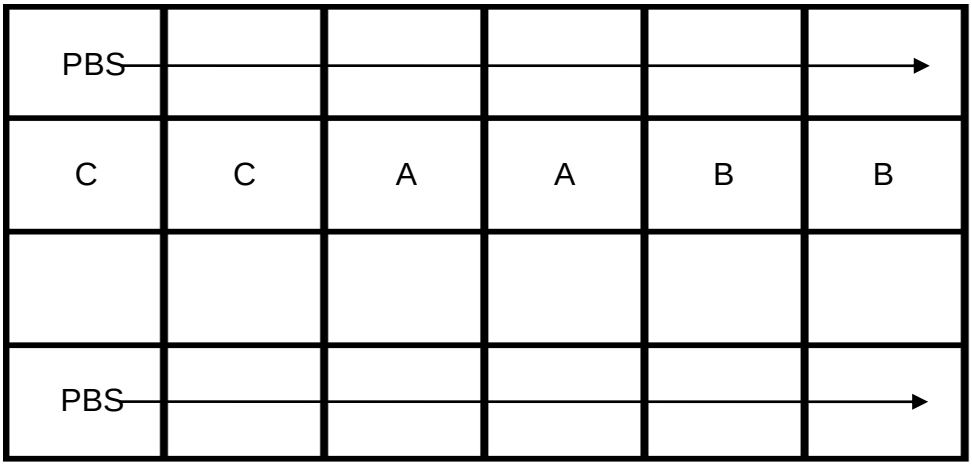

Figure 11. 24-well plate setting for a comet assay. A separate plate was used for each experiment and each treatment to ensure no fumes produced from one treatment could affect another. PBS was placed in the wells of the top and bottom row to minimise evaporation. C = control (no Se); A = Se concentration 1; B = Se concentration 2.

2.7.2 Microscope Slide Preparation

The day before the comet assay was carried out, two 26 x 76 mm microscope slides (Fronine) per well were pre-coated with agarose. Each slide was labelled with a diamond pen and wiped with 70% ethanol using Kimwipes. The slides were then dipped into 1% normal melting point agarose (NMPA) (60°C) (to cover the lower two thirds of the slide). The underside was wiped clean, and left lying flat in a level microscope slide humidity incubation container to set at RT.

2.7.3 Comet Assay Protocol

After the 24 hr incubation period with the Se compounds, the cells were harvested (protocol 2.1.2) and counted (protocol 2.1.3), and then resuspended in an appropriate volume of 1X PBS to make a final concentration on 5 X 10^4 cells/10 µl. A 10 µl volume of these cells was mixed in 80 µl of melted 0.5% low melting point agarose (LMPA) (37°C) and then placed vertically on the bottom of the pre-agarose-coated slides prepared the previous day. A 22 x 44 mm coverslip (LabServ®) was then gently placed on top to avoid air bubbles and ensure even coverage of cells on the slide, and the slides were incubated at 4°C for 20 minutes to allow the gel to solidify. Once set, the 22 x 44 mm coverslips (LabServ®) were able to be removed without disrupting the gel.

The agarose-coated slides were submersed in the lysis solution at 4°C for 90 minutes. Following cell lysis, the slides were washed in chilled 1X PBS for 5 minutes, and submerged in the chilled alkaline electrophoresis buffer for 30 minutes to allow for denaturation. The slides were then electrophoresed using an Owl gel electrophoresis tank for 20 minutes at 300 mA (between 17-24 V) at 4°C. After the cells were electrophoresed, the slides were washed in neutralisation buffer three times for 5 minutes, and then finally rinsed in mQ H_2O for 5 minutes and allowed to dry at RT. The slides could then be stored in the dark at RT for up to two months before staining and imaging was necessary.

2.7.4 Bleomycin Incubation Step

When investigating the repair capacity of the Se compounds on DNA damage in the cells, an incubation period with bleomycin was carried out. The comet assay protocol (2.7.3) was altered to include an incubation period before the cells were harvested. The media containing the Se compounds was removed, and replaced with growth media containing 1 µg/ml bleomycin, and left to incubate for 10 minutes. Following that incubation period, the growth media/bleomycin was removed, and replaced with normal growth media and left to incubate for 10 minutes to allow the cells to undergo the repair process. The process of the comet assay protocol (2.7.3) was then continued.

2.7.5 Staining and Imaging the Comets

The cells were stained with SYBR® Gold (Invitrogen, USA) to visualise the comets. A 1X solution of SYBR® Gold was added directly onto the gel with a coverslip placed on top to evenly distribute the stain and left to incubate at 4°C for 10 minutes. The slides were then rinsed twice in mQ H_2O for 5 minutes each wash to remove excess stain. The comets were then visualised using the Leica DMRE fluorescence microscope (Bio-strategy), and images were taken using the Olympus DP70 camera to examine 50 comets per slide.

2.7.6 Comet Analysis

The images obtained from visualising the comets were then analysed using the CometScore software (TriTek). Output from the CometScore software was further analysed using Microsoft Excel. Data (mean ± sd) were considered to be statistically significant when the two-tailed *p*-value was <0.05.

Chapter Three

Results

This chapter outlines the results from culturing *in vitro* two *BRCA1*-mutated cell lines, extracting the nuclear DNA, amplification and sequencing of the *BRCA1* gene to identify the respective mutations and, finally, carrying out the MTT assay to determine the IC_{50} of the cell lines following Se treatment and the level of DNA damage through the comet assay. In addition, results of the *Mycoplasma* PCR diagnostic test that was established for the first time.

3.1 Growth of Two Human Breast Cancer Cell Lines

The SUM149PT and MDA-MB-436 cell lines were received frozen in a cryotube from the University of Auckland on the 20 November, 2013, and the 2 July, 2014 respectively. Once transferred to the University of Waikato with MPI approval (permit number 759), the cells were revived (protocol 2.1.1), and then maintained and subcultured when necessary (2.1.2). Cells were cultured using aseptic techniques and monitored for microbe contamination using direct microscopy observation. A molecular protocol to detect *Mycoplasma* contamination in the two cell lines will be discussed in more detail in Chapter 3.5.

Figure 12 shows a representative image of the two adherent epithelial cell lines used for the purposes of this study. Cultured cells were used for various experiments, and any superfluous cells were frozen down and stored in the -80°C freezer in the C.2.10 laboratory at the University of Waikato.

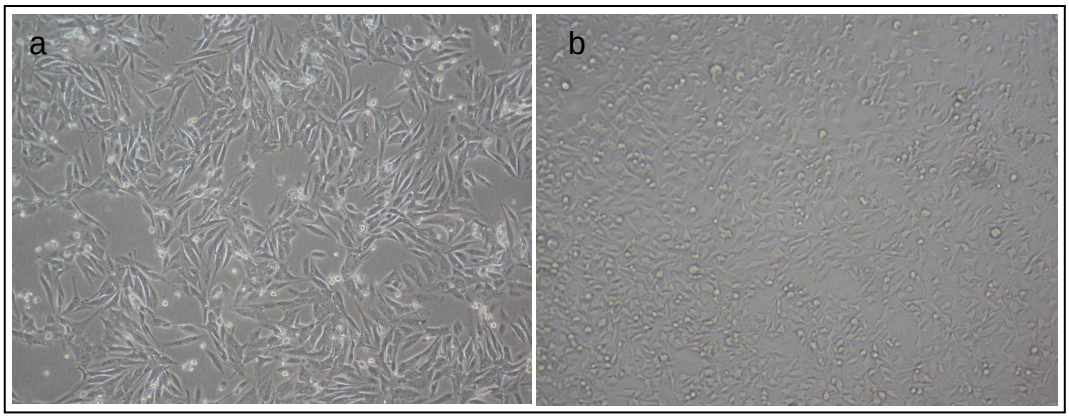

Figure 12. Photomicrographs of Epithelial growth of *BRCA1*-mutated cell lines. a) SUM149PT cell line. b) MDA-MB-436 cell line. Cells were cultured in a T25 flask. Photomicrographs capture at 10X magnification on the Nikon Eclipse TS100 microscope.

3.2 Extraction of Genomic DNA from Breast Cancer Cell Lines

One hundred microlitres of genomic DNA was extracted from the SUM149PT and MDA-MB-436 *BRCA1*-mutated cell lines using the protocol outlined in chapter 2.2 and quantified using the NanoDrop (see 2.3). The NanoDrop results of the two cell lines can be seen in Table 13. The absorbance of the 260/280 ratio was within the expected range of 1.8-2.0, indicating a pure sample. Also, contaminants such as phenol that are used during the extraction process can be visualised on the chromatogram as a peak at 230 nm if present. In both cases, there was no peak at 230 nm, therefore, based on the purity and lack of contaminants, these DNA samples were able to be used for further downstream applications. The total yield of genomic DNA extracted for SUM149PT was 839.2 ng/µl, and 1219.5 ng/µl for MDA-MB-436, respectively.

Table 13. DNA extraction NanoDrop results showing purity, contamination and concentration.

Sample	A260/280 ratio	A260/230 ratio	Contamination	Concentration (ng/µl)
SUM149PT	2.03	2.13	Negligible	839.2
MDA-MB-436	2.01	2.01	Negligible	1219.5

3.3 Optimisation of PCR Conditions

PCR was carried out to amplify the *BRCA1* mutations that were previously identified in the SUM149PT and MDA-MB-436 cell lines (Elstrodt et al., 2006). This was achieved using the protocol 2.4 which outlines the PCR reaction mix, and the conditions used for optimal results.

To optimise the PCR reaction, different concentrations of the components in the reaction mix were used, and the annealing temperatures were altered. Observation of a single, bright, sharp band of the expected size on the agarose gel was considered an optimal result to enable these products to be utilised for further downstream testing (e.g. DNA sequencing). These optimal results were achieved using HOT FIREPol® 10X Buffer 2 (Solis Biodyne). The difference between the HOT FIREPol® 10X Buffer 1 and 2 is that Buffer 2 contains a detergent. The annealing temperature that was used to achieve optimal results for the KM2F/R primer set and the KM4F/R primer set was 61°C.

3.3.1 HOT FIREPol® 10X Buffer 2 Optimisation

Using the SUM49PT extracted gDNA and the KM2F/R primer set, Figure 13 shows the PCR products using the HOT FIREPol® 10X Buffer 1 with a range of three annealing temperatures. Lanes 2-4 show different annealing temperatures (53, 57 and 61°C) using the KM2F/R primer set where no product was observed. Lane 5 contained the negative control

(-ve) which had no template DNA. Lane 6 contained the positive control (+ve) which used a validated set of primers targeting a known PCR product of 516 bp for the *GAPDH* gene (Crossan, 2014). As no amplification products were observed using the B1 buffer with the KM2F/R primer set, subsequent PCR reactions were carried out using the HOT FIREPol® 10X Buffer B2 as a replacement.

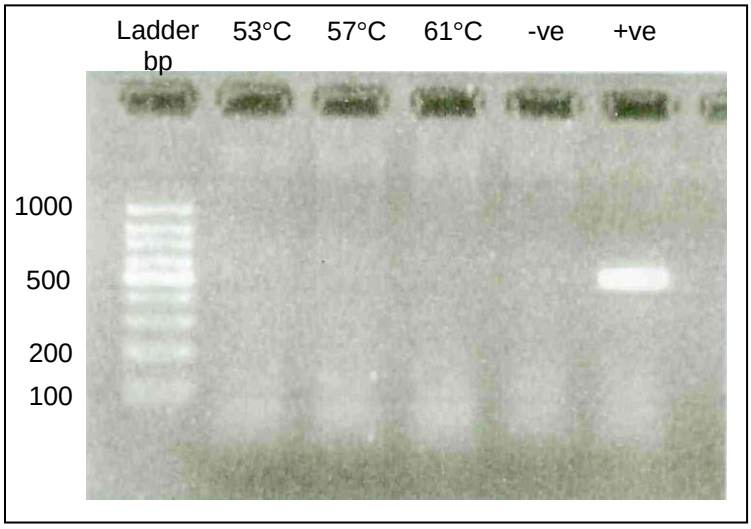

Figure 13. Gradient PCR of SUM149PT gDNA with the KM2F/R primer and HOT FIREPol® 1X Buffer B1. PCR products were electrophoresed for 30 min at 90 V on a 1.5% 1X TAE, agarose gel stained with RedSafe™ and compared to the 100 bp molecular weight ladder (Solis Biodyne) in Lane 1. Bands lower than 100 bp are primer dimers. -ve = negative control (no template DNA); +ve = positive control (validated primer set targeting the *GAPDH* gene).

3.3.2 Annealing Temperature Optimisation

Figure 14 shows the PCR products using the B2 buffer at a range of annealing temperatures using the SUM149PT extracted DNA. Lanes 2-5 show different annealing temperatures (53, 55, 58 and 61°C) using the KM2F/R primer set with the expected product of 250 bp. Lane 6 is a positive control (+ve) using the validated *GAPDH* primer set (516 bp). Lane 7 is a negative control (-ve) containing no template DNA. Lane 4 (61°C) appeared to have the brightest band, and therefore, 61°C was used as the annealing temperature for any subsequent PCR reactions using the KM2F/R primer set to achieve optimal results.

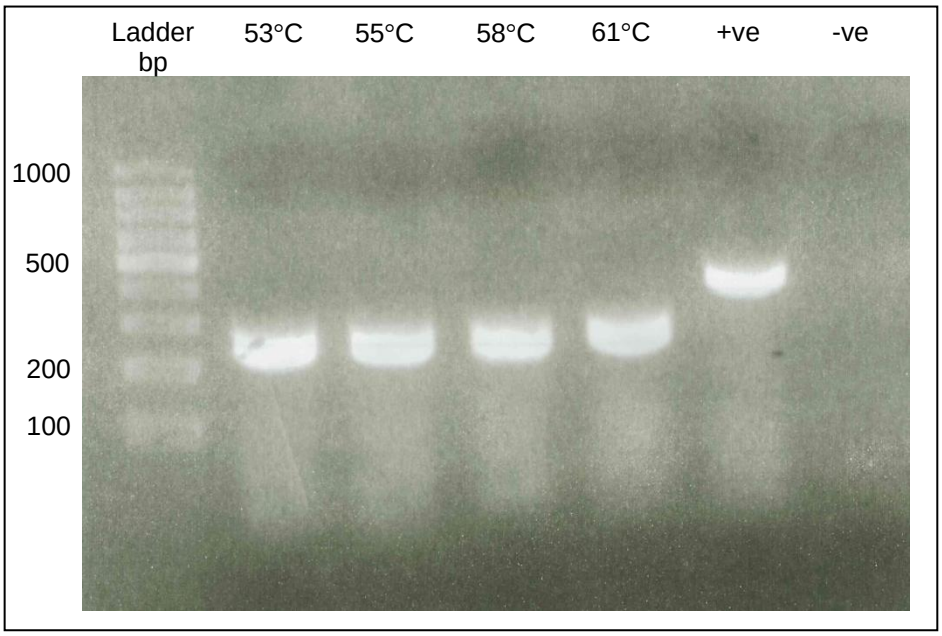

Figure 14. Gradient PCR of SUM149PT DNA with the KM2F/R primer and HOT FIREPol® 1X Buffer B2. The four annealing temperatures resulted in the expected band of 254 bp. PCR products were electrophoresed for 30 min at 90 V on a 1.5% 1X TAE, agarose gel stained with RedSafe™ and compared to the 100 bp molecular weight ladder (Solis Biodyne) in Lane 1. Bands lower than 100 bp are primer dimers. -ve = negative control (no template DNA); +ve = positive control.

Figure 15 shows the PCR products using the B2 buffer at a range of annealing temperatures using the MDA-MB-436 extracted DNA and the KM4F/R primer set. Lane 2 is a positive control (+ve) using the validated KM2F/R primer set (Figure 14) for the *BRCA1* mutation at an expected size of 250 bp. Lane 3 is a negative control (-ve) containing no template DNA. Lanes 4-7 show different annealing temperatures (53, 55, 58 and 61°C) using the KM4F/R primer set with the expected product of 400 bp. Lane 7 (61°C) appeared to have the brightest band, and therefore, 61°C was used as the annealing temperature for any subsequent PCR reactions using the KM4F/R primer set to achieve optimal results.

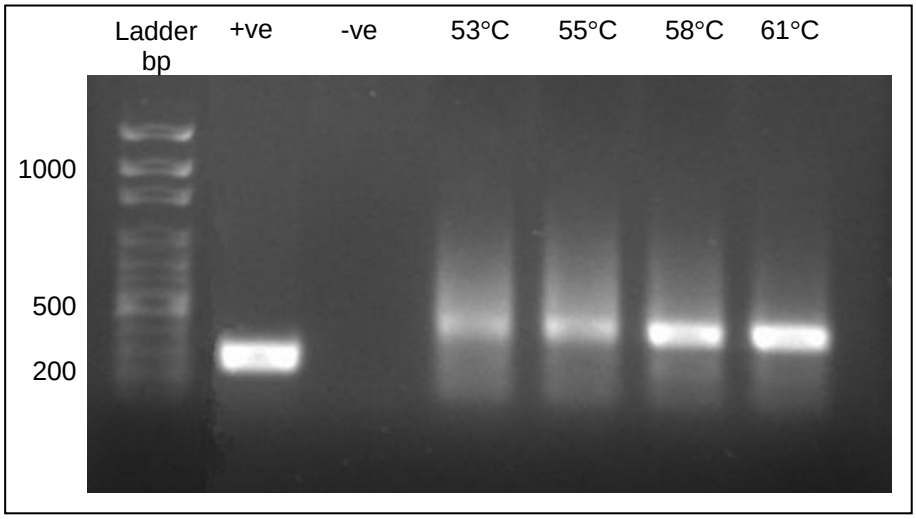

Figure 15. Gradient PCR of MDA-MB-436 DNA amplified with the KM4F/R primer set. The four annealing temperatures resulted in the expected band of 400 bp. PCR products were electrophoresed for 30 min at 90 V on a 1.5% 1X TAE, agarose gel stained with RedSafe™ and compared to the 100 bp molecular weight ladder (Solis Biodyne). Bands lower than 100 bp are primer dimers. -ve = negative control (no template DNA); +ve = positive control.

3.3.3 Amplification of *BRCA1* Gene Under Optimised Conditions

The DNA extracted from the two *BRCA1*-mutated cell lines (SUM149PT and MDA-MB-436) was amplified with each set of primers (KM2F/R and KM4F/R) that target the identified mutations (2288delT and 5396+1G>A) found in the corresponding cell line (Table 4). Each primer set was amplified at their optimal annealing temperature. Figure 16 shows the amplification products generated. Lane 2 and lane 5 are negative controls containing no template DNA with primer set KM4F/R and KM2F/R respectively. Lane 3 contains the SUM149PT DNA, and lane 4 contains the MDA-MB-436 DNA, both of which were amplified with the KM4F/R primer set to produce products of 400 bp. Lane 6 and 7 also contain the SUM149PT and MDA-MB-436 DNA respectively, but with the KM2F/R primer set to produce a product of 250 bp.

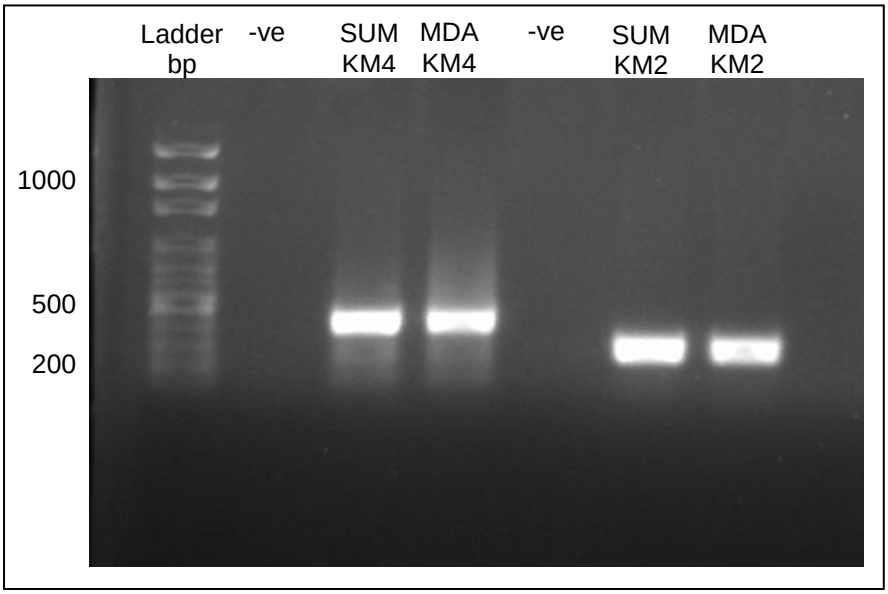

Figure 16. SUM149PT and MDA-MB-436 DNA amplified with the KM2F/R and KM4F/R primer sets. The KM4 primers resulted in the expected band of 400 bp, and the KM2 primers resulted in the expected band of 254 bp. PCR products were electrophoresed for 30 min at 90 V on a 1.5% 1X TAE, agarose gel stained with RedSafe™ and compared to the 100 bp molecular weight ladder (Solis Biodyne) in Lane 1. Bands lower than 100 bp are primer dimers. SUM = SUM149PT; MDA = MDA-MB-436; KM2 = KM2F/R; KM4 = KM4F/R; -ve = negative control (no template DNA); +ve = positive control.

3.4 DNA Sequencing

The PCR products obtained from Figure 16 were purified using the Zymo Clean and Concentrate Kit (protocol 2.4.3), and sent to be sequenced at the University of Waikato DNA Sequencing Facility. DNA sequencing results obtained were analysed using Geneious software to compare them against the 81,188 bp *BRCA1* gene reference sequence (U14680). The forward and/or reverse sequences were aligned to the reference sequence to identify the expected mutations in the cell lines. Figure 17 shows the DNA sequencing results of the two cell lines each targeted with the two primer sets. Firstly, SUM149PT DNA amplified with the KM2F/R primer set shows the expected deletion of an adenine nucleotide at position 49,068. The position number is based on the gDNA of the *BRCA1* gene that corresponds to the mRNA sequence position number of 2288. In comparison, Figure 17b shows SUM149PT DNA amplified with the KM4F/R primer set with no mutation. Secondly, Figure 17c shows MDA-MB-436 DNA amplified with the KM2F/R primer set with no mutation. In comparison, the MDA-MB-436 DNA amplified with the KM4F/R primer set has the expected substitution of a cytosine nucleotide for a thymine

nucleotide at position 12,757. This position number is based on the gDNA of the *BRCA1* gene that corresponds to the mRNA sequence position number of 5396+1. The sequence that was aligned to the reference sequence was chosen based on the sequence that was of the highest quality (evenly spaced peaks of the same width, no miscalls). An additional primer was included for the PCR amplicons with the KM4F/R primer set, KM5R. This is an internal reverse primer to ensure the mutation was sequenced. The internal reverse primer targets the exonic region, whereas the KM4F/R primers target the intronic region. The SUM149PT DNA with the KM2F/R primer set was aligned to the reverse complement of the reverse sequence, with 100% identity except for the expected mutation. The MDA-MB-436 DNA with the KM2F/R primer set was aligned to the forward sequence with 100% identity. The SUM149PT DNA with the KM4F/R primer set was aligned to the KM5R internal reverse sequence with 100% identity. The MDA-MB-436 DNA with the KM4F/R primer set was aligned to the KM5R internal reverse sequence with 100% identity, except for the expected mutation.

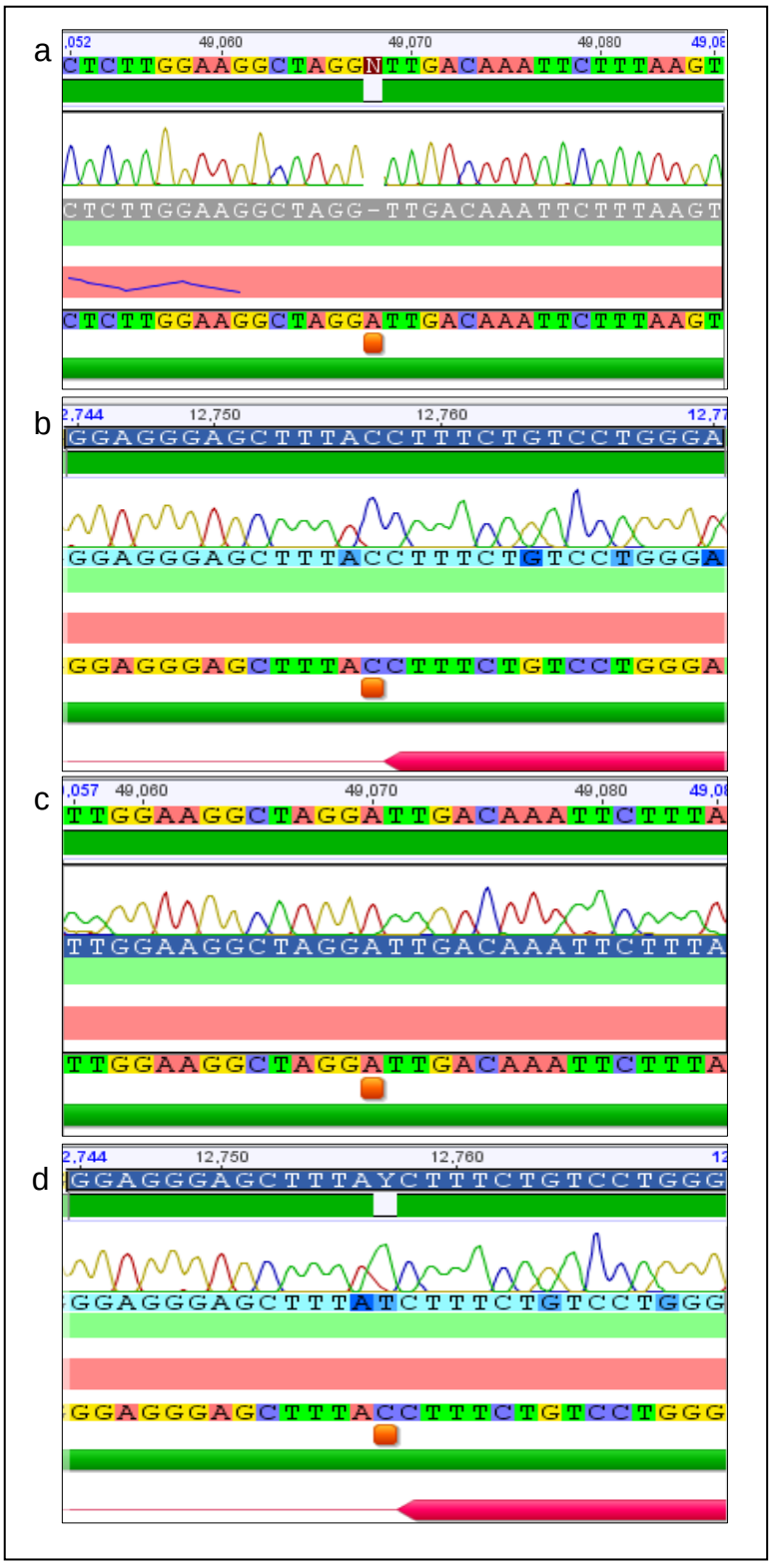

Figure 17. Alignment sequencing results of the *BRCA1* reference sequence (U14680). The top sequence is the nucleotide sequence from the cell line DNA with the electropherogram from the UoW DNA Sequencing facility depicted underneath. The bottom sequence is the reference sequence. The dark green bar shows nucleotide identity. The bright pink bar with an arrow head shows the exon. a) SUM149PT DNA amplified with the KM2F/R primer set and sequenced using the primer KM2R showing the expected genomic mutation 49,068delA (corresponds to mRNA 2288delT mutation. b)SUM149PT DNA amplified with the KM4F/R primer set and sequenced using the primer KM5R showing no mutation. c) MDA-MB-436 DNA amplified with the KM2F/R primer set and sequenced using the primer KM2F with no mutation. d) MDA-MB-436 DNA amplified with the KM4F/R primer set and sequenced using primer KM5R with the expected genomic DNA mutation of a C for a T at position 12,757 (corresponds to showing the 5396+1G>A mutation in mRNA).

3.5 Optimisation of a PCR Diagnostic Assay for *Mycoplasma* Contamination

A PCR diagnostic assay was developed by Uphoff and Drexler (1999) to test cell culture samples for contamination with *Mycoplasma*. PCR was carried out to detect *Mycoplasma* contamination in cell culture samples using this method. However, a different *Taq* DNA polymerase was used. Figure 18 shows the agarose gel electrophoresis results following the PCR protocol outlined by Uphoff and Drexler (1999). All PCR samples were run with and without an internal control template DNA. The internal control is expected to amplify a product of 986 bp in size. Lanes 2 and 3 contained the PCR reactions with MDA-MB-436 DNA template, with lane 3 also containing the internal control template DNA. Lanes 4 and 5 were negative/water controls (no template DNA), with lane 5 also containing the internal control. Lanes 6 and 7 contained a positive *Mycoplasma* DNA sample (DSMZ), with lane 7 also containing the internal control. The internal control band was visible in all test samples (lanes 3, 5, and 7), showing a band near 1000 bp. The *Mycoplasma* positive control was not visible (expected size of 502-520 bp) in lanes 6 and 7. As the positive control sample did not amplify, the lack of band in the MDA-MB-436 sample (lanes 2 and 3) cannot be taken as negative for *Mycoplasma* contamination. As a result, further optimisation of this protocol was necessary. Because the internal control sample was amplified, this indicates that the PCR reaction was successful. However, as the positive control sample was not present, it indicates that the positive control sample may not have sufficient, or degraded *Mycoplasma* DNA present, or the primer mix is not annealing to the template DNA efficiently. Therefore, the next step was to determine which primers target each sample (either *Mycoplasma* or internal control), and to test the primers separately on the samples.

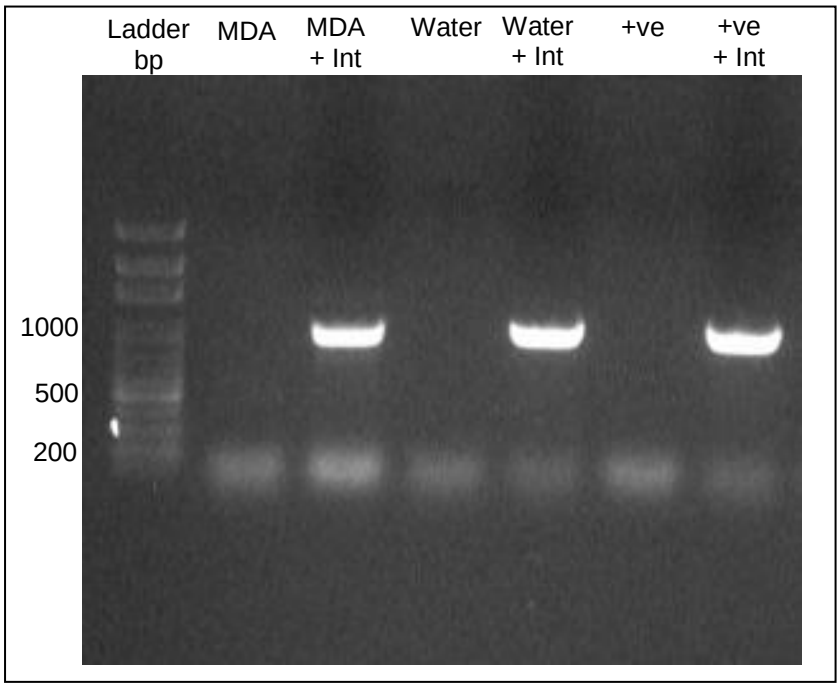

Figure 18. MDA-MB-436 DNA PCR test for *Mycoplasma* contamination using the DSMZ *Mycoplasma* DNA positive sample. The Intron PCR Master Mix solution containing the Taq DNA polymerase was used. The PCR conditions used were those developed by Uphoff and Drexler (1999). PCR products were electrophoresed for 30 min at 90 V on a 1.3% 1X TAE, agarose gel stained with RedSafe™ and compared to the 100 bp molecular weight ladder (Solis Biodyne) in Lane 1. Bands lower than 100 bp are primer dimers. MDA = MDA-MB-436; Int = Internal control; water = negative control (no template DNA); +ve = positive control.

3.5.1 Validation of Primer Sets and *Mycoplasma* Positive Control

The six primers that are used in the primer mix (LMP13-18) for the diagnostic PCR assay were blasted using the NCBI nucleotide blast tool (blastn) to determine which primers targeted the internal control, and which targeted the *Mycoplasma* genus. It was found that LMP13 (forward) and LMP18 (reverse) hit the internal control (*A. laidlawii*), and LMP15 (forward) and LMP17 (reverse) hit a range of *Mycoplasma* species. These two primer sets were amplified with the appropriate sample (either the *Mycoplasma* positive control or the internal control DNA sample) to determine if there was any DNA in the positive *Mycoplasma* sample, and to check the primers were amplifying their targets.

Figure 19 shows the results of testing the primer pairs separately with the suitable sample. Lane 2 is a negative control (no template DNA) with the

LMP13-18 primer mix. Lane 3 is the LMP15/17 primer set with the *Mycoplasma* positive control DNA (DSMZ). Lane 4 is the LMP13/18 primer set with the internal control DNA showing the expected product of 986 bp. Lane 5 is a positive control for the PCR reaction containing the MDA-MB-436 DNA with the KM4F/R primer set showing the expected product of 400 bp. The *Mycoplasma* positive control sample with the specific primer set did not amplify, suggesting an issue with the quality or quantity of the sourced positive control, sensitivity of Taq DNA Polymearse, or possible primer degradation. Consequently, a new *Mycoplasma* positive sample was acquired to further validate the protocol.

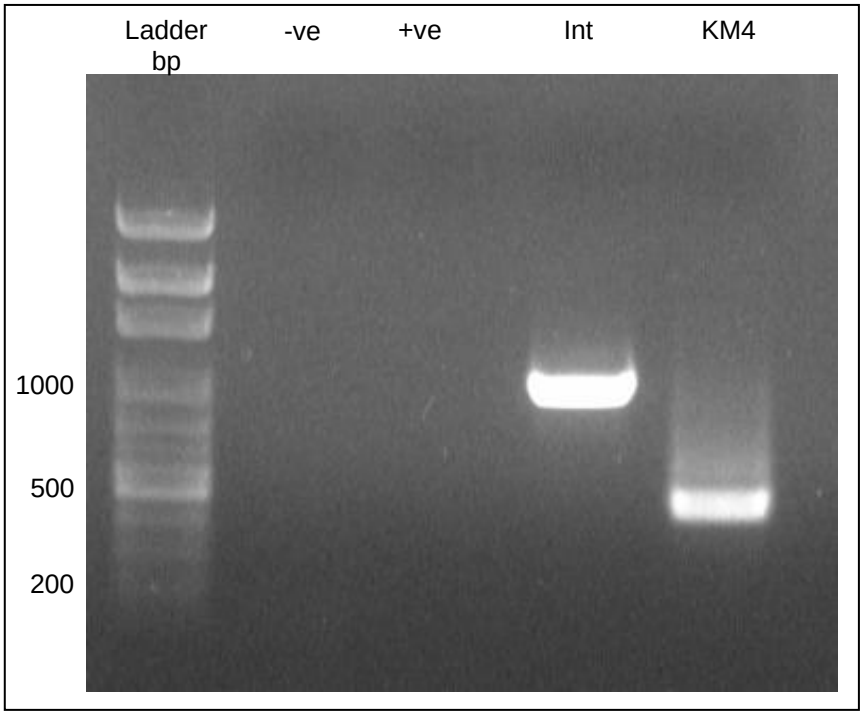

Figure 19. *Mycoplasma* positive control sample PCR test using individual primer sets. The Intron PCR Master Mix containing the Taq DNA polymerase was used. The PCR conditions used were 35 cycles of 94°C for 20 sec, 60°C for 20 sec, and 72°C for 60 sec. PCR products were electrophoresed for 30 min at 90 V on a 1.3% 1X TAE, agarose gel stained with RedSafe™ and compared to the 100 bp molecular weight ladder (Solis Biodyne) in Lane 1. Bands lower than 100 bp are primer dimers. +ve = *Mycoplasma* positive sample; Int = Internal control; KM4 = KM4F/R; -ve = negative control (no template DNA).

3.5.2 Validation of the PCR Protocol using a New *Mycoplasma* Positive Sample

A new *Mycoplasma* cell lysate positive sample was sourced locally from AgResearch. Figure 20 shows the agarose gel electrophoresis results of the PCR reaction as outlined by Uphoff and Drexler (1999), with the new *Mycoplasma* positive cell lysate sample. All PCR samples were amplified with and without an internal DNA control. Lanes 2 and 3 contained the MDA-MB-436 DNA, with lane 3 also containing the internal control. Lanes 4 and 5 were negative/water controls (no template DNA), with lane 5 also containing the internal control. Lanes 6 and 7 contained a positive *Mycoplasma* sample (AgResearch), with lane 7 also containing the internal control. The internal control band was only visible in two out of three test samples (lanes 3 and 5), showing a band at 986 bp. The *Mycoplasma* positive control was not visible (expected size of 502-520 bp) in lanes 6 and 7. As the *Mycoplasma* positive samples did not amplify, and the internal control did not amplify with the *Mycoplasma* positive control (lane 7), a different Taq DNA polymerase was then tested to improve amplification.

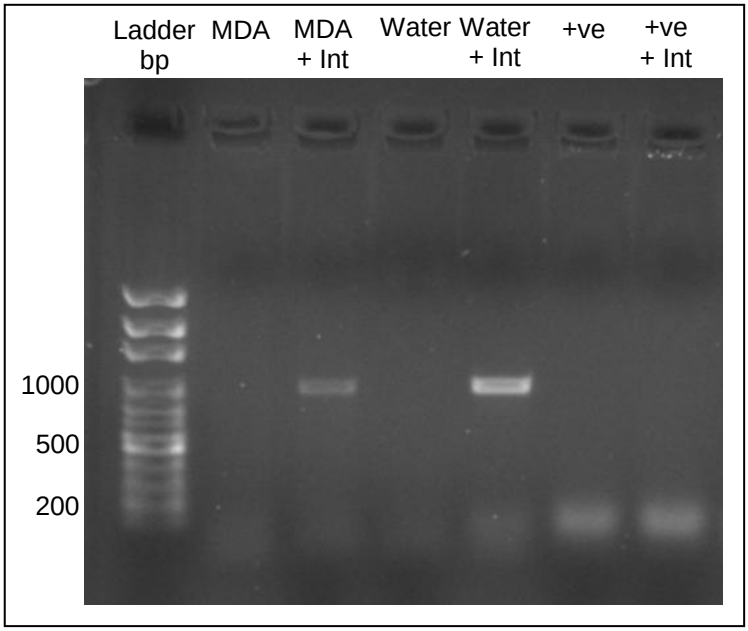

Figure 20. MDA-MB-436 DNA PCR test for *Mycoplasma* contamination using the AgResearch *Mycoplasma* positive sample. The Intron PCR Master Mix containing the Taq DNA polymerase was used. The PCR conditions used were those developed by Uphoff and Drexler (1999). PCR products were electrophoresed for 30 min at 90 V on a 1.3% 1X TAE, agarose gel stained with RedSafe™ and compared to the 100 bp molecular weight ladder (Solis Biodyne) in Lane 1. Bands lower than 100 bp are primer dimers. MDA = MDA-MB-436; Int = Internal control; water = negative control (no template DNA); +ve = positive control.

3.5.3 Optimisation of the *Mycoplasma* Detection PCR

Instead of using the 2X PCR Master Mix Solution (i-Taq™) (Intron), the master mix was prepared using the HOT FIREPol® DNA Polymerase (Solis BioDyne) and other components as outlined in protocol 2.4.5 with minor modifications. Briefly, 4 µl of DNA template was added instead of 1 µl. In addition, 1 µl of internal control DNA was added to the reactions requiring an internal control. The PCR reactions were then run for 35 cycles with temperature and time specifications outlined in the HOT FIREPol® DNA Polymerase (Solis BioDyne) Data sheet. The annealing temperature was set at 54°C for 30 seconds, followed by extension at 72°C for 60 seconds.

Figure 21 shows the results of the adapted protocol for the detection of *Mycoplasma* contamination. All samples were run by themselves, and with an internal control. Lanes 2 and 3 contained the SUM149PT DNA, with lane 3 also containing the internal control. Lanes 4 and 5 contained the MDA-MB-436 DNA, with lane 5 also containing the internal control. Lanes

6 and 7 were negative/water controls (no template DNA), with lane 7 also containing the internal control. Lanes 8 and 9 contained a positive *Mycoplasma* sample (AgResearch), with lane 9 also containing the internal control. Neither the internal control (expected size of 986 bp) nor the *Mycoplasma* positive sample (expected size of 502-520bp) bands were amplified. Only a smear of non-specific DNA amplification and a bright band of primer dimers were observed on the agarose gel (lanes 2-5 and 8-9) was observed. As this reaction did not produce a positive result as expected, the next step was to optimise the PCR reaction by extracting and purifying the DNA from the *Mycoplasma* cell lysate.

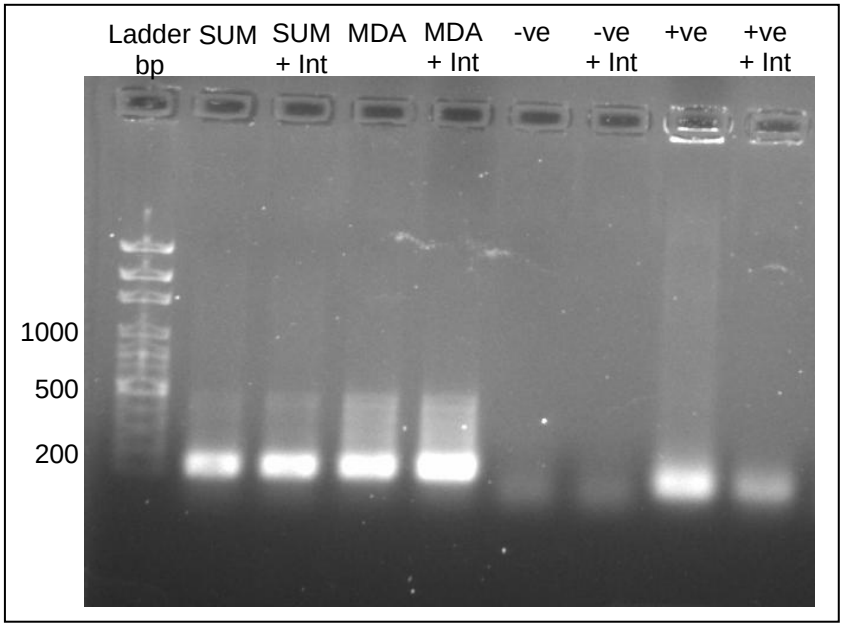

Figure 21. SUM149PT and MDA-MB-436 DNA PCR test for *Mycoplasma* contamination using the new AgResearch *Mycoplasma* positive sample. The HOT FIREPol® DNA Polymerase (Solis BioDyne) was used. The PCR conditions used were those recommended by the manufacturer of the Taq DNA polymerase. PCR products were electrophoresed for 30 min at 90 V on a 1.3% 1X TAE, agarose gel stained with RedSafe™ and compared to the 100 bp molecular weight ladder (Solis Biodyne) in Lane 1. Bands lower than 100 bp are primer dimers. SUM = SUM149PT; MDA = MDA-MB-436; Int = Internal control; -ve = negative control (no template DNA); +ve = positive control.

3.5.4 Optimisation of the Protocol using Extracted DNA from the *Mycoplasma* Cell Lysate

Mycoplasma DNA from the cell lysate was kindly donated by Holly Sprosen and was used as a template in the PCR reaction following the protocol outlined in 2.4.5. The concentration of extracted DNA was too low to be detected with the NanoDrop (H. Sprosen, personal communication, 30 January, 2014). All PCR samples were amplified with and without an internal control. Figure 22 shows the PCR results on an agarose gel. Lanes 2 and 3 contained the SUM149PT DNA, with lane 3 also containing the internal control. Lanes 4 and 5 contained the MDA-MB-436 DNA, with lane 5 also containing the internal control. Lanes 6 and 7 contained a 1:10 dilution of the extracted *Mycoplasma* DNA, with lane 7 also containing the internal control. Lanes 8 and 9 were negative/water controls (no template DNA), with lane 8 also containing the internal control. The internal control band was visible in all of the expected test samples (lanes 3, 5, 7, and 8), indicating the PCR was successful. The *Mycoplasma* positive control was visible (expected size of 502-520 bp) in lanes 6 and 7. No band of the expected size for *Mycoplasma* contamination (502-520 bp) was present in the SUM149PT sample (lanes 2 and 3), or the MDA-MB-436 sample (lanes 4 and 5). As a band for the positive control was present, it can be concluded that the SUM149PT and the MDA-MB-436 cell cultures are not contaminated with *Mycoplasma*.

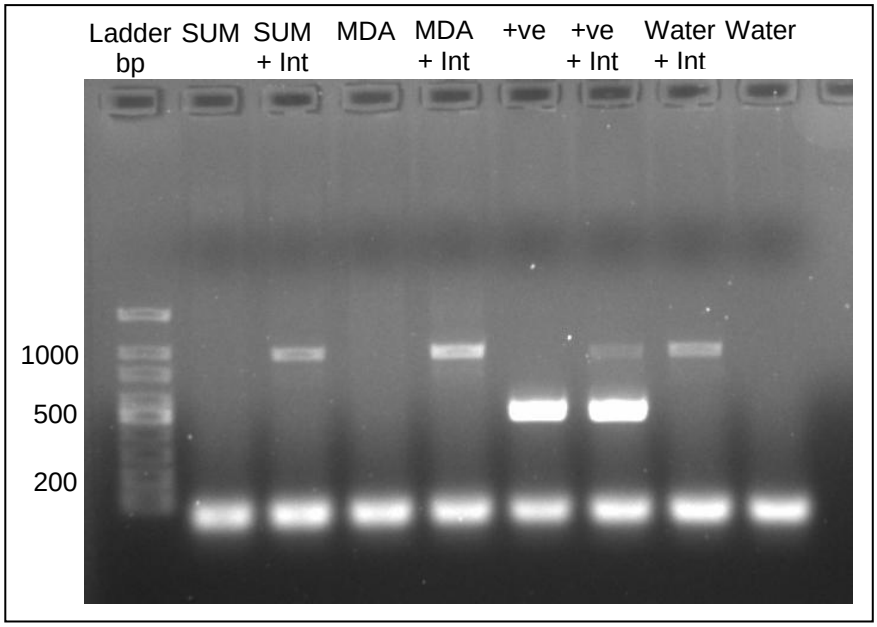

Figure 22. SUM149PT and MDA-MB-436 DNA PCR test for *Mycoplasma* contamination using the extracted *Mycoplasma* DNA sample. The Intron PCR Master Mix containing the Taq DNA polymerase was used. The PCR conditions used were those optimised and outlined in 2.4.5. PCR products were electrophoresed for 30 min at 90 V on a 1.3% 1X TAE, agarose gel stained with RedSafe™ and compared to the 100 bp molecular weight ladder (GenScript) in Lane 1. Bands lower than 100 bp are primer dimers. SUM = SUM149PT; MDA = MDA-MB-436; Int = Internal control; water = negative control (no template DNA); +ve = positive control.

3.6 MTT Assay

The MTT assay was used to analyse the cytotoxic effects of sodium selenite and MSA on the two *BRCA1*-mutated cell lines. All experiments were carried out in triplicate. The relative inhibitory activity is expressed as a percentage of the SC.

Figure 23 shows the inhibitory rate of the two Se compounds on the SUM149PT cell line. From this graph, the IC_{50} was calculated as 45 µM and 500 µM for sodium selenite and MSA, respectively. The standard error of the mean (SEM) at 10 µM for sodium selenite was quite large in comparison to the other data points. This was due to visible differences in colour of the MTT crystals; for all experiments the crystals appeared a brownish colour expect for occasional inconsistent wells at 10 µM which appeared purple/blue and had a much greater absorbance reading. There was a statistically significant difference between the two IC_{50} values (p=0.023, at 95% CI). Therefore, sodium selenite was more cytotoxic than MSA in this cell line.

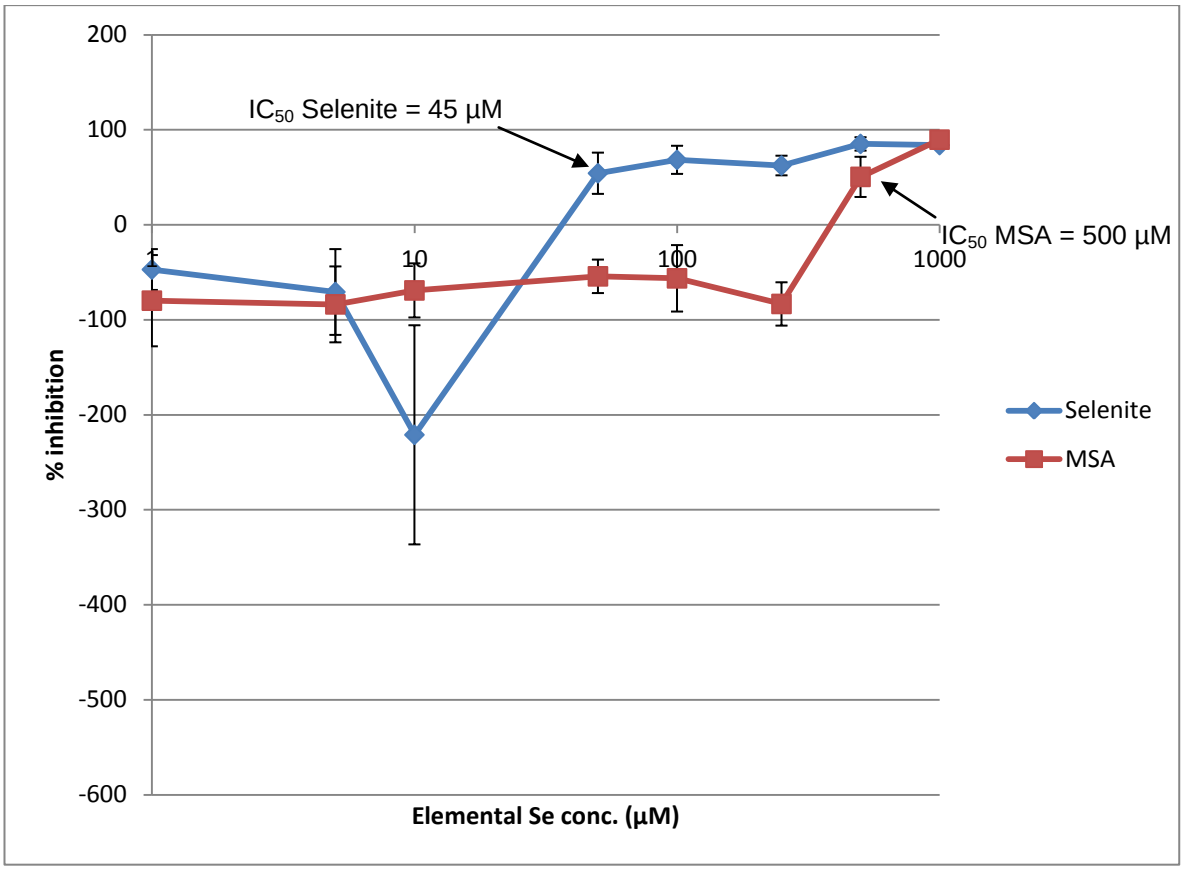

Figure 23. Line graph of percent inhibition of cell growth against elemental Se concentration for the SUM149PT cell line. Percent inhibition was estimated using an MTT assay followed by a 24hr exposure to Se in a 96-well plate. The data are expressed as mean ± the SEM for at least three independent determinations in triplicate for each experimental point (*n*=9).

Figure 24 shows the inhibitory rate of the two Se compounds on the MDA-MB-436 cell line. From this graph, the IC_{50} was calculated as 300 µM and 500 µM for sodium selenite and MSA, respectively. The SEM at 5, 10 and 50 µM for sodium selenite was quite large in comparison to the other data points. This was due to visible differences in colour of the MTT crystals; for all experiments the crystals appeared a brownish colour expect for occasional inconsistent wells at 5, 10 and 50 µM which appeared purple/blue and had a much greater absorbance reading. There was no statistically significant difference between the two IC_{50} values (p= 0.155, at 95% CI) for this cell line.

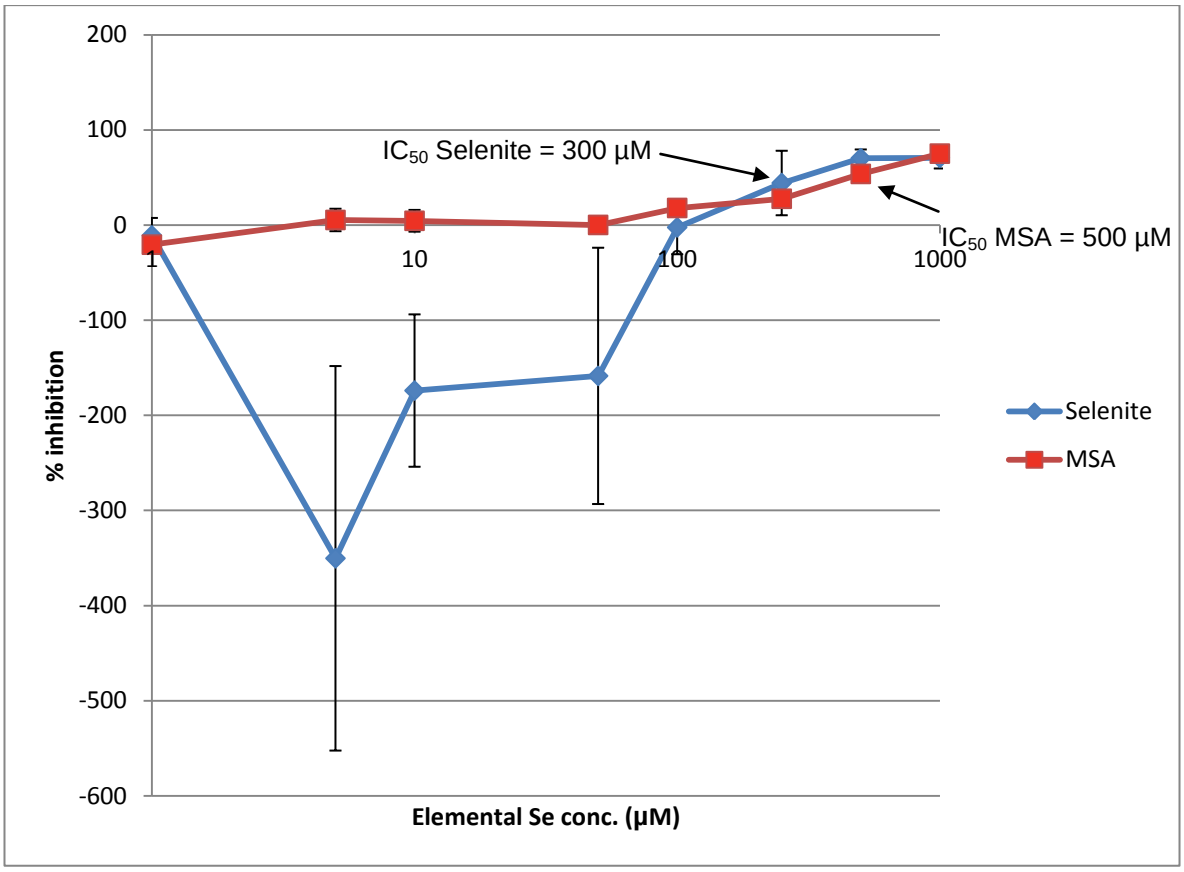

Figure 24. Line graph of percent inhibition of cell growth against elemental Se concentration for the MDA-MB-436 cell line. Percent inhibition was estimated using an MTT assay followed by a 24hr exposure to Se in a 96-well plate. The data are expressed as mean ± the SEM for at least three independent determinations in triplicate for each experimental point (*n*=9).

The negative inhibition observed with 1-50 µM sodium selenite and 1-500 µM MSA with the SUM149PT cell line (Figure 23), and similarly with 1-100 µM sodium selenite and 1-10 µM MSA with the MDA-MB-436 cell line (Figure 24) represent an increase in cell growth in relation to the solvent control growth. At the lower concentrations of Se, growth rate was increased, indicating that Se is a valuable nutrient for cell growth and survival. Once the concentration of Se became too high, it inhibited the growth of cells to the point of becoming toxic and killing the cells.

3.7 Comet Assay

The comet assay was used to assess the level of DNA damage the cells acquired when treated with either sodium selenite or MSA following protocol 2.7. Briefly, cells were exposed to the Se compounds for 24 hrs, then loaded onto a pre-agarose-coated slide, lysed, electrophoresed, and stained to visualise the comets and analyse the levels of DNA damage present in the cells. All experiments were carried out in triplicate. At least 50 comets were obtained per slide for each treatment (two slides per treatment), and analysed using the CometScore software, using the percentage of DNA present in the tail calculation (% DNA in tail).

For analysis of the comets, the CometScore software changes the colour spectrum from a single hue to a full spectrum to perform the calculations. Healthy cells with undamaged DNA appeared as just the head of the comet, as can be seen in Figure 25a. When the DNA in the cells become damaged, that DNA spreads to form the comet tail when electrophoresed, as can be seen in Figure 26a. Figure 25b/26b shows the comet pictures after application of the CometScore software. It can be seen that the more damage present, the smaller the head of the comet. Two waves are used to carry out all calculations: the first wave (green) measuring the head, and the second wave (purple) measuring the tail.

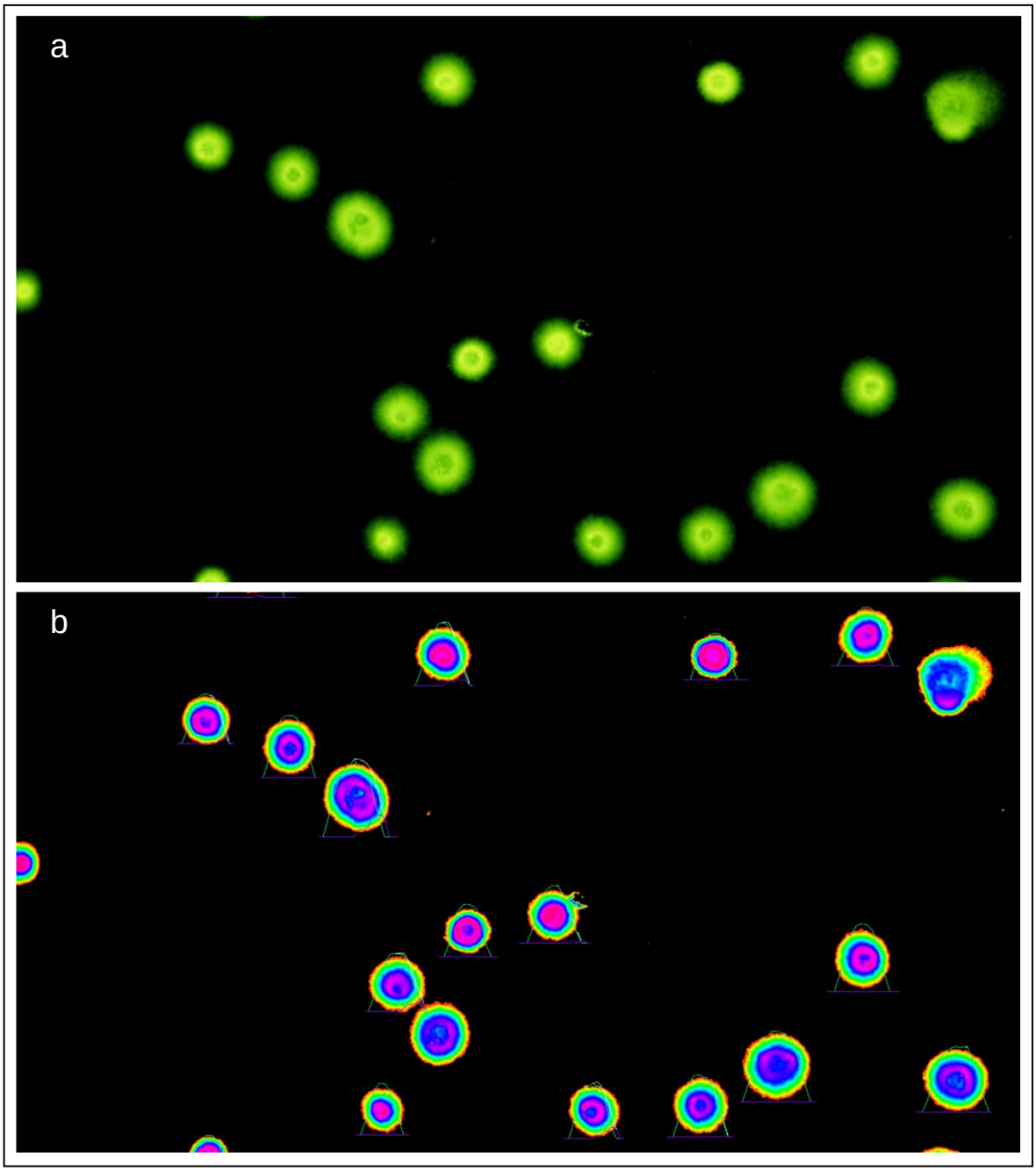

Figure 25. Representative images and analysis of the comets from the CometScore software for control cells. a) Images produced after staining with SYBR® Gold and visualising the microscope slides using the fluorescent microscope (X10 lens). b) Analysis output produced by the CometScore software.

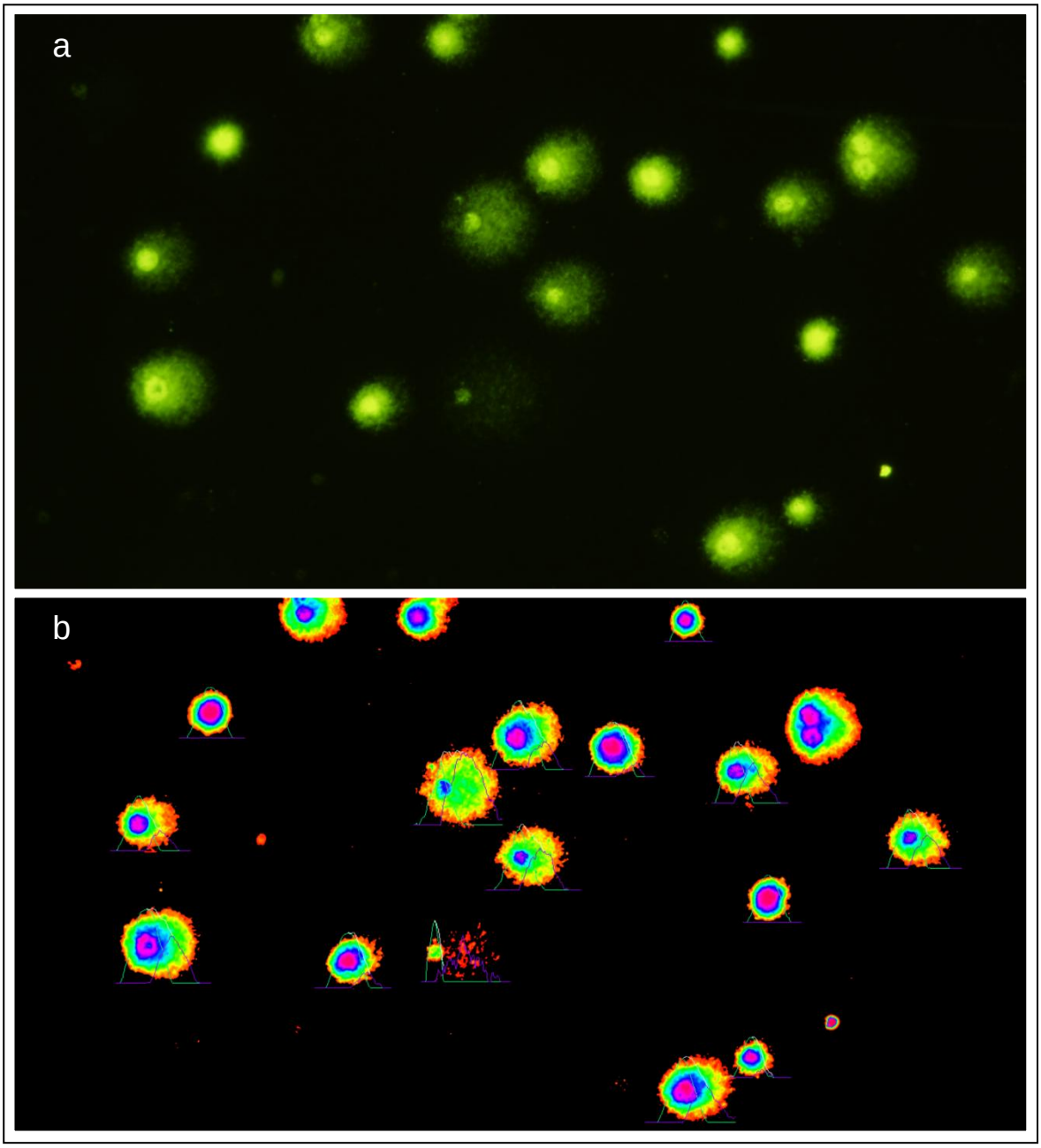

Figure 26. Representative images and analysis of the comets from the CometScore software for cells treated with Se (2 µM sodium selenite). Cells were treated with Se for 24 hrs**.** a) Images produced after staining with SYBR® Gold and visualising the microscope slides using the fluorescent microscope (X10 lens). b) Analysis output produced by the CometScore software.

Figure 27 shows the levels of DNA damage present (measured by the percentage of DNA present in the tail), when the SUM149PT cells were subjected to sodium selenite and MSA for 24 hrs. The cells were treated with approximately one quarter and one half of the preliminary IC_{50} for each treatment; for sodium selenite, approximately 1/4 IC_{50} was 12.5 µM and 1/2 IC_{50} was 25 µM, and for MSA, approximately 1/4 IC_{50} was 25 µM

and 1/2 IC_{50} was 50 µM. There was a statistically significant difference between DNA damage with treatment at 1/4 IC_{50} and 1/2 IC_{50} for this cell line, with a *p*-value of 0.0004 and 0.001, respectively, at 95% confidence. This again demonstrates that sodium selenite is more genotoxic to the cells than MSA.

Interestingly, as seen in Figure 27, there was a significant difference between the levels of DNA damage present in the controls (0 µM) under the two different treatment conditions, with control cells incubated on the same plate as others treated with MSA having less than half the amount of DNA damage seen in cells incubated on plates with sodium selenite in other wells (*p*-value=0.0003, at 95% CI). The two treatments were conducted on different plates, and in separate incubators, thus, each treatment condition cannot influence the effects of the other treatment. A great increase in the levels of DNA damage after treatment with sodium selenite in comparison to the control is evident (*p*-value=0.0014, at 95% CI). Similarly, the difference between the MSA treatment and control, even though smaller in comparison to sodium selenite, still shows statistical significance (*p*-value=0.02, at 95% CI). However, the level of DNA damage present in the cells treated with 50 µM MSA is lower than that present in the sodium selenite control treatment, though the difference is not statistically significant (*p*=0.498, with 95% CI).

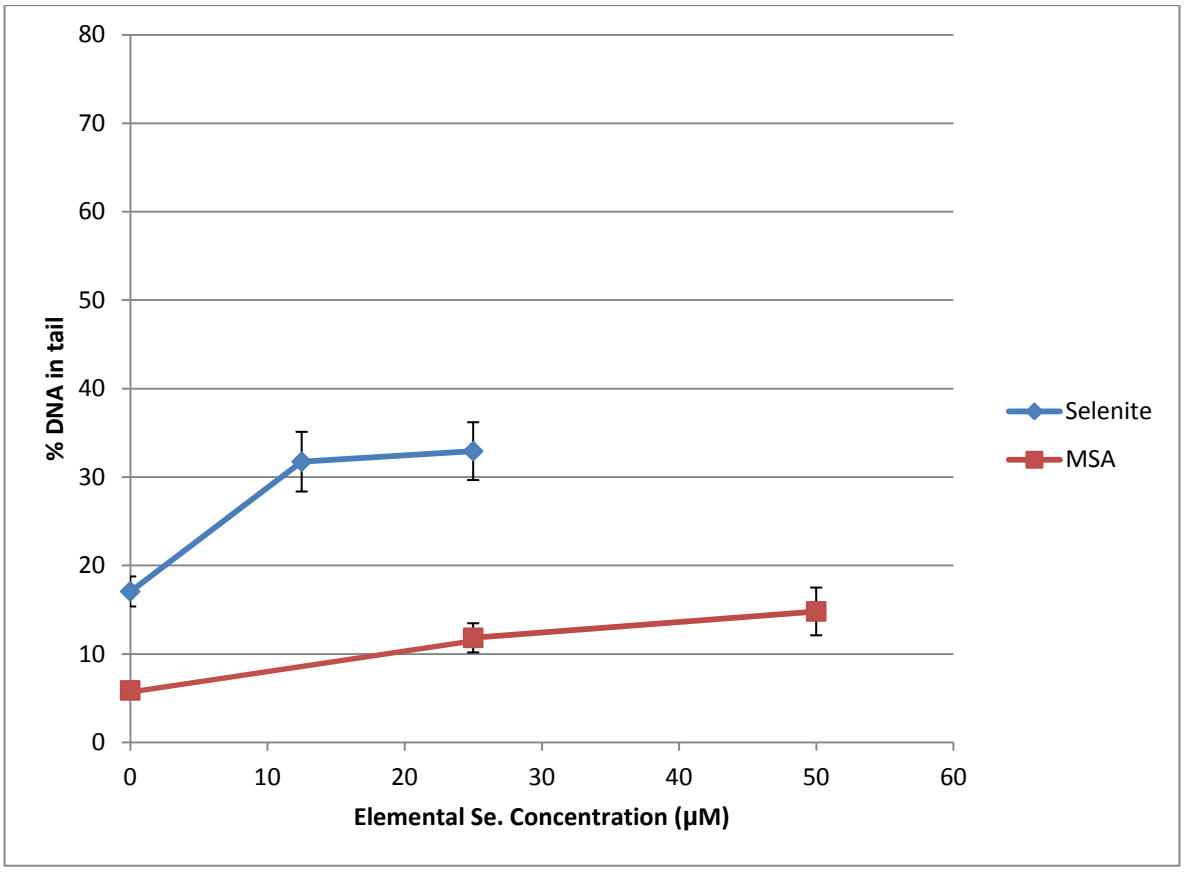

Figure 27. Line graph of SUM149PT cell line comet assay results.. Three independent comet assay experiments were conducted for each Se compound (sodium selenite and MSA) in 24-well plates. Each treatment was in duplicate. Cells were treated with Se for 24 hrs**.** Two microscope slides per treatment were produced and analysed using the CometScore software. Score ~50 comets/slide. The data are expressed as mean ± SEM (bars).

The effects of the two Se treatments on the DNA damage in the MDA-MB-436 cell line was then investigated. The cells were treated with a much lower concentration of Se (2 µM) that is more physiologically relevant and preliminary results can be seen in Figure 28. There was a significant increase in DNA damage with sodium selenite compared to controls (p=0.01, at 95% CI), and compared to MSA (p=0.006, at 95% CI). In contrast to sodium selenite, a non-significant reduction in DNA damage was seen with MSA compared to controls. At this concentration sodium selenite is genotoxic whereas MSA is not. Overall, this result is promising in showing the beneficial effects of Se at lower (non-toxic) doses, and the possibility of it being able to reduce native or induced DNA damage in cells. The following steps to evaluate this hypothesis would be to test the lower doses of Se with an incubation period with bleomycin. However, due

to time constraints, this was not able to be completed during this research thesis.

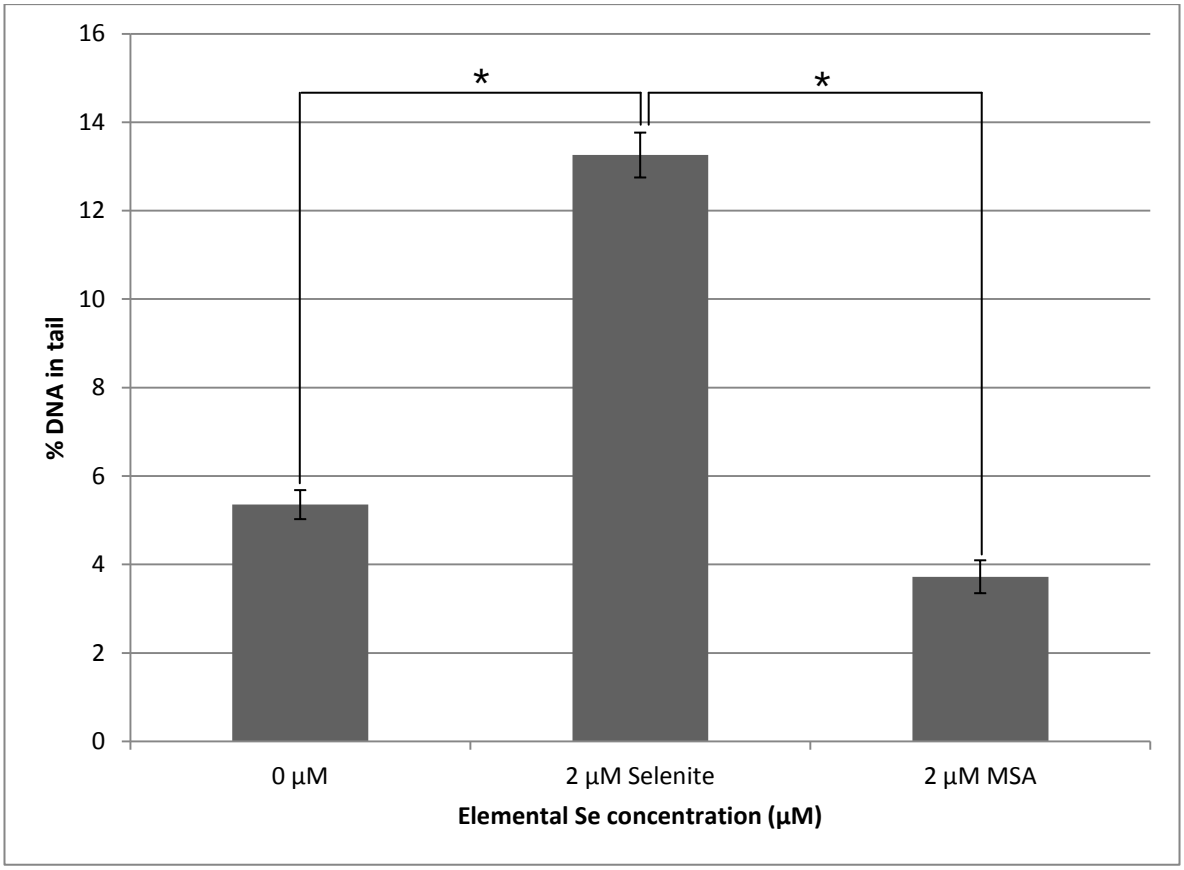

Figure 28. Bar graph of the comet assay for the MDA-MB-436 cell line treated with 2 µM sodium selenite and MSA. Two microscope slides per treatment were produced. This experiment was completed once with duplicates per treatment. Analysis of comet assay was conducted using the CometScore software. Score ~50 comets/slide. * = p<0.05.

3.7.1 Comet Assay with Bleomycin

Following on from determining the genotoxicity levels of the two Se treatments, the effects of the Se treatment in reducing the levels of induced DNA damage were investigated. This was carried out using the comet assay protocol 2.7.4, incorporating an incubation period with bleomycin, a chemotherapy drug which induces DNA damage to the cells.

Figure 29 shows the preliminary data when the SUM149PT cells were treated with one quarter of the IC_{50} (the lower concentration used in the initial comet assay (Figure 27)), followed by a 10 minute incubation with

1 µg/ml bleomycin, and finally, a repair period of 10 minutes. The levels of DNA damage produced in cells that were only treated with bleomycin was similar to levels of damage produced with a Se treatment alone (Figure 27). Conversely, the levels of DNA damage produced between the Se treatment on the same plate are not similar. The difference between the control and Se treatment had great statistical significance (p=3.5x10^{-12}, with 95% CI). There was statistical significance between the levels of DNA damage present in the control (0 µM Se), and the control plus bleomycin (p=4.9x10^{-9}). In comparison, there was no statistical significance between the levels of DNA damage present in the 1/4 IC_{50} and 1/4 IC_{50} plus bleomycin (p=0.152, at 95% CI). The differences between the levels of damage present in the cells that underwent a repair incubation phase in comparison to those that were just treated with bleomycin was not statistically significant (p=0.939, at 95% CI). The levels of damage produced when treated with this level of Se as well as with bleomycin were very high, and perhaps a decrease in DNA damage levels may be seen if the concentration of Se was dropped to a more beneficial and physiologically obtainable level (as opposed to a level where it may be starting to produce more toxic effects).

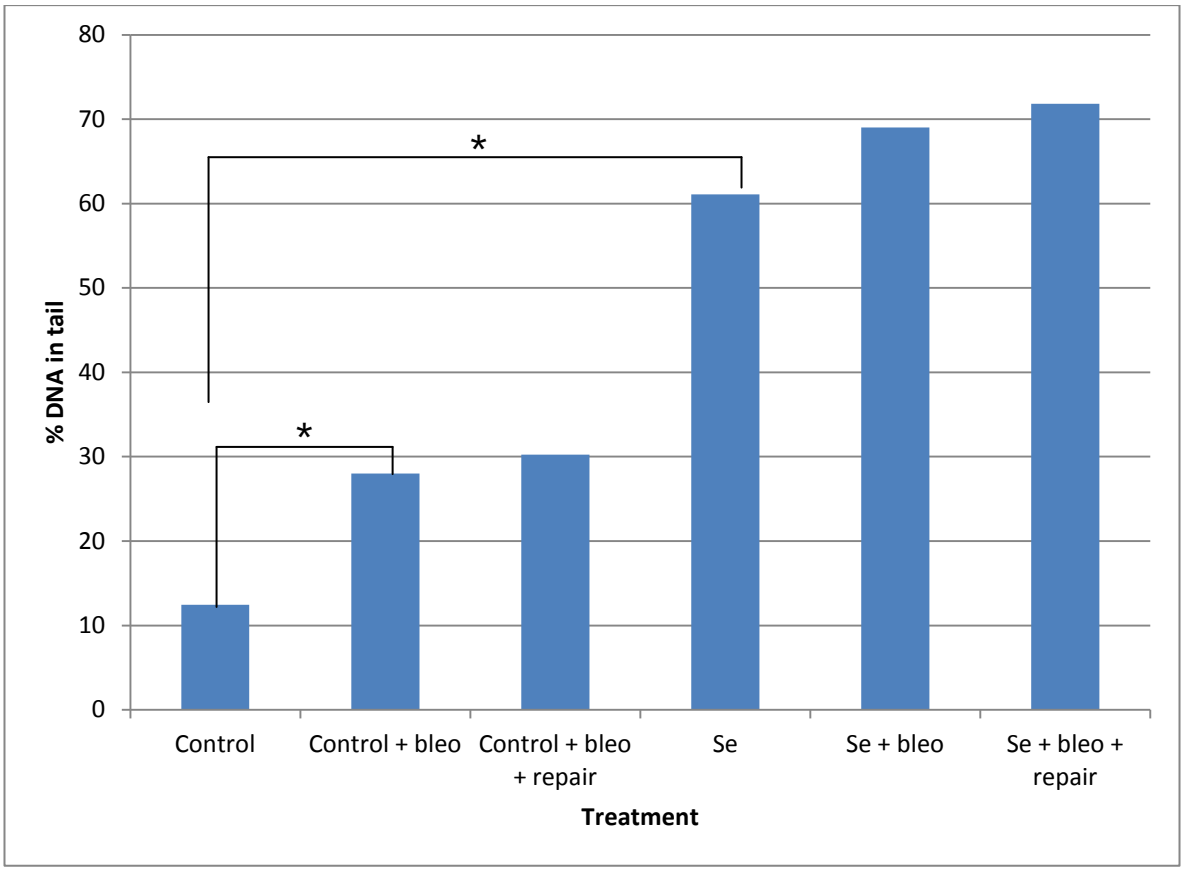

Figure 29. Bar graph of comet assay for the SUM149PT cell line treated with sodium selenite and bleomycin. SUM149PT cells were treated with one quarter of the sodium selenite IC_{50} (12.5 µM), followed by a 10 minute incubation with 1 µg/ml bleomycin (bleo), and finally, a repair period of 10 minutes. Two microscope slides per treatment were produced. This experiment was completed once. Analysis of comet assay was conducted using the CometScore software. Score ~50 comets/slide. Control/Se + bleo = treatment with a 10 minute incubation with bleomycin. Control/Se + bleo + repair = treatment with a 10 minute incubation with bleomycin followed by a 10 minute incubation period to allow for repair of DNA damage. * = $p<0.05$.

Chapter Four

Discussion

The aim of this project was to investigate the effects of Se supplementation as a possible chemoprotective agent against breast cancer. The toxicity of inorganic and organic Se compounds at various concentrations was investigated *in vitro* on human *BRCA1*-mutated cancer cells, and the differential effects that these compounds at different concentrations had on the levels of DNA damage present in the cells.

4.1 Amplification and Sequencing of the *BRCA1* Gene

The SUM149PT and MDA-MB-436 cell lines used during this research each harboured a mutation that resulted in the loss of the wild-type *BRCA1* allele. In order to validate that these mutations were present in each respective cell line, and the alternative mutation was absent, DNA had to be isolated from the cultured cells, amplified in the target region, purified, and sequenced. This was achieved using an array of molecular biology techniques, the first of which was to extract the genomic DNA from the two cell lines.

4.1.1 DNA Extraction

Extraction of high yield pure, DNA from cells is crucial for obtaining quality results during further downstream experiments. A chloroform extraction protocol was used for this research, and is a commonly used extraction method that is simple, non-kit based, and effective at producing a high quantity and quality of DNA.

The genomic DNA (gDNA) extracted from the two cell lines, SUM149PT and MDA-MB-436, was of high concentration and purity with negligible amounts of organic contaminants.

4.1.2 Optimisation of *BRCA1* Mutation Amplification from gDNA

In order to optimise the amplification of the target region containing the *BRCA1* mutation using the gDNA isolated from the two cell lines, factors such as primer design, particular components of the PCR reaction mixture (e.g. the buffer used), and the annealing temperature of the primers need to be altered. These factors will be discussed in more detail in the next section.

4.1.2.1 Primer Design

A primer set for each of the two *BRCA1* mutations reported by Elstrodt et al., (2006), were designed to amplify genomic DNA. The KM2F/R primer set was designed to target the 2288delT mutation present in exon 11 of mRNA, and expected to amplify a PCR product of 250 bp. The position of the deletion is based on the mRNA *BRCA1* sequence (U14680.1) and, as genomic DNA was used, the sequence was compared to the whole *BRCA1* gene (U14680). As a result, the position number of the mutation will be different; the position of the mutation in the gene is 49,068. The KM4F/R primer set was designed to target the 5396+1G>A mutation present at the splice donor site of exon 20, and produces a PCR product of 400 bp. Again, the position of the mutation is based on the mRNA sequence. Therefore, the position number of the mutation when comparing the sequencing to the *BRCA1* gene becomes 12,757. Due to the 5396+1G>A mutation being at the splice site, a second, internal reverse primer, KM5R, was designed to ensure the mutation was covered during the sequencing reaction.

4.1.2.2 Composition of PCR Buffer

Buffers used during PCR are necessary to control the pH levels to ensure the Taq DNA polymerase can work effectively. Initially, the HOT FIREPol® 10X Buffer B1 was used for PCR reactions, which did not contain any detergent. Using this buffer, the DNA was not able to be amplified (Figure 13). The B1 buffer was therefore replaced with the HOT FIREPol® 10X Buffer B2, which contained detergent, Tris-HCl and ammonium sulphate. Using the B2 buffer, a single band of the expected size (250 bp using the KM2F/R primer set) was observed on the agarose gel (Figure 14).

4.1.2.3 Annealing Temperature

The composition and length of the primers used during amplification will alter the optimal annealing temperature required. Lower annealing temperatures decrease the specificity with which the primer binds to the target DNA, resulting in an increased risk of amplification of non-specific DNA, but also the chance of an increased yield of the target product. A range of annealing temperatures was tried for both the KM2F/R and the KM4F/R primer set using gradient PCR. The optimal annealing temperature determined for amplification of a single, bright, clear band on the agarose gel was 61°C for both primer sets (Figure 14 and 15). As this annealing temperature is higher than the recommended IDT melting temperature, the risk of non-specific amplification is reduced, resulting in better quality products.

In conclusion, PCR reactions for the KM2F/R and KM4F/R primer sets were carried out using the B2 buffer instead of the B1 buffer, and the optimal annealing temperatures for both primer sets was 61°C. The gDNA from the SUM149PT and the MDA-MB-436 cell lines was amplified with each of the primer sets (KM2F/R and KM4F/R) and resulted in a single, sharp band of expected size on the agarose gel; a 250 bp band was present for both cell lines using the KM2F/R primer set, and a 400 bp band using the KM4F/R primer set (Figure 16). No contamination was observed in the negative control.

The remainder of the amplified samples were cleaned and concentrated using the Zymo Clean and Concentrate Kit (protocol 2.4.3), run through the NanoDrop to determine the concentration, and then sent to the Waikato DNA Sequencing Facility.

4.1.3 DNA Sequencing

Generally, for each PCR product to be DNA sequenced, two sequencing reactions are carried out; one in the forward direction, and the other in the reverse direction. This ensures that the entire product is 100% covered and an accurate consensus sequence is generated for analysis. This is important since there is a small area at the beginning of the sequencing run before the chemistry stabilises and produces single, evenly spaced peaks, with little baseline noise and no miscalls. The resulting chromatograms were analysed for miscalls, and edited to remove noise from the beginning and ends of the sequence to ensure that the highest quality sequencing data was used to align against the NCBI *BRCA1* gene reference sequence (U14680).

Six out of ten reactions run were of high quality. All the sequencing reactions chosen for alignment to the reference sequence were of very high quality and show that each cell line used for this study harboured the specific mutation in the *BRCA1* gene as reported by Elstrodt et al., (2006).

The KM4F/R primer set targeted the splice site at the end of exon 20 but anneals to intronic regions of the *BRCA1* gene. An additional internal reverse primer was designed (KM5R) for sequencing of the purified PCR products that annealed at a region within the exon. This primer was included as a secondary precaution to ensure the target mutation region was sequenced. The KM4 forward and reverse sequences for both the SUM149PT DNA and the MDA-MB-436 DNA were of very poor quality with multiple peaks present throughout the entire sequence. As these are cancer cells, they harbour many mutations within their genes, especially in the intronic regions. Due to these mutations frame shifts are more likely to have occurred, resulting in multiple different transcripts being produced,

and therefore multiple peaks being produced for each nucleotide position in the chromatogram. Consequently, these sequences were not able to be used to align to the reference sequence to identify the expected mutation. For future screening of cell passages, it is recommended to use the KM5R internal primer to confirm the absence/presentation of the mutation in the amplified KM4F/R PCR product or, alternatively, extract RNA from the cell line, convert to complementary DNA and repeat the PCR and sequencing reactions.

4.2 Optimisation of Diagnostic *Mycoplasma* Contamination PCR

PCR can be used to detect *Mycoplasma* contamination within cell cultures. A protocol developed by Uphoff and Drexler (1999) uses a mix of six primers to target a broad range of *Mycoplasma* species, as well as targeting an internal control that is of a larger size than the positive *Mycoplasma* sample. This method required optimisation in order to develop a molecular assay that the Laboratory of Molecular Genetics could use to detect *Mycoplasma* contamination of imported cell lines.

Firstly, the brand of Taq DNA polymerase differed from the published protocol, which used Taq DNA polymerase supplied by Qiagen, whereas we used Taq DNA polymerase supplied by Intron for PCR experiments (except for one case). This Taq was selected as it came in a prepared master mix, which reduced preparation time and gel loading time since it already contains the gel loading dye. Also, as the master mix is already prepared, pipetting error is reduced, resulting in more reliable results. This Taq is very affordable, and is easily stored in 1 ml aliquots at 4°C.

During PCR, Taq DNA polymerase can be inhibited due to the presence of contaminants such as organic compounds, heavy metals, and constituents of bacterial cells (Wilson, 1997). Therefore, to confirm that the Taq DNA polymerase is unaffected by contaminants, an internal control DNA

sample was incorporated into the PCR reaction mix for every sample tested. The internal control is added at a limiting dilution to the PCR reaction mixture, and the sensitivity of the PCR reaction will therefore be shown on the agarose gel (Uphoff & Drexler, 2011).

Following the recommendation of Uphoff and Drexler's protocol, using a positive *Mycoplamsa* and internal control DNA sample sourced from DSMZ, a band at the expected position for the internal control (986 bp) was present in each sample on the agarose gel, indicating that no inhibiting contaminants were present in the reaction mixture. Therefore amplification was successful using the selected Taq DNA polymerase. However, no band at the expected size of 502-520 bp was present in the *Mycoplasma* positive sample and MDA-MB-436 DNA sample, even though the internal control was amplified in both cases. Therefore, we were unable to conclude that our PCR results for MDA-MB-436 were indeed negative for *Mycoplasma*. To address why the positive *Mycoplasma* sample did not amplify, we investigated if there was any evidence that *Mycoplasma* DNA was present in the sample by using the NanoDrop, if the lyophilised pellet had fully solubilised, and if the purchased primers were correctly ordered, resuspended and finally, confirm their DNA target using bioinformatics analysis.

4.2.1 Validation of the *Mycoplasma* Positive Control Sample

To ensure that the DNA pellet was fully solubilised, the sample was heated at 65°C for 24 hrs. The NanoDrop reading of 0.1 ng/µl showed that there was practically no DNA present in the positive *Mycoplasma* sample. However, the sensitivity of DNA detection for the NanoDrop is reported to be 2-100 ng/ul ± 2 ng/ul (Thermo Fisher Scientific, 2008).

To determine if the primers were the issue, rather than a multiplex PCR, a single primer set was used. No errors were made in the purchase of the primers or in the preparation of the primer stocks. In addition, the nucleotide sequences of primers LMP13-18 were analysed by using the blastn program available on the NCBI database (Appendix 3). Results

showed that the LMP13 (forward) and LMP18 (reverse) hit the internal control *Mycoplasma*, *A. laidlawii,* with 100% nucleotide identity. LMP14, 15, and 16 (forward), and LMP17 (reverse), all hit a broad range of *Mycoplasma* species as expected. Even when using a single primer set (LMP15/17) for PCR, no band was present on the agarose gel at the expected size using the *Mycoplasma* positive sample DNA. However, a band was still observed for the internal control using the LMP13/18 primer set (Figure 19).

Based on these results, it was concluded that the *Mycoplasma* positive DNA sample received from DSMZ did not have enough DNA in the sample for detection using the Intron Taq Polymerase. Therefore, to validate the PCR protocol and test for the presence of *Mycoplasma* contamination in the cell cultures, a new *Mycoplasma* positive sample was required.

4.2.2 Validation of a New *Mycoplasma* Positive Sample

A new *Mycoplasma* positive cell lysate sample was sourced from AgResearch. This sample of NIH 3T3 mouse embryo fibroblast cells had been previously confirmed via PCR to be contaminated with *Mycoplasma*, as opposed to a DNA sample. It was advised to centrifuge the sample prior to use (Olivia Wallace, personal communication, January 13, 2015), and take the template sample from the bottom of the tube where the *Mycoplasma* cells would be present.

The original Uphoff and Drexler protocol was tested using this new *Mycoplasma* positive sample. Again, the internal control band at 986 bp was present for the MDA-MB-436 cell line and the negative control reactions, but interestingly, no internal control band was present for the new *Mycoplasma* positive sample (Figure 20). As mentioned earlier, the internal control is an indicator of inhibitory contaminants in the sample. As no band was present for this sample, it may be possible that there are inhibitory substances present. However, there was still a lack of a PCR band of the expected size for the *Mycoplasma* positive sample.

This inconclusive result may have been due to the Taq DNA polymerase not working effectively. Consequently, the next step in validating the protocol was to investigate the use of a different Taq DNA polymerase.

4.2.3 Validation of a Different Taq DNA Polymerase

The application of HOT FIREPol® DNA Polymerase (Solis BioDyne) for the amplification of the *BRCA1* gene (3.3.1) was successful, and therefore was selected to optimise the PCR diagnostic test. Due to different recommendations from the manufacturer, the PCR conditions were altered, and based on the conditions shown in Table 3. With a change in PCR conditions, no amplification of either the positive *Mycoplasma* sample (502-520 bp) nor the internal control sample (986 bp) was observed on the agarose gel.

In order to validate this protocol further, optimisation of this PCR reaction would be necessary. Factors such as the $MgCl_2$ concentration, the buffer used, the annealing temperature, and the primer and DNA concentration could all be altered to optimise this reaction. However, as the internal control wasn't amplified, but was using the Intron Taq, the final steps of optimisation of this protocol was carried out using the Intron Taq as it was shown to be working in the early stages of optimisation.

The final step in the optimisation of the protocol was to extract DNA from the cell lysate *Mycoplasma* sample received from AgResearch. A second option was obtaining a bacterial sample from the Special Bacteriology and Culture Collection, Institute of Environmental Science and Research Limited, Wellington, New Zealand (Linda Peters, personal communication, January 23, 2015).

4.2.4 Optimisation of the Protocol using Extracted DNA from the *Mycoplasma* Cell Lysate

The DNA from the cell lysate of the *Mycoplasma* positive cell sample received from AgResearch was extracted, purified and concentrated. This *Mycoplasma* DNA sample was then used as a template in the PCR reaction. Even though the NanoDrop did not detect evidence of DNA, the sample was diluted to ensure adequate sample volume was available for future PCR reactions, plus PCR requires a minimum of 300 picograms for bacterial genomes. Thus, a 1:10 dilution was made, and only 1 µl of the diluted DNA sample was added to the PCR reaction mixture. Following PCR using the extracted DNA, Intron Taq and a higher annealing temperature recommended by Uphoff and Drexler (1999), the positive and internal controls were successfully amplified. Using the extracted DNA, the expected band for a *Mycoplasma* positive sample was present, thus confirming optimisation of the protocol. No band was observed on the agarose gel for the negative PCR. Therefore, no contamination was present during the experiment. As a result, the lack of band observed in the SUM149PT and MDA-MB-436 DNA samples indicates that those cell cultures were not contaminated with *Mycoplasma*.

Alternative options are available for the detection of *Mycoplasma* contamination in cell cultures. These include commercial testing facilities, or *Mycoplasma* detection kits. These options could be utilised as a secondary confirmation for the status of cell cultures.

In conclusion, the monitoring of cell morphology, and the turbidity of growth media were used in conjunction with this molecular technique to confirm that the cell cultures utilised during this research thesis were not contaminated with *Mycoplasma.* Therefore, the results obtained can be regarded as a true representation of the effects of Se on these cell lines.

4.3 MTT Assay

The MTT assay was used to investigate the first aim of this research; to assess the viability of the SUM149PT and MDA-MB-436 *BRCA1*-mutated cell lines when treated for 24 hours with sodium selenite and MSA at a concentration range of 0-1000 µM elemental Se. All treatments were carried out in triplicate, and each individual experiment was repeated three times. The same Se compounds and MTT assay kit were used for all experiments for reproducibility purposes.

The SUM149PT cell line showed a significant difference between IC_{50} values of the two Se compounds, with sodium selenite being more cytotoxic than MSA (Figure 23) (p=0.023404, at 95% CI). This result, of an inorganic Se compound being more toxic than an organic Se compound at higher concentrations, is in agreement with Valdiglesia et al., (2010). Clinical studies also suggest this possibility. A cohort of 1135 *BRCA1*-mutation carriers from Poland received an oral supplement of 250 µg daily of sodium selenite for 6-62 months. However, this study was terminated early due to a higher incidence of breast cancer cases in the treatment group (Lubinski et al., 2011). In comparison, a randomised placebo-controlled trial of 35,000 American men who were supplemented with 200 µg of an organic Se compound (selenomethionine) daily showed no increase in the incidence of prostate cancer (Lippman et al., 2009). Thus in human trials using comparable supranutritional doses of Se, organic compounds (selenomethionine) did not lead to increases in cancer cases, whereas, inorganic compounds (sodium selenite) did, again demonstrating the relatively genotoxic effects of the inorganic Se compounds.

In comparison to the SUM149PT cell line, the MDA-MB-436 cell line showed no significant difference between the IC_{50} values of the two Se compounds (Figure 24) (p= 0.155, at 95% CI). This differential effect of the same Se compounds on two *BRCA1*-mutated breast cancer cell lines could indicate that responses to Se could be altered due to genotypic differences. Further analysis into other *BRCA1*-mutated cell lines would help develop a greater understanding on the differential effects of these

compounds due to genotypic differences. Also, differences could be observed with other, non-*BRCA1*-mutated breast cancer cell lines such as MCF-7 and MDA-MB-231, and further analysis into this area will also be very beneficial to gain a greater, overall, understanding of the effects of Se.

For both the SUM149PT and MDA-MB-436 cell line, the OD readings of the MTT plate at the lower sodium selenite concentrations showed great variation, producing large error bars. When the solubilising solution was added to the wells to dissolve the formazan crystals, a yellowy-brown solution remained (as opposed to the expected purple/blue colour). The absorbance at this colour produced much lower OD values than the purple/blue solution. In addition, at lower concentrations of sodium selenite, the occasional well would appear purple, which lead to large error bars at these concentrations.

The yellowy-brown colour produced during the MTT assay may be due to the pH of the solution, but that does not account for the discrepancies between the triplicates during the single experiment in which all wells were treated with the same solutions. The lower concentrations (0-10 µM) represent the levels of Se pharmacologically-achievable in humans. Therefore, further analysis into the cause of these few purple/blue wells is necessary to produce reliable results without as much variability between wells.

The negative inhibition values seen from 1-50 µM for sodium selenite and 1-500 µM for MSA with the SUM149PT cell line (Figure 23), and 1-100 µM for sodium selenite and 1-10 µM for MSA with the MDA-MB-436 cell line (Figure 24) represent increased growth rates in comparison to the controls (0 µM Se). This leads to the conclusion that, at lower concentrations, Se promotes cell growth and survival, but then becomes toxic to the cells at higher concentrations. This result was similar for the sodium selenite treatment between the two cell lines (1-50 µM for SUM149PT and 1-100 µM for MDA-MB-436). However, due to the great variation at these

lower concentrations, there are no observable trends with this treatment, and the effects cannot be predicted.

For the MSA treatment, the variability between the two cell lines in the concentration range at which increased growth occurred was very large (1-500 µM for SUM149PT and 1-10 µM for MDA-MB-436). This difference between the two cell lines could again indicate different effects of the Se compounds due to genotypic differences. However, overall, there is much more of a linear trend observed with MSA, which suggests that the effects of this compound are more predictable than with selenite, which is an important characteristic clinically. Also, although no increase in growth was observed for the MDA-MB-436 cell line with MSA, the lower concentrations of MSA didn't affect the growth of the cells, as the inhibition rate stayed consistently at 0% until the concentration increased beyond physiological levels of Se.

In conclusion, the overall trend observed with these results supports the observation from other clinical investigators that sodium selenite, an inorganic form of Se, is more genotoxic than MSA, an organic form of Se. However, there is the possibility that the effects of Se may differ due to genotypic differences between cell lines . Over time, cell lines accumulate genomic aberrations, resulting in differences between the same cell line from two different suppliers, and differences from the original primary tumour (Burdall, Hanby, Lansdown, & Speirs, 2003; Tsuji et al., 2010). Also, only a partial sequence of the *BRCA1* gene has been sequenced, but other harmful mutations may be present, which could again alter the effects observed in the different cell lines. As a result, the observed effects of Se on these particular cell lines may not be a true representation of the effects Se would have *in vivo* due to differences in genotype, and a lack of cell-cell interactions that would be present in the primary tumour (Burdall et al., 2003; Tsuji et al., 2010). Therefore, further investigation is required to develop a greater understanding of the effects of Se (see 6.1).

4.4 Comet Assay

The second part of the aim was to investigate the differential effects of the two Se compounds on the levels of DNA damage in the two cell lines using the comet assay.

Due to the nature of the comet assay protocol, the cells are subjected to great stress as a result of mechanical manipulation. This could, in turn, result in bias in the results, leading to greater levels of DNA damage being observed. This issue is not able to be completely avoided, but could be minimised and kept uniform across all treatments and experiments by ensuring all cells were manipulated for the same amount of time, and subjected to the same conditions across each replicate.

All comet assay analysis was completed using the CometScore software (TriTek) which measured all the variables within each individual comet to present overall calculations of comets. For the purposes of this research thesis, the percentage of DNA present in the tail calculation (% DNA in tail) was analysed as this directly correlated with the percentage of damaged DNA in each cell (damaged DNA is found in the tail of the comet). For every treatment well, two slides were prepared, and approximately 50 comets were analysed per slide to ensure a fair representation of the cells was analysed. The CometScore software was reliable, and visual scoring of the comets matched the calculations performed by the software.

The SUM149PT cell line was treated with one quarter and one half of the preliminary IC_{50} values obtained via the MTT assay; the cells were treated with 12.5 and 25 µM sodium selenite, and 25 and 50 µM MSA. Analysis found that sodium selenite was more genotoxic in comparison to MSA at both one quarter, and one half of their respective IC_{50} values (Figure 27). This again coincides with research stating that inorganic forms of Se are more genotoxic than organic forms (Valdiglesias et al., 2010). Interestingly, there was a statistically significant difference between the levels of DNA damage present in the control selenite and MSA treatment

wells (0 µM Se), with a *p*-value of 0.0003 (95% CI). Specifically, the level of DNA damage was lower in cells in the control wells on the plates in which MSA was present in other (treatment) wells than that found in cells in control wells on selenite plates. The two Se compounds were incubated on separate culture plates in two different incubators. It has been reported that metabolism of MSA produces the two volatile Se species, dimethylselenide and dimethyldiselenide, within 10-20 minutes after exposure. These two volatile species (which could be smelt in the incubator in which MSA was present) are metabolites of selenol (the active form of Se in the body), and are considered to be the most potent, biologically active form of Se (Jüliger, Goenaga-Infante, Lister, Fitzgibbon, & Joel, 2007). It is possible that these volatile species produced by MSA metabolism resulted in significant exposure of cells in control wells on these MSA plates to biologically-active Se and may thus be responsible for the observed decrease in DNA damage in control cells on MSA plates compared to control cells on selenite plates.

A demonstration of the relatively low genotoxicity of MSA is the lower levels of DNA damage produced by 50 µM of MSA (1/2 IC_{50}) compared to that measured in cells from the control wells on sodium selenite plates (Figure 27). While this difference was not statistically significant, it indicates that MSA is not increasing DNA damage in the cells at these concentrations; in fact the exposure to volatile Se compounds reduced the native DNA damage present in this malignant cell line under these conditions.

At elemental Se concentrations far in excess of those achievable nutritionally, let alone the optimal levels of plasma Se (1.65 µM) in the body (Rayman, 2012), each Se compound induced a significant increase in the levels of DNA damage. These Se concentrations are known to be toxic *in vivo.* Therefore to better understand the effects of these Se compounds on the levels of DNA damage in cells, lower concentrations around the optimal levels of plasma Se would be more beneficial to demonstrate the effects that these compounds could have on the body.

Following on from the results obtained with Se treatments alone, the effects of Se on induced DNA damage were investigated to determine if Se was capable of reducing the levels of damage present. The SUM149PT cells were treated with the lowest dose of sodium selenite used in the initial comet assay (12.5 µM). Bleomycin induced significant levels of DNA damage to control cells, and when allowed a repair phase, the cells were not able to repair the DNA strand breaks, with levels of damage increasing by a small, non-significant amount (Figure 29). In comparison, there was no statistically significant difference between the levels of damage present in the 12.5 µM sodium selenite treatment and the same treatment plus bleomycin. This suggests that the effects of bleomycin are reduced when cells are pre-treated with Se. Also, the levels of damage present in the cells that underwent a repair incubation phase, compared to those that did not have a repair phase was not statistically different. The difference between the levels of DNA damage produced when treated with Se alone in Figure 27 and Figure 29 is very large, despite both being treated with the same concentration (12.5 µM). The data produced with the bleomycin incubation is only preliminary, therefore, further investigations into the cause of this vast difference is necessary.

In comparison to these results, other research has shown a reduction in the levels of DNA damage when *BRCA1*-mutation carriers were supplemented with 140 µg of sodium selenite orally daily (Kowalska et al., 2005). The concentration of sodium selenite that those *BRCA1*-mutation carriers were treated with was close to optimal plasma concentrations of Se (140 µg = ~1.75 µM), whereas the SUM149PT cells in this experiment were treated with a much higher dose (12.5 µM). The very high levels of damage that were produced with bleomycin in addition to the high concentrations of Se, and the lack of DNA repair, may be due to concentrations of Se that are reaching toxic levels in the cells. A decrease in the levels of initial DNA damage, and an increase in the repair capacity of the cells might be observed if the concentration of Se is dropped to a more physiologically relevant concentration.

The MDA-MB-436 cell line was then treated with a more physiologically relevant concentration (2 µM) of the two Se compounds, and incubated on the same plate. Preliminary results again demonstrated the higher genotoxicity of sodium selenite in comparison to MSA, with statistical significance between the levels of DNA damage with the two treatments (Figure 28). The levels of damage present in the MSA treated cells was lower than that of the control, but not at statistically significant levels. This indicates that low levels of MSA do not affect the normal baseline levels of DNA damage present in the cells. In comparison, there was a great difference between the levels of DNA damage present in the controls and with sodium selenite treatment.

The control treatment for this experiment again demonstrates the low DNA damage levels seen when MSA is present on the plate. In contrast, the levels of damage produced by a low concentration of sodium selenite were comparable to the levels of damage present in the control when only the sodium selenite treatment was present in the plate. These lower levels of DNA damage observed in control cells when incubated on a plate with MSA suggest that the volatile metabolites of MSA, which appear to produce protective effects in the cells, could be masking the effects of sodium selenite when incubated on the same plate. To obtain a true evaluation of the effects of sodium selenite at these physiologically relevant concentrations, separate plates for each treatment are necessary to cancel out any effects the MSA metabolites may have on the cells.

Overall, these results show the more positive effects of Se at physiologically relevant Se concentrations and again demonstrate the beneficial effects of organic Se compounds in reducing DNA damage levels in *BRCA1*-mutated cells. If these lower levels of Se were to be tested with bleomycin, similar results to the work by Kowalska et al. (2005) might be seen.

In conclusion, the overall trend of the data supported the contention that sodium selenite is more genotoxic than MSA. The initial concentrations of Se to which the *BRCA1*-mutated cells were subjected were too high to

represent physiological plasma Se concentrations. Possibly as a result of this, an enhanced DNA repair capacity on induced DNA strand breaks was not visible with these Se compounds. Lower, more physiologically relevant concentrations of Se showed more promising results in terms of lower levels of DNA damage, and further investigation into these lower levels with bleomycin might produce results that hopefully support the research emphasising the valuable DNA repair capacity of Se.

Chapter Five

Conclusions

The original aim of this research was to investigate the *in vitro* toxicity of inorganic and organic Se compounds to human *BRCA1*-mutated cancer cells, as well as non-*BRCA1*-mutated cancer cells, by evaluating a) the dose-response for lethality of sodium selenite and MSA, and b) the dose-response of these two Se compounds on native and bleomycin-induced DNA damage. The hypothesis is that inorganic forms of Se are more genotoxic than organic Se compounds and therefore the latter are likely to be more suitable as chemoprotective agents against breast cancer.

The data presented within this thesis demonstrates that a commonly-used inorganic form of Se, sodium selenite, is more genotoxic than the organic Se compound, MSA, in two malignant *BRCA1*-mutated cell lines.

Sodium selenite also has more direct cytotoxicity in these cells than MSA, as demonstrated by the MTT assay.

However the enhanced repair capacity from Se on DNA damage in cells demonstrated by others has not been reproduced, though preliminary data testing the effects of lower doses of Se show promising results. Interestingly, the volatile metabolites produced from MSA appear to reduce DNA damage, also supportive of this hypothesis.

The next chapter outlines future recommendations for the detection of *Mycoplasma* contamination, the validation of the differential genotoxicity of inorganic vs. organic Se compounds, and the increased repair capacity of Se in breast cancer.

Chapter Six

Future Recommendations

Based on the results obtained in this thesis, the following five recommendations are suggested for future experiments.

6.1 Non-malignant Cell Lines

This *in vitro* project evaluated Se in *BRCA1*-mutated cancer cells. Using these cells will provide preliminary data on DNA damage modification with differing Se compounds and concentrations and may suggest appropriate dosing guidelines. However, an option that would provide information into the effects of Se on non-malignant *BRCA1*-mutated cells is to use PMBC from *BRCA1*-mutation carriers. Thus, the first recommendation, in order to develop a greater understanding of the effects of Se as a possible chemopreventive agent, is to carry out these experiments (MTT assay and comet assay) on PBMC obtained from *BRCA1* carriers who have not yet presented with breast cancer. It is noted that an application for ethical approval would be required so individuals who are *BRCA1*-mutation carriers could give their informed consent to participate in this study.

6.2 *Mycoplasma* Contamination PCR

The internal control (DSMZ) and positive *Mycoplasma* (AgResearch) DNA samples were used in the optimised PCR protocol for the detection of *Mycoplasma* contamination. The PCR amplicons were of the correct size on the agarose gel for each sample, but the nucleotide sequence was not determined to validate that the samples received contained the expected

DNA. Therefore, it is recommended that these PCR amplicons be purified and sequenced.

6.3 MTT Assay

Results were obtained from the MTT assay on the two *BRCA1*-mutated cell lines treated with the two Se compounds at a concentration range of 0-1000 µM. The effects of the two Se compounds were quite variable at the lower concentrations (1-10 µM). The lower concentrations are more representative of physiologically obtainable Se plasma levels (with pharmacological dosing) and, therefore, a more thorough evaluation of the effects of these two compounds at these concentrations is necessary.

Also, the MTT assay was only carried out on *BRCA1*-mutated cell lines. In order to understand if the effects observed are linked specifically to the *BRCA1* mutation or breast cancer in general, it is recommended that other, non-*BRCA1*-mutated breast cancer cell lines such as MCF-7 (see 1.8) be tested to evaluate the effects.

6.4 Comet Assay

Results obtained from the comet assay on the two *BRCA1*-mutated cell lines treated with the two Se compounds provided preliminary data into the effects of Se on DNA damage and repair in the cells. At this stage, the DNA repair capacity of Se has not been clearly demonstrated in this work, but these recommendations for future experiments may help elucidate the action of Se.

The first recommendation is to repeat the experiment at least twice more, treating the MDA-MB-436 cell line with 1-2.5 µM concentrations of both sodium selenite and MSA. This will produce reproducible data for that cell line and demonstrate the effects of Se at these lower concentrations. Following this, the SUM149PT cell line will need to be tested at these

concentrations as well to allow more reliable comparisons between the two *BRCA1*-mutated cell lines. Additional investigations into differences that occur between co-incubation of the two Se compounds and separate incubations should be carried out to determine if the volatile Se metabolites produced by MSA influence the results obtained for the sodium selenite treatment.

The second recommendation is to repeat the experiment with the bleomycin/repair incubation, but at lower Se concentration (1-2.5 µM) on both cell lines. As these lower concentrations are comparable to the range of physiological levels of plasma Se seen clinically, the DNA repair capacity of Se could be better determined, and may suggest a threshold concentration above which each Se compound may show toxicity as opposed to beneficial effects.

The final recommendation is to repeat these experiments on non-*BRCA1*-mutated cell lines. This will determine if the observed effects of Se are linked specifically to *BRCA1* mutations or to breast cancer in general.

6.5 Alternative Methodologies

An alternative method to investigate the levels of DNA damage in cells is LORD-Q PCR. LORD-Q is a high-sensitivity, real-time PCR technique that produces sequence-specific quantification of DNA damage present in both mitochondrial and genomic DNA, in comparison to the comet assay which only provides information on global DNA damage (Lehle et al., 2014). This procedure would reduce the time necessary to obtain results as it produces quantitative results rapidly in comparison to the comet assay. It also eliminates the unknown biases that are encountered with the comet assay due to manual manipulation during each step of the procedure. Therefore, a greater, more reliable amount of information on the effects of Se on DNA damage in cells would be able to be collated in a shorter span of time.

Also, as it is thought that Se enhances the DNA repair capacity of cells, it would be of interest to determine the repair genes that are affected. Possible DNA repair candidates could be identified through full transcriptome analysis, and quantitative PCR could then be used to determine the effects of Se on these particular genes. This would generate a broader understanding of the effects of Se, and could result in many exciting discoveries.

6.6 Conclusion

Overall, the five recommendations stated above will further refine and evaluate the effects of Se at physiologically relevant levels of Se. Through the testing of other non-*BRCA1*-mutated breast cancer cell lines, the observed effects of Se can be linked to either the *BRCA1* mutation, or to breast cancer in general.

References

Abdulah, R., Miyazaki, K., Nakazawa, M., & Koyama, H. (2005). Chemical forms of selenium for cancer prevention. *Journal of Trace Elements in Medicine and Biology, 19*(2–3), 141-150. doi: http://dx.doi.org/10.1016/j.jtemb.2005.09.003

Aro, A., Alfthan, G., & Varo, P. (1995). Effects of supplementation of fertilizers on human selenium status in Finland. *Analyst, 120*(3), 841-843. doi: 10.1039/AN9952000841

Arpino, G., Bardou, V., Clark, G., & Elledge, R. (2004). Infiltrating lobular carcinoma of the breast: tumor characteristics and clinical outcome. *Breast Cancer Res, 6*(3), R149 - R156.

Arps, D., Healy, P., Zhao, L., Kleer, C., & Pang, J. (2013). Invasive ductal carcinoma with lobular features: a comparison study to invasive ductal and invasive lobular carcinomas of the breast. *Breast Cancer Research and Treatment, 138*(3), 719-726. doi: 10.1007/s10549-013-2493-2

Asterand. (2014). Instructions for Growth of SUM149PT Cell Line. Retrieved 7 October, 2014, from http://www.asterand.com/Asterand/human_tissues/Instructions%20for%20Growth%20of%20SUM149PT%20Cell%20Line.pdf

ATCC. (2014a). MCF7 (ATCC® HTB-22™). Retrieved 2 October, 2014, from http://www.atcc.org/products/all/HTB-22.aspx

ATCC. (2014b). MDA-MB-231 (ATCC® HTB-26™). Retrieved 2 October, 2014, from http://www.atcc.org/products/all/HTB-26.aspx

ATCC. (2014c). MDA-MB-436 (ATCC® HTB-130™). Retrieved 2 October, 2014, from http://www.atcc.org/products/all/HTB-130.aspx

Baliga, M., Wang, H., Zhuo, P., Schwartz, J., & Diamond, A. (2007). Selenium and GPx-1 overexpression protect mammalian cells against UV-induced DNA damage. *Biological Trace Element Research, 115*(3), 227-241. doi: 10.1007/BF02685998

Barber, M., Thomas, J., & Dixon, J. M. (2008). *Epidemiology of breast cancer*. Oxford: Clinical Publishing, An Imprint of Atlas Medical Publishing Ltd.

Bera, S., Rosa, V. D., Rachidi, W., & Diamond, A. M. (2013). Does a role for selenium in DNA damage repair explain apparent controversies in its use in chemoprevention? *Mutagenesis, 28*(2), 127-134. doi: 10.1093/mutage/ges064

Berry, M. J., Banu, L., Chen, Y., Mandel, S. J., Kieffer, J. D., Harney, J. W., & Larsen, P. R. (1991). Recognition of UGA as a selenocysteine codon in Type I deiodinase requires sequences in the 3' untranslated region. *Nature, 353*, 273-276. doi: 10.1038/353273a0

Böck, A. (2000). Biosynthesis of selenoproteins — an overview. *BioFactors, 11*(1-2), 77-78. doi: 10.1002/biof.5520110122

Boeri, L., Canzonieri, C., Cagioni, C., Ornati, F., & Danesino, C. (2011). Breast cancer and genetics. *Journal of Ultrasound, 14*(4), 171-176. doi: doi.org/10.1016/j.jus.2011.10.002

Borzekowski, D. L. G., Guan, Y., Smith, K. C., Erby, L. H., & Roter, D. L. (2014). The Angelina effect: immediate reach, grasp, and impact of going public. *Genet Med, 16*(7), 516-521. doi: 10.1038/gim.2013.181

Bravard, A., Vacher, M., Moritz, E., Vaslin, L., Hall, J., Epe, B., & Radicella, J. P. (2009). Oxidation Status of Human OGG1-S326C Polymorphic Variant Determines Cellular DNA Repair Capacity. *Cancer Research, 69*(8), 3642-3649. doi: 10.1158/0008-5472.can-08-3943

Brinkley, B. R., Beall, P. T., Wible, L. J., Mace, M. L., Turner, D. S., & Cailleau, R. M. (1980). Variations in Cell Form and Cytoskeleton in Human Breast Carcinoma Cells in Vitro. *Cancer Research, 40*(9), 3118-3129.

Budiman, M. E., Bubenik, J. L., Miniard, A. C., Middleton, L. M., Gerber, C. A., Cash, A., & Driscoll, D. M. (2009). Eukaryotic Initiation Factor 4a3 Is a Selenium-Regulated RNA-Binding Protein that Selectively Inhibits Selenocysteine Incorporation. *Molecular Cell, 35*(4), 479-489. doi: 10.1016/j.molcel.2009.06.026

Burdall, S., Hanby, A., Lansdown, M., & Speirs, V. (2003). Breast cancer cell lines: friend or foe? *Breast Cancer Res, 5*(2), 89 - 95.

Cailleau, R., Olivé, M., & Cruciger, Q. V. J. (1978). Long-Term Human Breast Carcinoma Cell Lines of Metastatic Origin: Preliminary Characterization. *In Vitro, 14*(11), 911-915. doi: 10.2307/4292143

Chavatte, L., Brown, B. A., & Driscoll, D. M. (2005). Ribosomal protein L30 is a component of the UGA-selenocysteine recoding machinery in eukaryotes. *Nat Struct Mol Biol, 12*(5), 408-416. doi: http://www.nature.com/nsmb/journal/v12/n5/suppinfo/nsmb922_S1.html

Chavez, K. J., Garimella, S. V., & Lipkowitz, S. (2010). Triple negative breast cancer cell lines: One tool in the search for better treatment of triple negative breast cancer. *Breast Disease, 32*(1), 35-48. doi: 10.3233/BD-2010-0307

Combs, G., Jr., & Lü, J. (2006). Selenium as a cancer preventive agent. In D. Hatfield, M. Berry & V. Gladyshev (Eds.), *Selenium* (pp. 249-264): Springer US.

Combs, G. F. (2001). Selenium in global food systems. *British Journal of Nutrition, 85*(05), 517-547. doi: doi:10.1079/BJN2000280

Combs Jr, G. F., & Gray, W. P. (1998). Chemopreventive Agents: Selenium. *Pharmacology & Therapeutics, 79*(3), 179-192. doi: http://dx.doi.org/10.1016/S0163-7258(98)00014-X

Copeland, P. R., Fletcher, J. E., Carlson, B. A., Hatfield, D. L., & Driscoll, D. M. (2000). A novel RNA binding protein, SBP2, is required for the translation of mammalian selenoprotein mRNAs. *The EMBO Journal, 19*(2), 306-314.

Crossan, H. (2014). *Characterisation of VMO1 in Human Tissues.* (MSc), University of Waikato.

Davies, E. L. (2012). Breast cancer. *Medicine, 40*(1), 5-9. doi: doi.org/10.1016/j.mpmed.2011.09.010

de Rosa, V., Erkekoğlu, P., Forestier, A., Favier, A., Hincal, F., Diamond, A. M., . . . Rachidi, W. (2012). Low doses of selenium specifically stimulate the repair of oxidative DNA damage in LNCaP prostate cancer cells. *Free Radical Research, 46*(2), 105-116. doi: doi:10.3109/10715762.2011.647009

Diamond, A., Dudock, B., & Hatfield, D. (1981). Structure and properties of a bovine liver UGA suppressor serine tRNA with a tryptophan anticodon. *Cell, 25*(2), 497-506. doi: 10.1016/0092-8674(81)90068-4

Diamond, A. M., Choi, I. S., Crain, P. F., Hashizume, T., Pomerantz, S. C., Cruz, R., . . . McCloskey, J. A. (1993). Dietary selenium affects methylation of the wobble nucleoside in the anticodon of selenocysteine tRNA([Ser]Sec). *Journal of Biological Chemistry, 268*(19), 14215-14223.

Elstrodt, F., Hollestelle, A., Nagel, J. H. A., Gorin, M., Wasielewski, M., van den Ouweland, A., . . . Schutte, M. (2006). BRCA1 Mutation Analysis of 41 Human Breast Cancer Cell Lines Reveals Three New Deleterious Mutants. *Cancer Research, 66*(1), 41-45. doi: 10.1158/0008-5472.can-05-2853

Ethier, S. P., Mahacek, M. L., Gullick, W. J., Frank, T. S., & Weber, B. L. (1993). Differential Isolation of Normal Luminal Mammary Epithelial Cells and Breast Cancer Cells from Primary and Metastatic Sites Using Selective Media. *Cancer Research, 53*(3), 627-635.

Forozan, F., Veldman, R., Ammerman, C. A., Parsa, N. Z., Kallioniemi, A., Kallioniemi, O. P., & Ethier, S. P. (1999). Molecular cytogenetic analysis of 11 new breast cancer cell lines. *British Journal of Cancer, 81*(8), 1328-1334. doi: 10.1038/sj.bjc.6695007

Gammelgaard, B., Jackson, M., & Gabel-Jensen, C. (2011). Surveying selenium speciation from soil to cell—forms and transformations. *Analytical and Bioanalytical Chemistry, 399*(5), 1743-1763. doi: 10.1007/s00216-010-4212-8

Guimarães, M. J., Peterson, D., Vicari, A., Cocks, B. G., Copeland, N. G., Gilbert, D. J., . . . Zlotnik, A. (1996). Identification of a novel selD homolog from Eukaryotes, Bacteria, and Archaea: Is there an autoregulatory mechanism in selenocysteine metabolism? *Proceedings of the National Academy of Sciences, 93*(26), 15086-15091.

Hall, J. M., Lee, M. K., Newman, B., Morrow, J. E., Anderson, L. A., Huey, B., & King, M.-C. (1990). Linkage of Early-Onset Familial Breast Cancer to Chromosome 17q21. *Science, 250*(4988), 1684-1689. doi: 10.2307/2878541

Hanahan, D., & Weinberg, Robert A. (2011). Hallmarks of Cancer: The Next Generation. *Cell, 144*(5), 646-674. doi: http://dx.doi.org/10.1016/j.cell.2011.02.013

Hatfield, D., Lee, B. J., Hampton, L., & Diamond, A. M. (1991). Selenium induces changes in the selenocysteine tRNA[Ser]Sec population in mammalian cells. *Nucleic Acids Research, 19*(4), 939-943. doi: 10.1093/nar/19.4.939

Hatfield, D. L., Carlson, B. A., Xu, X. M., Mix, H., & Gladyshev, V. N. (2006). Selenocysteine Incorporation Machinery and the Role of Selenoproteins in Development and Health. In M. Kivie (Ed.), *Progress in Nucleic Acid Research and Molecular Biology* (Vol. Volume 81, pp. 97-142): Academic Press.

Hatfield, D. L., Tsuji, P. A., Carlson, B. A., & Gladyshev, V. N. (2014). Selenium and selenocysteine: roles in cancer, health, and development. *Trends in Biochemical Sciences, 39*(3), 112-120. doi: 10.1016/j.tibs.2013.12.007

Ip, C. (1981). Prophylaxis of Mammary Neoplasia by Selenium Supplementation in the Initiation and Promotion Phases of Chemical Carcinogenesis. *Cancer Research, 41*(11 Part 1), 4386-4390.

Ip, C., & Ip, M. M. (1981). Chemoprevention of mammary tumorigenesis by a combined regimen of selenium and vitamin A. *Carcinogenesis, 2*(9), 915-918. doi: 10.1093/carcin/2.9.915

Ip, C., & Sinha, D. (1981). Anticarcinogenic effect of selenium in rats treated with dimethylbenz[a]anthracene and fed different levels and types of fat. *Carcinogenesis, 2*(5), 435-438. doi: 10.1093/carcin/2.5.435

Johnson, C. C., Fordyce, F. M., & Rayman, M. P. (2010). Symposium on 'Geographical and geological influences on nutrition' Factors controlling the distribution of selenium in the environment and their impact on health and nutrition. *Proceedings of the Nutrition Society, 69*(01), 119-132. doi: doi:10.1017/S0029665109991807

Judson, P. L., & Van Le, L. (1998). Familial breast and ovarian cancer: the role of the BRCA genes. *Primary Care Update for OB/GYNS, 5*(3), 140-143. doi: doi.org/10.1016/S1068-607X(98)00020-1

Jüliger, S., Goenaga-Infante, H., Lister, T. A., Fitzgibbon, J., & Joel, S. P. (2007). Chemosensitization of B-Cell Lymphomas by Methylseleninic Acid Involves Nuclear Factor-κB Inhibition and the Rapid Generation of Other Selenium Species. *Cancer Research, 67*(22), 10984-10992. doi: 10.1158/0008-5472.can-07-0519

Kamenova, K., Reshef, A., & Caulfield, T. (2014). Angelina Jolie/'s faulty gene: newspaper coverage of a celebrity/'s preventive bilateral mastectomy in Canada, the United

States, and the United Kingdom. *Genet Med, 16*(7), 522-528. doi: 10.1038/gim.2013.199

Karunasinghe, N., Ryan, J., Tuckey, J., Masters, J., Jamieson, M., Clarke, L. C., . . . Ferguson, L. R. (2004). DNA Stability and Serum Selenium Levels in a High-Risk Group for Prostate Cancer. *Cancer Epidemiology Biomarkers & Prevention, 13*(3), 391-397.

Key, T. J., Verkasalo, P. K., & Banks, E. (2001). Epidemiology of breast cancer. *The Lancet Oncology, 2*(3), 133-140. doi: doi.org/10.1016/S1470-2045(00)00254-0

Kluger, J., & Park, A. (2013, May 27). The Angelina Effect. *Time*.

Kowalska, E., Narod, S. A., Huzarski, T., Zajaczek, S., Huzarska, J., Gorski, B., & Lubinski, J. (2005). Increased Rates of Chromosome Breakage in BRCA1 Carriers Are Normalized by Oral Selenium Supplementation. *Cancer Epidemiology Biomarkers & Prevention, 14*(5), 1302-1306. doi: 10.1158/1055-9965.epi-03-0448

Krol, A. (2002). Evolutionarily different RNA motifs and RNA–protein complexes to achieve selenoprotein synthesis. *Biochimie, 84*(8), 765-774. doi: http://dx.doi.org/10.1016/S0300-9084(02)01405-0

Kryukov, G. V., Castellano, S., Novoselov, S. V., Lobanov, A. V., Zehtab, O., Guigó, R., & Gladyshev, V. N. (2003). Characterization of Mammalian Selenoproteomes. *Science, 300*(5624), 1439-1443. doi: 10.2307/3833993

Labunskyy, V. M., Hatfield, D. L., & Gladyshev, V. N. (2014). Selenoproteins: Molecular Pathways and Physiological Roles. *Physiological Reviews, 94*(3), 739-777.

Laffon, B., Valdiglesias, V., Pásaro, E., & Méndez, J. (2010). The Organic Selenium Compound Selenomethionine Modulates Bleomycin-Induced DNA Damage and Repair in Human Leukocytes. *Biological Trace Element Research, 133*(1), 12-19. doi: 10.1007/s12011-009-8407-9

Lee, B. J., Worland, P. J., Davis, J. N., Stadtman, T. C., & Hatfield, D. L. (1989). Identification of a selenocysteyl-tRNA(Ser) in mammalian cells that recognizes the nonsense codon, UGA. *Journal of Biological Chemistry, 264*(17), 9724-9727.

Lehle, S., Hildebrand, D. G., Merz, B., Malak, P. N., Becker, M. S., Schmezer, P., . . . Rothfuss, O. (2014). LORD-Q: a long-run real-time PCR-based DNA-damage quantification method for nuclear and mitochondrial genome analysis. *Nucleic Acids Research, 42*(6), e41. doi: 10.1093/nar/gkt1349

Levenson, A. S., & Jordan, V. C. (1997). MCF-7: The First Hormone-responsive Breast Cancer Cell Line. *Cancer Research, 57*(15), 3071-3078.

Li, C. I., Uribe, D. J., & Daling, J. R. (2005). Clinical characteristics of different histologic types of breast cancer. *British Journal of Cancer, 93*, 1046–1052. doi: doi:10.1038/sj.bjc.6602787

Lippman, S. M., Klein, E. A., Goodman, P. J., & et al. (2009). Effect of selenium and vitamin e on risk of prostate cancer and other cancers: The selenium and vitamin e cancer prevention trial (select). *JAMA, 301*(1), 39-51. doi: 10.1001/jama.2008.864

Lobanov, A. V., Hatfield, D. L., & Gladyshev, V. N. (2009). Eukaryotic selenoproteins and selenoproteomes. *Biochimica et Biophysica Acta (BBA) - General Subjects, 1790*(11), 1424-1428. doi: http://dx.doi.org/10.1016/j.bbagen.2009.05.014

Low, S. C., Grundner-Culemann, E., Harney, J. W., & Berry, M. J. (2000). SECIS–SBP2 interactions dictate selenocysteine incorporation efficiency and selenoprotein hierarchy. *The EMBO Journal, 19*(24), 6882-6890.

Lubinski, J., Jaworska, K., Durda, K., Jakubowska, A., Huzarski, T., Byrski, T., . . . Narod, S. (2011). Selenium and the risk of cancer in BRCA1 carriers. *Hereditary Cancer in Clinical Practice, 9*(Suppl 2), A5.

Lymberis, S. C., Parhar, P. K., Katsoulakis, E., & Formenti, S. C. (2004). Pharmacogenomics and breast cancer. *Pharmacogenomics, 5*(1), 31-55.

MacMahon, B. (2006). Epidemiology and the causes of breast cancer. *International Journal of Cancer, 118*(10), 2373-2378. doi: 10.1002/ijc.21404

Medina, D., & Shepherd, F. (1980). Selenium-mediated inhibition of mouse mammary tumorigenesis. *Cancer Letters, 8*(3), 241-245. doi: http://dx.doi.org/10.1016/0304-3835(80)90009-9

Meerloo, J., Kaspers, G. L., & Cloos, J. (2011). Cell Sensitivity Assays: The MTT Assay. In I. A. Cree (Ed.), *Cancer Cell Culture* (Vol. 731, pp. 237-245): Humana Press.

Miniard, A. C., Middleton, L. M., Budiman, M. E., Gerber, C. A., & Driscoll, D. M. (2010). Nucleolin binds to a subset of selenoprotein mRNAs and regulates their expression. *Nucleic Acids Research, 38*(14), 4807-4820. doi: 10.1093/nar/gkq247

Ministry of Health. (2012). Cancer: New Registrations and Deaths 2009.

Ministry of Health. (2014). *Cancer: New Registrations and Deaths 2011*. Ministry of Health.

Mosmann, T. (1983). Rapid colorimetric assay for cellular growth and survival: Application to proliferation and cytotoxicity assays. *Journal of Immunological Methods, 65*(1–2), 55-63. doi: http://dx.doi.org/10.1016/0022-1759(83)90303-4

Murray, A. J. (2010). The genetics of breast cancer. *Surgery (Oxford), 28*(3), 103-106. doi: doi.org/10.1016/j.mpsur.2009.11.005

Murray, A. J., & Davies, D. M. (2013). The genetics of breast cancer. *Surgery (Oxford), 31*(1), 1-3. doi: doi.org/10.1016/j.mpsur.2012.10.019

Nathanson, K. N., Wooster, R., & Weber, B. L. (2001). Breast cancer genetics: What we know and what we need. *Nature Medicine, 7*(5), 552-556. doi: doi.org/10.1038/87876

Navarro-Alarcon, M., & Cabrera-Vique, C. (2008). Selenium in food and the human body: A review. *Science of The Total Environment, 400*(1–3), 115-141. doi: http://dx.doi.org/10.1016/j.scitotenv.2008.06.024

NCBI BLAST (Basic Local Alignment Search Tool). (2013). Blastp of Human Breast Cancer type 1 against Human Breast Cancer type 2. Retrieved 9 August, 2013, from http://blast.ncbi.nlm.nih.gov/Blast.cgi

NCBI ClinVar. (2013a). BRCA1 genetic variants of clinical significance. Retrieved 9 August 2013, from http://www.ncbi.nlm.nih.gov/clinvar?term=BRCA1

NCBI ClinVar. (2013b). ClinVar. Retrieved 9 August, 2013, from http://www.ncbi.nlm.nih.gov/clinvar/

NCBI GenBank. (2013a). Homo sapiens breast cancer 1, early onset (BRCA1), RefSeqGene (LRG_292) on chromosome 17. Retrieved 9 August, 2013, from http://www.ncbi.nlm.nih.gov/nuccore/NG_005905.2

NCBI GenBank. (2013b). Homo sapiens breast cancer 2, early onset (BRCA2), RefSeqGene (LRG_293) on chromosome 13. Retrieved 9 August, 2013, from http://www.ncbi.nlm.nih.gov/nuccore/NG_012772.3

NCBI HomoloGene. (2013). HomoloGene:5276. Gene conserved in Amniota. Retrieved 9 August, 2013, from http://www.ncbi.nlm.nih.gov/homologene?LinkName=gene_homologene&from_uid=672

Ohama, T., Yang, D. C. H., & Hatfield, D. L. (1994). Selenocysteine tRNA and Serine tRNA Are Aminoacylated by the Same Synthetase, but May Manifest Different Identities with Respect to the Long Extra Arm. *Archives of Biochemistry and Biophysics, 315*(2), 293-301. doi: http://dx.doi.org/10.1006/abbi.1994.1503

Orban, T. I., & Olah, E. (2003). Emerging roles of BRCA1 alternative splicing. *Journal of Clinical Pathology, 56*(4), 191-197.

Ostling, O., & Johanson, K. J. (1984). Microelectrophoretic study of radiation-induced DNA damages in individual mammalian cells. *Biochemical and Biophysical Research Communications, 123*(1), 291-298. doi: http://dx.doi.org/10.1016/0006-291X(84)90411-X

Painter, E. P. (1941). The Chemistry and Toxicity of Selenium Compounds, with Special Reference to the Selenium Problem. *Chemical Reviews, 28*(2), 179-213. doi: 10.1021/cr60090a001

Pecorino, L. (2005). *Molecular Biology of Cancer: Mechanisms, Targets and Therapeutics* (3rd ed.). Oxford: Oxford University Press.

Rayman, M. P. (2005). Selenium in cancer prevention: a review of the evidence and mechanism of action. *Proceedings of the Nutrition Society, 64*(04), 527-542. doi: doi:10.1079/PNS2005467

Rayman, M. P. (2012). Selenium and human health. *The Lancet, 379*(9822), 1256-1268.

Roszkowski, K., Jozwicki, W., Blaszczyk, P., Mucha-Malecka, A., & Siomek, A. (2011). Oxidative damage DNA: 8-oxoGua and 8-oxodG as molecular markers of cancer. *Medical Science Monitor, 17*(6), CR329-333.

Sasco, A. J. (2001). Epidemiology of breast cancer: an environmental disease?Note. *APMIS, 109*(5), 321-332. doi: 10.1034/j.1600-0463.2001.090501.x

Schrauzer, G., White, D., & Schneider, C. (1976). Inhibition of the genesis of spontaneous mammary tumors in C3H mice: effects of selenium and of selenium-antagonistic elements and their possible role in human breast cancer. *Bioinorganic Chemistry, 6*(3), 265-270.

Schwarz, K., & Foltz, C. M. (1957). SELENIUM AS AN INTEGRAL PART OF FACTOR 3 AGAINST DIETARY NECROTIC LIVER DEGENERATION. *Journal of the American Chemical Society, 79*(12), 3292-3293. doi: 10.1021/ja01569a087

Seo, Y., Sweeney, C., & Smith, M. (2002). Selenomethionine induction of DNA repair response in human fibroblasts. *Oncogene, 21*(23), 3663-3669.

Singh, N. P., McCoy, M. T., Tice, R. R., & Schneider, E. L. (1988). A simple technique for quantitation of low levels of DNA damage in individual cells. *Experimental Cell Research, 175*(1), 184-191. doi: http://dx.doi.org/10.1016/0014-4827(88)90265-0

Sørlie, T., Perou, C. M., Tibshirani, R., Aas, T., Geisler, S., Johnsen, H., . . . Børresen-Dale, A.-L. (2001). Gene expression patterns of breast carcinomas distinguish tumor subclasses with clinical implications. *Proceedings of the National Academy of Sciences, 98*(19), 10869-10874. doi: 10.1073/pnas.191367098

Soule, H. D., Vazquez, J., Long, A., Albert, S., & Brennan, M. (1973). A Human Cell Line From a Pleural Effusion Derived From a Breast Carcinoma. *Journal of the National Cancer Institute, 51*(5), 1409-1416. doi: 10.1093/jnci/51.5.1409

Thermo Fisher Scientific. (2008). NanoDrop 1000 Spectrophotometer V3.7 User's Manual. USA: Thermo Fisher Scientific Inc.

Thompson, D., & Easton, D. (2004). The Genetic Epidemiology of Breast Cancer Genes. *Journal of Mammary Gland Biology and Neoplasia, 9*(3), 221-236. doi: 10.1023/B:JOMG.0000048770.90334.3b

Thomson, C. D., & Robinson, M. F. (1980). Selenium in human health and disease with emphasis on those aspects peculiar to New Zealand. *The American Journal of Clinical Nutrition, 33*(2), 303-323.

Tice, R., & Vasquez, M. (1998). Protocol for the application of the pH>13 alkaline single cell gel (SCG) assay to the detection of DNA damage in mammalian cells. Durham, NC, USA: Integrated Laboratory Systems.

Tsuji, K., Kawauchi, S., Saito, S., Furuya, T., Ikemoto, K., Nakao, M., . . . Sasaki, K. (2010). Breast cancer cell lines carry cell line-specific genomic alterations that are distinct from aberrations in breast cancer tissues: Comparison of the CGH

profiles between cancer cell lines and primary cancer tissues. *BMC Cancer, 10*(1), 15.

Tujebajeva, R. M., Copeland, P. R., Xu, X. M., Carlson, B. A., Harney, J. W., Driscoll, D. M., . . . Berry, M. J. (2000). Decoding apparatus for eukaryotic selenocysteine insertion. *EMBO reports, 1*(2), 158-163.

UCSC Genome Bioinformatics. (2013a). UCSC Genome Browser on Human Feb. 2009 (GRCh37/hg19) Assembly. BRCA1. Retrieved 9 August, 2013, from http://genome.ucsc.edu/cgi-bin/hgTracks?hgsid=343670627

UCSC Genome Bioinformatics. (2013b). UCSC Genome Browser on Human Feb. 2009 (GRCh37/hg19) Assembly. BRCA2. . Retrieved 9 August, 2013, from http://genome.ucsc.edu/cgi-bin/hgTracks?position=chr13:32889617-32973809&hgsid=343847579&refGene=pack&hgFind.matches=NM_000059,

Uphoff, C., & Drexler, H. (1999). Detection of mycoplasma contaminations in cell cultures by PCR analysis. *Human Cell, 12*(4), 229-236.

Uphoff, C. C., & Drexler, H. G. (2011). Detecting Mycoplasma Contamination in Cell Cultures by Polymerase Chain Reaction. In I. A. Cree (Ed.), *Cancer Cell Culture* (Vol. 731, pp. 93-103): Humana Press.

Valdiglesias, V., Pásaro, E., Méndez, J., & Laffon, B. (2010). In vitro evaluation of selenium genotoxic, cytotoxic, and protective effects: a review. *Archives of Toxicology, 84*(5), 337-351. doi: 10.1007/s00204-009-0505-0

Vanderhaeghe, L. (2004, Apr/May). What's Causing Breast Cancer? *Total Health, 26,* R8-R9.

Wang, H. H., & Chung, U. L. (2012). Relationships between cause of cancer and breast cancer-related factors in breast cancer survivors. *Asian Pac J Cancer Prev, 13*(8), 3889-3892.

Wang, Y., Cortez, D., Yazdi, P., Neff, N., Elledge, S. J., & Qin, J. (2000). BASC, a super complex of BRCA1-associated proteins involved in the recognition and repair of aberrant DNA structures. *Genes & Development, 14*(8), 927-939. doi: 10.1101/gad.14.8.927

Washbrook, E. (2006). Risk factors and epidemiology of breast cancer. *Women's Health Medicine, 3*(1), 8-14. doi: doi.org/10.1383/wohm.2006.3.1.8

Waters, D. J., Shen, S., Cooley, D. M., Bostwick, D. G., Qian, J., Combs, G. F., . . . Morris, J. S. (2003). Effects of Dietary Selenium Supplementation on DNA Damage and Apoptosis in Canine Prostate. *Journal of the National Cancer Institute, 95*(3), 237-241. doi: 10.1093/jnci/95.3.237

Weekley, C. M., & Harris, H. H. (2013). Which form is that? The importance of selenium speciation and metabolism in the prevention and treatment of disease. *Chemical Society Reviews, 42*(23), 8870-8894. doi: 10.1039/C3CS60272A

Weigelt, B., Baehner, F. L., & Reis-Filho, J. S. (2010). The contribution of gene expression profiling to breast cancer classification, prognostication and prediction: a retrospective of the last decade. *The Journal of Pathology, 220*(2), 263-280. doi: 10.1002/path.2648

Weigelt, B., Geyer, F. C., & Reis-Filho, J. S. (2010). Histological types of breast cancer: How special are they? *Molecular Oncology, 4*(3), 192-208. doi: doi.org/10.1016/j.molonc.2010.04.004

Weigelt, B., & Reis-filho, J. S. (2009). Histological and molecular types of breast cancer: is there a unifying taxonomy? *Nature Reviews. Clinical Oncology, 6*(12), 718-730. doi: doi.org/10.1038/nrclinonc.2009.166

Welcsh, P. L., & King, M.-C. (2001). BRCA1 and BRCA2 and the genetics of breast and ovarian cancer. *Human Molecular Genetics, 10*(7), 705-713. doi: 10.1093/hmg/10.7.705

Westermarck, T., Latvus, A., & Atroshi, F. (2014). The Pharmacology and Biochemistry of Selenium in Cancer. In F. Atroshi (Ed.), *Pharmacology and Nutritional Intervention in the Treatment of Disease* (pp. 295-311). InTech.

Wilson, I. G. (1997). Inhibition and facilitation of nucleic acid amplification. *Applied and Environmental Microbiology, 63*(10), 3741-3751.

Wu, X.-Q., & Gross, H. J. (1993). The long extra arms of human tRNA(Ser)Sec and tRNASer function as major identity elements for serylation in an orientation-dependent, but not sequence-specific manner. *Nucleic Acids Research, 21*(24), 5589-5594. doi: 10.1093/nar/21.24.5589

Xu, X.-M., Carlson, B. A., Mix, H., Zhang, Y., Saira, K., Glass, R. S., . . . Hatfield, D. L. (2006). Biosynthesis of Selenocysteine on Its tRNA in Eukaryotes. *PLoS Biol, 5*(1), e4. doi: 10.1371/journal.pbio.0050004

Yang, G. Q., Wang, S. Z., Zhou, R. H., & Sun, S. Z. (1983). Endemic selenium intoxication of humans in China. *The American Journal of Clinical Nutrition, 37*(5), 872-881.

Yerushalmi, R., Hayes, M. M., & Gelmon, K. A. (2009). Breast carcinoma—rare types: review of the literature. *Annals of Oncology, 20*(11), 1763-1770. doi: 10.1093/annonc/mdp245

Yuan, J., Palioura, S., Salazar, J. C., Su, D., O'Donoghue, P., Hohn, M. J., . . . Söll, D. (2006). RNA-dependent conversion of phosphoserine forms selenocysteine in eukaryotes and archaea. *Proceedings of the National Academy of Sciences, 103*(50), 18923-18927. doi: 10.1073/pnas.0609703104

Zeng, H., Davis, C. D., & Finley, J. W. (2003). Effect of selenium-enriched broccoli diet on differential gene expression in min mouse liver1,2. *Journal of Nutritional Biochemistry, 14*(4), 227-231. doi: 10.1016/S0955-2863(03)00005-6

Zeng, H., Jackson, M., Cheng, W.-H., & Combs, G., Jr. (2011). Chemical Form of Selenium Affects Its Uptake, Transport, and Glutathione Peroxidase Activity in the Human Intestinal Caco-2 Cell Model. *Biological Trace Element Research, 143*(2), 1209-1218. doi: 10.1007/s12011-010-8935-3

Zhou, B., Stamler, J., Dennis, B., Moag-Stahlberg, A., Okuda, N., Robertson, C., . . . Elliott, P. (2003). Nutrient intakes of middle-aged men and women in China, Japan, United Kingdom, and United States in the late 1990s: The INTERMAP Study. *Journal of Human Hypertension, 17*, 623-630. doi: 10.1038/sj.jhh.1001605

Appendix One

Buffers and Solutions

Digestion buffer

500 µl	10 mM Tris-Cl (pH 8.0)
1 ml	10 mM EDTA (pH 8.0)
1 ml	100 mM NaCl
2.5 ml	0.5% SDS

Make up to 50 ml with sterile mQ H_2O

Digestion buffer with 500 µg/ml fresh proteinase K

5 uL	20 mg/ml proteinase K
195 µl	Digestion buffer

0.5M EDTA pH 8.0

Dissolve 93.05 g of EDTA in 500 ml of mQ H_2O
Autoclave

Electrophoresis buffer stock solution 1

200 g	NaOH	Final concentration = 10N
500 ml	dd H_2O	

Electrophoresis buffer stock solution 2

14.89 g	EDTA	Final concentration = 200 mM
200 ml	dd H_2O	

Adjust pH to 10 with NaOH

Electrophoresis buffer working solution

30 ml	Electrophoresis buffer stock solution 1
5 ml	Electrophoresis buffer stock solution 2

Make up to 1000 ml with dd H_2O

Freezing media (10 ml)

9.5 ml	Growth media
500 µl	DMSO

Growth media for the MDA-MB-436 cell line (50 ml)

44 ml	MEM
5 ml	Filter sterilised FBS
500 µl	1 mg/ml Insulin (Sigma)
500 µl	100X Pen/strep (Gibco® Life Technologies)

Growth media for the SUM149PT cell line (50 ml)

46.2 ml	Nutrient Mixture F-12 Ham (Sigma)
2.5 ml	Filter sterilised FBS
500 µl	1M HEPES
250 µl	1 mg/ml Insulin (Sigma)
50 µl	Hydrocortisone
500 µl	100X Pen/strep (Gibco® Life Technologies)

1M HEPES buffer

11.93g HEPES
Make up to 50 mL with mQ H_2O in a cell culture hood
Filter sterilise with 0.2 µM filter
Aliquot out 5 mL into 15 mL falcon tubes
Store at 4°C

1 mg/ml Hydrocortisone

Make up solution in a cell culture hood
Dissolve 40 mg Hydrocortisone in 20 ml 100% ethanol
Add 20 ml mQ H_2O
Aliquot 1 ml in 2 ml eppendorf tubes
Store at -20°C

1 mg/ml Insulin

Make up solution in a cell culture hood

1 ml	Insulin solution, human, 10 mg/ml in 25 mM HEPES, pH 8.2 (Sigma. LOT SLBG7397)
9 ml	mQ H_2O

Filter sterilise with 0.2 µM filter
Aliquot out ml into 2 ml eppendorf tubes
Wrap all solutions in tinfoil
Store at 4°C

6X Loading buffer

0.025 g	Bromophenol Blue	Final concentration = 0.25%
0.025g	Xylene Cyanol	Final concentration = 0.25%
3 mL	Glycerol FC = 30%	Final concentration = 30%

Make up to 10 ml with mQ H_2O

0.5% Low melting point agarose

125 mg	Low melting point agarose
25 ml	1X PBS

Microwave until agarose dissolves
Make in glass bottle, and transfer to a 50 ml falcon tube once dissolved
Store at RT

Lysis stock solution

146.1 g	NaCl	Final concentration = 2.5M
37.2 g	EDTA	Final concentration = 100 mM
1.2 g	Tris	Final concentration = 10 mM

700 ml dd H_2O
Stir till dissolved
12 g NaOH
Stir till dissolved
Adjust pH to 10
Adjust final volume to 890 ml
The Triton X-100 will increase the volume to the correct amount when preparing the lysis working solution

Lysis working solution

72.81 ml Lysis stock solution
2.19 ml 0.5% Triton X-100

2M $MgCl_2$

31.8g $MgCl_2$
Make up to 200mL with mQ H_2O
Autoclave

1M MSA

Dissolve 0.4064 g of MSA in 2 ml of 1X PBS
Filter sterlise
Store at -20°C

Neutralisation buffer

48.5 g 0.4M Tris
800 ml dd H_2O
Adjust pH to 7.5 with concentration HCl
Adjust final volume to 1000 ml with dd H_2O

1% Normal melting point agarose

500 mg Normal melting point agarose
50 ml 1X PBS
Microwave until agarose dissolves
Make in glass bottle, and transfer to a 50 ml falcon tube once dissolved
Store at RT

10X Phosphate buffered saline (PBS) solution

80g NaCl
20g KCl
14.4g Na_2HPO_4
2.4g KH_2PO_4
Adjust pH to 7.4, make up to 1 L with mQ H_2O and autoclave.

20 mg/ml Proteinase K

20 mg Proteinase K
10 µl 1M Tris (pH 8.0)
2 µl 0.5M EDTA (pH 8.0)
Make up to 1 ml with sterile mQ H_2O
Store at -20°C

3M Sodium Acetate pH 5.2

Dissolve 40.8 g of sodium acetate in 80 ml of H_2O
Adjust the pH to 5.2 with glacial acetic acid
Adjust the volume to 100 ml with H_2O
Autoclave

1M Sodium Selenite

Dissolve 3.784 g of sodium selenite in 10 ml of 1X PBS
Filter sterilise
Store at -20°C

SYBR® Gold fluorescent stain

1.3 µl 1000X SYBR Gold
1298.7 µl mQ H_2O
Store at -20°C

50X TAE - Tris-acetate EDTA buffer

242g Tris base dissolved in 800 mL mQ H_2O
57.1mL Glacial acetic acid
100mL 0.5M EDTA (pH 8.0)
Make up to 1L with mQ H_2O

1X TAE running buffer

20mL 50X TAE
980mL mQ H_2O

TE buffer – Tris EDTA pH 8.0

10mL 1M Tris-HCl pH 8.0
2mL 0.5M EDTA pH 8.0

1M Tris pH 8.0

Dissolve 60.5 g of Tris in 500 ml of H_20
Adjust the pH to 8.0
Autoclave

0.5% Triton-X 100

250µl Triton-X 100
Make up to 50mL with 1X PBS

Appendix Two

Vector Maps

2.1 *Mycoplasma* Internal Control Plasmid

The internal control DNA is a 3995 bp plasmid that contains a 516 bp DNA fragment derived from the *Mycoplasma* strain, *Acholeplasma laidlawii*. This fragment is disrupted by the insertion of a 476 bp Taq I fragment from pUC-19 plasmid DNA (Figure 30). Due to this disruption, the internal control product will appear as a 1 kb band on the agarose gel.

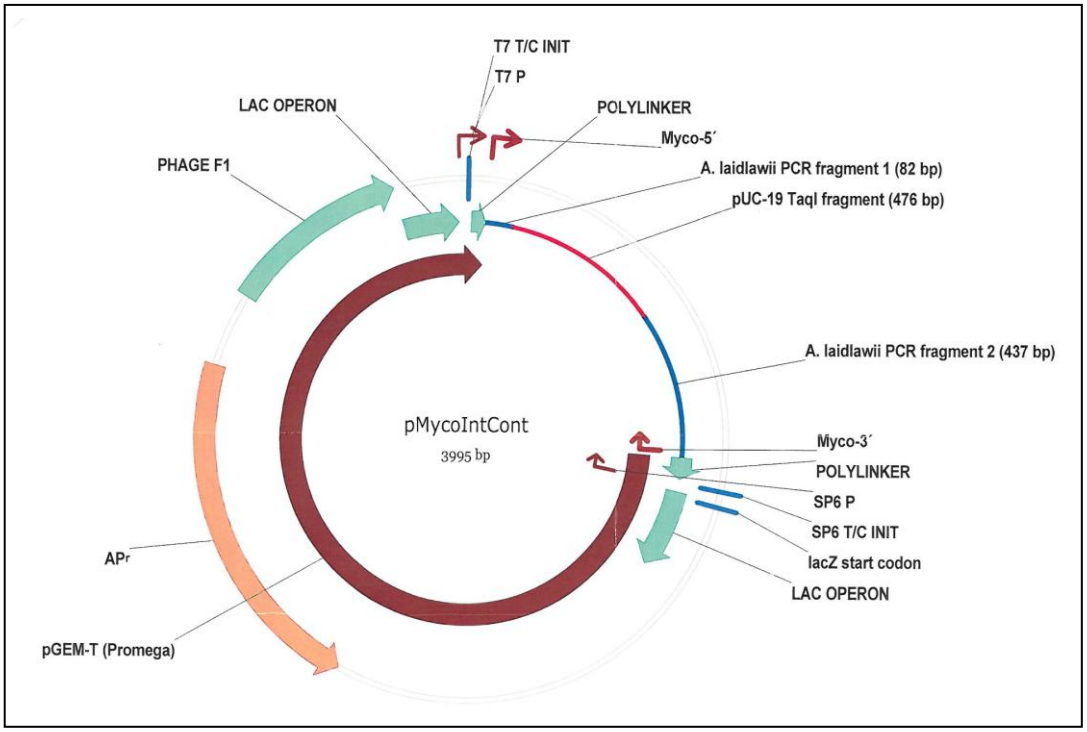

Figure 30. pMycoIntCont plasmid map of the internal control supplied from DSMZ.

Appendix Three

Primer Blast Results

The six published primers (Uphoff & Drexler, 1999) used for the detection of *Mycoplasma* contamination in cell cultures were run through the nucleotide blast program to identify which species the oligonucleotides were targeting.

3.1 LMP13 - CGCCTGAGTAGTACGTWCGC

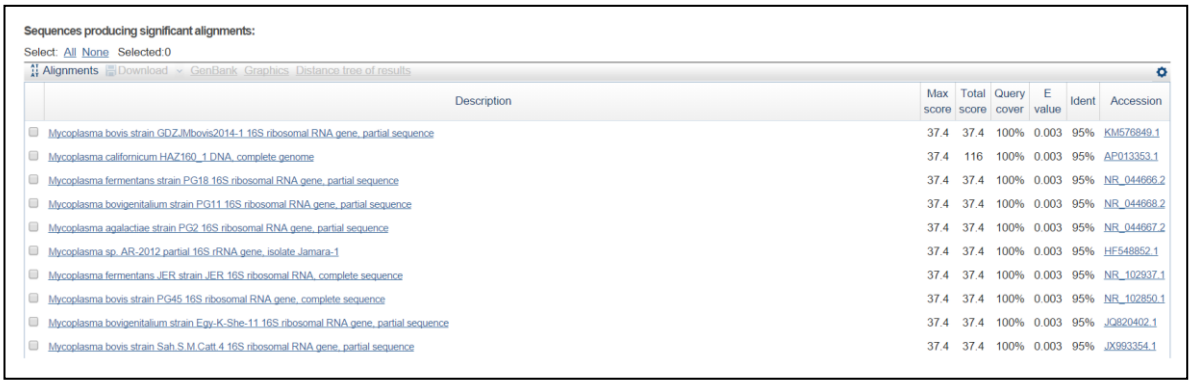

Sequences producing significant alignments:

Select: All None Selected:0

Alignments Download GenBank Graphics Distance tree of results

Description	Max score	Total score	Query cover	E value	Ident	Accession
Mycoplasma bovis strain GDZJMbovis2014-1 16S ribosomal RNA gene, partial sequence	37.4	37.4	100%	0.003	95%	KM576849.1
Mycoplasma californicum HAZ160_1 DNA, complete genome	37.4	116	100%	0.003	95%	AP013353.1
Mycoplasma fermentans strain PG18 16S ribosomal RNA gene, partial sequence	37.4	37.4	100%	0.003	95%	NR_044666.2
Mycoplasma bovigenitalium strain PG11 16S ribosomal RNA gene, partial sequence	37.4	37.4	100%	0.003	95%	NR_044668.2
Mycoplasma agalactiae strain PG2 16S ribosomal RNA gene, partial sequence	37.4	37.4	100%	0.003	95%	NR_044667.2
Mycoplasma sp. AR-2012 partial 16S rRNA gene, isolate Jamara-1	37.4	37.4	100%	0.003	95%	HF548852.1
Mycoplasma fermentans JER strain JER 16S ribosomal RNA, complete sequence	37.4	37.4	100%	0.003	95%	NR_102937.1
Mycoplasma bovis strain PG45 16S ribosomal RNA gene, complete sequence	37.4	37.4	100%	0.003	95%	NR_102850.1
Mycoplasma bovigenitalium strain Egy-K-She-11 16S ribosomal RNA gene, partial sequence	37.4	37.4	100%	0.003	95%	JQ820402.1
Mycoplasma bovis strain Sah.S.M.Catt.4 16S ribosomal RNA gene, partial sequence	37.4	37.4	100%	0.003	95%	JX993354.1

Figure 31. Nucleotide blast results for primer LMP13. Results show 95% identity with a range of *Mycoplasma* species, targeting the 16S rRNA gene. Only the first ten hits are shown.

3.2 LMP14 - TGCCTGRGTAGTACATTCGC

Sequences producing significant alignments:

Select: All None Selected:0

Alignments Download GenBank Graphics Distance tree of results

Description	Max score	Total score	Query cover	E value	Ident	Accession
Ureaplasma parvum serovar 3 DNA, complete genome, strain: SV3F4	37.4	137	100%	0.004	95%	AP014584.1
Mycoplasma gallisepticum S6, complete genome	37.4	118	100%	0.004	95%	CP006916.2
Uncultured Mycoplasma sp. clone D9 16S ribosomal RNA gene, partial sequence	37.4	37.4	100%	0.004	95%	KF631218.1
Uncultured Mycoplasma sp. clone D7 16S ribosomal RNA gene, partial sequence	37.4	37.4	100%	0.004	95%	KF631217.1
Uncultured Mycoplasma sp. clone D1 16S ribosomal RNA gene, partial sequence	37.4	37.4	100%	0.004	95%	KF631216.1
Uncultured Ureaplasma sp. clone H40-48 16S ribosomal RNA gene, partial sequence	37.4	37.4	100%	0.004	95%	JF975752.1
Uncultured Ureaplasma sp. clone H40-45 16S ribosomal RNA gene, partial sequence	37.4	37.4	100%	0.004	95%	JF975751.1
Uncultured Ureaplasma sp. clone H40-39 16S ribosomal RNA gene, partial sequence	37.4	37.4	100%	0.004	95%	JF975750.1
Uncultured Ureaplasma sp. clone H40-30 16S ribosomal RNA gene, partial sequence	37.4	37.4	100%	0.004	95%	JF975749.1
Uncultured Ureaplasma sp. clone H40-28 16S ribosomal RNA gene, partial sequence	37.4	37.4	100%	0.004	95%	JF975748.1

Figure 32. Nucleotide blast results for primer LMP14. Results show 95% identity with a range of *Mycoplasma* species, targeting the 16S rRNA gene. Only the first ten hits are shown.

3.3 LMP15 - CRCCRGAGTAGTATGCTCGC

Sequences producing significant alignments:

Select: All None Selected:0

Alignments Download GenBank Graphics Distance tree of results

Description	Max score	Total score	Query cover	E value	Ident	Accession
Uncultured Mycoplasma sp. clone AF 16S ribosomal RNA gene, partial sequence	32.3	32.3	75%	0.099	100%	KP292569.1
Mycoplasma flocculare ATCC 27399, complete genome	32.3	195	75%	0.099	100%	CP007585.1
Mycoplasma orale strain Minhan 16S ribosomal RNA gene, partial sequence	32.3	32.3	75%	0.099	100%	KM507723.1
Mycoplasma mycoides subsp. mycoides strain izsam_mm5713, complete genome	32.3	381	75%	0.099	100%	CP010267.1
Uncultured Mycoplasma sp. clone DE6 16S ribosomal RNA gene, partial sequence	32.3	32.3	75%	0.099	100%	KJ623625.1
Uncultured Mycoplasma sp. clone NJ15 16S ribosomal RNA gene, partial sequence	32.3	32.3	75%	0.099	100%	KJ623624.1
Uncultured Mycoplasma sp. clone NJ28 16S ribosomal RNA gene, partial sequence	32.3	32.3	75%	0.099	100%	KJ623623.1
Uncultured Mycoplasma sp. clone PA6 16S ribosomal RNA gene, partial sequence	32.3	32.3	75%	0.099	100%	KJ623622.1
Mycoplasma hominis ATCC 27545, complete genome	32.3	166	75%	0.099	100%	CP009652.1
Mycoplasma ovipneumoniae strain Dovre 16S ribosomal RNA gene, partial sequence	32.3	32.3	75%	0.099	100%	KJ433280.1

Figure 33. Nucleotide blast results for primer LMP15. Results show 100% identity with a range of *Mycoplasma* species, targeting the 16S rRNA gene. Only the first ten hits are shown.

3.4 LMP16 - CGCCTGGGTAGTACATTCGC

Sequences producing significant alignments:

Select: All None Selected:0

Alignments Download GenBank Graphics Distance tree of results

Description	Max score	Total score	Query cover	E value	Ident	Accession
Candidatus Mycoplasma girerdii strain VCU_M1, complete genome	40.1	82.8	100%	4e-04	100%	CP007711.1
Mycoplasma pneumoniae M29, complete genome	40.1	177	100%	4e-04	100%	CP008895.1
Uncultured Mycoplasma sp. clone SB6-42 16S ribosomal RNA gene, partial sequence	40.1	40.1	100%	4e-04	100%	KJ197810.1
Mycoplasma muris strain RIII-4 16S ribosomal RNA gene, partial sequence	40.1	40.1	100%	4e-04	100%	NR_044664.2
Mycoplasma iowae strain 695 16S ribosomal RNA gene, partial sequence	40.1	40.1	100%	4e-04	100%	NR_044669.2
Uncultured Mycoplasma sp. partial 16S rRNA gene, clone D08	40.1	40.1	100%	4e-04	100%	HG764212.1
Uncultured Mycoplasma sp. partial 16S rRNA gene, clone D04	40.1	40.1	100%	4e-04	100%	HG764211.1
Uncultured Mycoplasma sp. partial 16S rRNA gene, clone D06	40.1	40.1	100%	4e-04	100%	HG764210.1
Uncultured Mycoplasma sp. partial 16S rRNA gene, clone H07	40.1	40.1	100%	4e-04	100%	HG764209.1
Mycoplasma penetrans HF-2 strain HF-2 16S ribosomal RNA, complete sequence	40.1	40.1	100%	4e-04	100%	NR_074145.1

Figure 34. Nucleotide blast results for primer LMP16. Results show 100% identity with a range of Mycoplasma species, targeting the 16S rRNA gene. Only the first ten hits are shown.

3.5 LMP17 - GCGGTGTGTACAARACCCGA

Sequences producing significant alignments:

Select: All None Selected:0

Alignments Download GenBank Graphics Distance tree of results

Description	Max score	Total score	Query cover	E value	Ident	Accession
Mycoplasma ovipneumoniae strain Dovre 16S ribosomal RNA gene, partial sequence	37.4	37.4	100%	0.003	95%	KJ433280.1
Mycoplasma capricolum subsp. capripneumoniae genome assembly ILRI181.1, chromosome : 1	37.4	74.8	100%	0.003	95%	LN515399.1
Mycoplasma canadense DNA, complete genome, strain: HAZ360_1	37.4	95.7	100%	0.003	95%	AP014631.1
Mycoplasma capricolum subsp. capripneumoniae genome assembly F38.1, chromosome : 1	37.4	74.8	100%	0.003	95%	LN515398.1
Mycoplasma capricolum subsp. capripneumoniae genome assembly 9231-Abomsa assembly V8, chromosome : I	37.4	74.8	100%	0.003	95%	LM995445.1
Mycoplasma verecundum strain ATCC 27862 16S ribosomal RNA gene, complete sequence	37.4	37.4	100%	0.003	95%	NR_125608.1
Mycoplasma pneumoniae M29, complete genome	37.4	79.3	100%	0.003	95%	CP008895.1
Mycoplasma sp. Eis-1-PT-13 16S ribosomal RNA gene, partial sequence; 16S-23S ribosomal RNA intergenic spacer, complete sequence; and 23S ribosomal RNA gene, partial sequence	37.4	37.4	100%	0.003	95%	KJ700870.1
Mycoplasma sp. Eis-1-PN-14 16S ribosomal RNA gene, partial sequence; 16S-23S ribosomal RNA intergenic spacer, complete sequence; and 23S ribosomal RNA gene, partial sequence	37.4	37.4	100%	0.003	95%	KJ700869.1
Candidatus Hepatoplasma crinochetorum 16S ribosomal RNA, complete sequence	37.4	37.4	100%	0.003	95%	NR_121778.1

Figure 35. Nucleotide blast results for primer LMP17. Results show 95% identity with a range of Mycoplasma species, targeting the 16S rRNA gene. Only the first ten hits are shown.

3.6 LMP18 - GCGGTGTGTACAAACCCCGA

Sequences producing significant alignments:

Select: All None Selected:0

Alignments Download GenBank Graphics Distance tree of results

Description	Max score	Total score	Query cover	E value	Ident	Accession
Candidatus Phytoplasma solani isolate Lorestan 16S ribosomal RNA gene, partial sequence; 16S-23S ribosomal RNA intergenic spacer, complete sequence; and 23S ribosomal RNA gene, partial seque	40.1	40.1	100%	5e-04	100%	KF130968.1
Candidatus Phytoplasma solani isolate Fars 16S ribosomal RNA gene, partial sequence; 16S-23S ribosomal RNA intergenic spacer, complete sequence; and 23S ribosomal RNA gene, partial sequence	40.1	40.1	100%	5e-04	100%	KF130967.1
Sugarcane yellow leaf disease phytoplasma isolate CoSe92423 16S ribosomal RNA gene, partial sequence	40.1	40.1	100%	5e-04	100%	KJ599657.1
Sugarcane yellow leaf disease phytoplasma isolate CoLk94184 16S ribosomal RNA gene, partial sequence	40.1	40.1	100%	5e-04	100%	KJ599656.1
Acholeplasma oculi genome assembly Acholeplasma oculi strain 19L, chromosome : 1	40.1	376	100%	5e-04	100%	LK028559.1
Coconut lethal yellowing phytoplasma isolate Francisco de Montejo 16S ribosomal RNA gene, partial sequence	40.1	40.1	100%	5e-04	100%	KF277151.2
Candidatus Phytoplasma prunorum isolate PN115-NPA 16S ribosomal RNA gene and 16S-23S ribosomal RNA intergenic spacer, partial sequence	40.1	40.1	100%	5e-04	100%	KF932302.1
Candidatus Phytoplasma phoenicium isolate PN201-NPA 16S ribosomal RNA gene and 16S-23S ribosomal RNA intergenic spacer, partial sequence	40.1	40.1	100%	5e-04	100%	KF932301.1
Candidatus Phytoplasma phoenicium isolate PN199-NPA 16S ribosomal RNA gene and 16S-23S ribosomal RNA intergenic spacer, partial sequence	40.1	40.1	100%	5e-04	100%	KF932300.1
Candidatus Phytoplasma phoenicium isolate PN193-NPA 16S ribosomal RNA gene and 16S-23S ribosomal RNA intergenic spacer, partial sequence	40.1	40.1	100%	5e-04	100%	KF932299.1

Figure 36. Nucleotide blast results for primer LMP18. Results show 100% identity with the internal control species, *Acholeplasma*. Only the first ten hits are shown.